SN-140A

INVESTIGATION OF THE RELATION BETWEEN SOLAR VARIATIONS AND WEATHER ON EARTH AS SHOWN BY STUDY OF SIMULTANEOUS DATA FROM THE SUN, MARINER II, NEAR-EARTH SATELLITES AND THE ATMOSPHERE BELOW THE MESOSPHERE

FINAL REPORT

CONTRACT NO. NASw-724
AMENDMENT NO. 2

nes co

DECEMBER 1965

NATIONAL ENGINEERING SCIENCE CO.

PREPARED FOR

NATIONAL AERONAUTICS AND SPACE ADMINISTRATION

WASHINGTON, D.C.

INVESTIGATION OF THE RELATION BETWEEN SOLAR VARIATIONS AND WEATHER ON EARTH AS SHOWN BY STUDY OF SIMULTANEOUS DATA FROM THE SUN, MARINER II, NEAR-EARTH SATELLITES AND THE ATMOSPHERE BELOW THE MESOSPHERE

Prepared by

John C. Freeman, Jr. and W. H. Portig

with the support of

Leon F. Graves and Peter Hanna

Prepared for

NATIONAL AERONAUTICS AND SPACE ADMINISTRATION
Washington, D. C.

FINAL REPORT

Contract No. NASw-724
Amendment No. 2

December 1965

NATIONAL ENGINEERING SCIENCE COMPANY
8237 Lockheed Street, Houston, Texas 77017

PREFACE

The work reported here was accomplished in two major phases. The governing philosophy during the first phase was that the transient influence of the sun on the earth's atmosphere is controlled by the solar wind and that a stratospheric event would follow a magnetic storm in the ionosphere.

The analysis of the 10 mb data and TIROS photographs accomplished in the later stages of the second phase of the work gives indication of detectable characteristic height patterns at 10 mb 4 to 5 days preceding a magnetic storm. This time is near the time of the visibility of radiative aspects of a well established solar disturbance, especially the first appearance of faculae.

There is little doubt about the method of transport or the possibility of absorption of very short wave radiation from flares and faculae. The increased heating of the equatorial region of the absorbing layers would be expected.

The solar wind is also an attractive source of energy to influence the weather because of its scale of time variation, its variability, and the likelihood that its energy can be collected from a large area near the earth and can be concentrated in a local area on the earth.

The form of the solar wind energy concentration is debatable but it certainly affects the ionosphere and the auroral zones near the poles. We have concentrated on magnetic waves as the primary means of transmitting this energy but the possibility of collection of high energy protons near the pole seems just as attractive.

We postulate that this energy heats the poles at very high levels and causes a high cell there. One possible method of heating the area 150 to 200 km would be by slowing the west winds there resulting in an increase in temperature and high pressure. The slowing could be brought about by increased ionization at levels near 150 km.

Our descriptive evidence shows that the significant effect on the lower atmosphere precedes the magnetic storm and probably precedes the reported data of the solar event. We postulate that there is a leading event on the sun that affects the earth.

We have a theory for the transmission of a disturbance downward (feeding on the energy of the lower atmosphere).

34626

ABSTRACT

A recognizable disturbance of a 10 mb chart is shown to accompany a solar disturbance. The 10 mb disturbance precedes the magnetic storm. An effect of increased organization of clouds as shown by TIROS photographs also accompanies the solar disturbance.

The idea is promoted that energy is available from small scales at any level in the atmosphere to force planetary motions to follow the thermal wind equation. This idea releases students of solar influence from seeking energy for solar influence on the weather. Control rather than energy is required.

With this new freedom a model of the atmosphere that allows control from above is developed. A similar model allows descending very long period waves at the equator.

TABLE OF CONTENTS

I SOLAR STORMS CAUSE WEATHER CHANGES

Introduction

Our work that follows shows that, concurrent with certain aspects of a solar event and before and during a magnetic storm on the earth, there is a detectable and characteristic change of the 10 mb map. The TIROS data also show a significant change in the circulation over the Gulf of Mexico. The results are striking in individual cases in contrast to the work of MacDonald and Roberts (1960, 1961), which shows that there is a statistically significant increase in the vorticity at 300 mb over the Gulf of Alaska about 3 days after the event. The work of Shapiro and Ward (1962) and Freeman, Graves and Portig (1963) show that there is a positive correlation between the K_p index and the zonal wind with a 5 day lag and a negative correlation with a 14 day lag. There is an unmistakable reaction of a 10 mb chart to a solar disturbance that is much more striking than results shown in previous work.

We slay the paper tiger that has chewed up all previous dynamic theories of interaction between the ionosphere (where the effect of the solar storms is accepted and well documented) and the troposphere, and we present a model of the atmosphere in which interaction is possible. In essence we show that control (and not energy) is all that is required to establish a link between ionosphere and troposphere. The energy is available from smaller scale motion at any level.

Solar and Magnetic Storms

A general description of magnetic storms and the mechanism by which the energy reaches the ionosphere from the sun has been developed by Chapman, Ferraro, Akasofu, Parker and Dessler in the last two decades. This work has been stimulated greatly by the measurements from satellites. The work of Jacchia and Slowey (1964) and of Paetzold (1963) have shown that satellite measurements of density can be used to estimate the temperature at 150 to 1500 km and that this varies significantly with solar activity. This is postulated by Johnson (1965) to be a result of absorbtion of very short ultra-violet radiation. Magnetic storms are very important in sun-atmosphere relations because they are an obvious disturbance in the atmosphere that is caused by a disturbance on the sun. There is no question of the occurrence and of the ultimate cause of magnetic storms. There is some question of the details of the mechanism by which the sun influences the ionosphere. There is no doubt that a solar storm manifest by flares and sunspots begins a chain of events that results in a magnetic storm in the ionosphere.

The solar storm begins with unusual activity on the face of the sun that generates flares, prominences and sunspots. (The sunspots can persist for days). This storm heats the sun's corona; there is some evidence for localization of this heating but it is usually assumed that the corona is heated all around the sun. If the storm is facing the earth, then the very short wave radiation from it reaches the earth as soon as the storm occurs (in 8 minutes) and begins to heat the lighted regions. If the storm is not facing the earth, we can only detect the increased temperature in the corona.

The corona of the sun consists of a glowing visible part, which is the traditional entity observed as the corona, and an invisible part, which is assumed to fill the entire solar system. The corona consists of hot gases streaming from the sun at 200 to 600 km/sec. Since these gases are moving in essentially the same direction and keep the same velocity over large areas, they have been given the very suggestive name "the solar wind." This follows the idea that the corona is actually the sun's atmosphere.

The solar wind is postulated to blow throughout the solar system with a significant change in its nature at about the orbit of Jupiter. Most important to us is the fact that it blows right past the earth and that in a very real sense the orbit of the earth is inside the atmosphere of the sun.

The solar wind is made up of a neutral plasma; that is, the positive ions and negative electrons are separate and free but equal in number. Such a plasma carries the lines of magnetic force of a magnetic field with the particles; thus the solar wind carries the magnetic field of the sun to the far reaches of the solar system. The classical solution of the combined magnetic field of earth and sun must be modified by the solar wind concept. Rather than the dipole field for earth and sun with those combined by addition, we have the concept of the solar wind blowing back the earth's magnetic field and restricting the influence of the earth so that we end up with a picture similar to that in Figure 1.

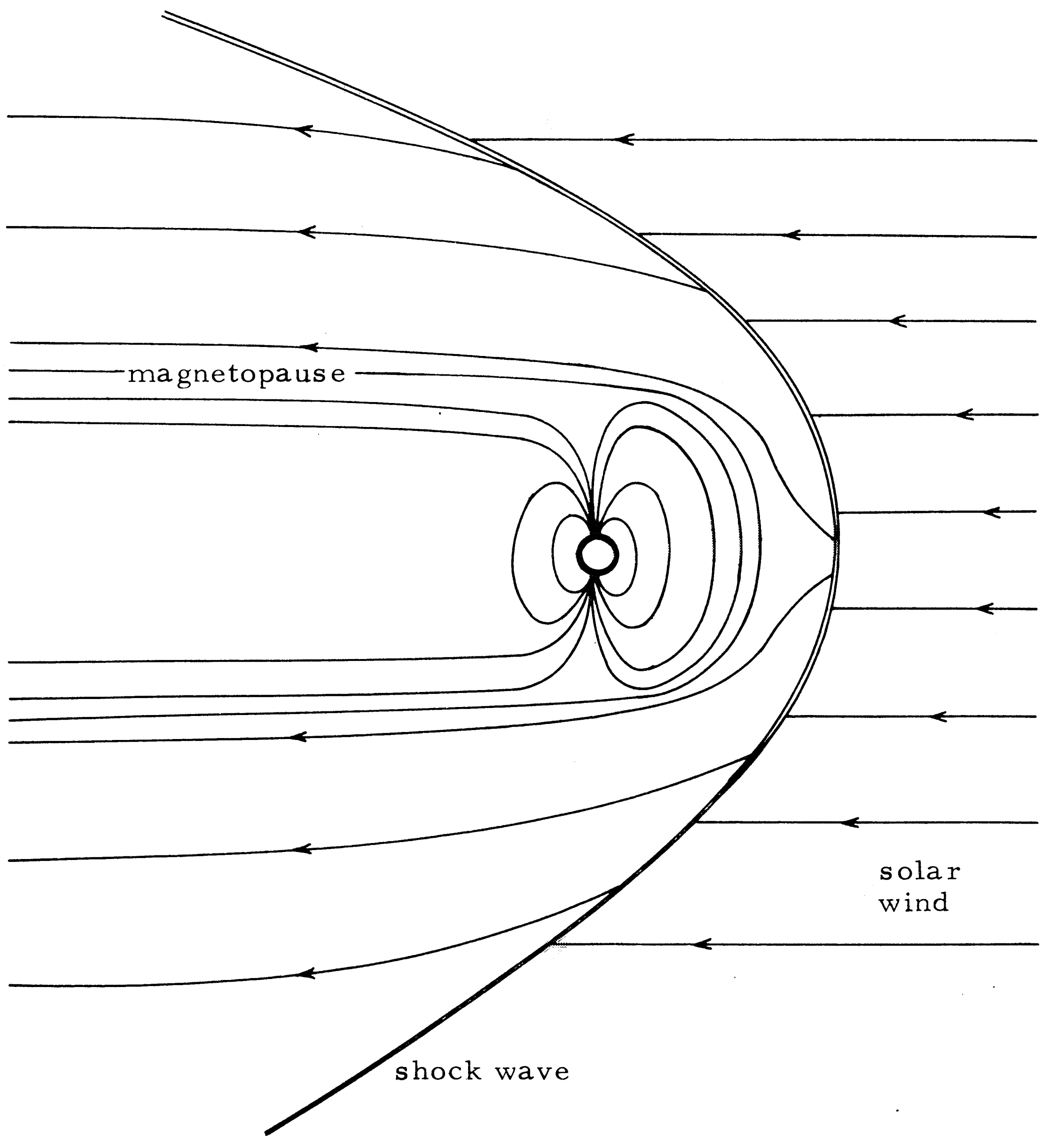

The solar cavity outlined by the magnetopause and the shock wave in the solar wind that precedes it.

Figure 1

The magnetopause is a natural boundary of the earth and is the absolute boundary of the earth's atmosphere and of all other earth influence other than gravitational.

The plasma acts very much like a fluid and the magnetosphere acts like a solid boundary with the fluid flowing around it. Hydromagnetic waves can be generated on the boundary of the magnetosphere and move in and affect the earth.

Some of the new ideas about the shape of the magnetic cavity include the concept that it is a long tail or wake streaming for millions of miles behind the earth. The idea of it being millions of miles long and capable of transmitting hydromagnetic waves makes it an attractive energy catcher.

The solar wind contains a very small amount of energy from the sun. The forward face of the magnetosphere is large enough to catch about 100 times the energy of the solar wind that would impinge on the frontal area of the earth. The long tail behind the earth can catch and transmit much more energy.

Every 100,000 miles of tail would gather 500 times the energy of the solar wind in one earth circle. Thus a 10 million mile long tail could gather 5×10^4 times the energy of the solar wind that would impinge on the earth's area. Thus, even if the energy of the solar wind is only a very small part of the total energy transmitted from the sun, we multiply its effect many times by gathering it all along the tail of the earth. In addition, we propose to use this energy on only about 1/20 of the earth's surface which gives us a factor of 10^6 to multiply by the energy in the solar wind in order to obtain the pool of energy available for phenomena governed by it.

Since about 10^{-6} of the energy in the solar constant is made up of the increased solar wind, we see that in a one or two day solar storm the equivalent of one or two days of full solar constant is potentially available to put into the upper atmosphere over the poles in winter. Actually, every hydromagnetic wave in the solar wind may bring energy to the cavity as a water wave brings energy to the shore.

In addition to the energy from the hydromagnetic waves that can be brought to the poles by hydromagnetic waves, we also propose that the poles are heated by high energy particles trapped from the solar wind. This is the alternate (and presently favored) theory of heating of the poles during magnetic storms.

However the poles are heated in the ionosphere, it seems to be a part of the same phenomenon as the magnetic storm and it is a result of a solar storm.

It is common that specialists in high altitude meteorology will assume that heating of the upper air leads to no significant pressure disturbance at low levels. They assume the heating at the pole at a high level causes the constant pressure surfaces to be raised in the upper levels as shown in Figure 2.

The achievement of geostrophic balance after the heating requires that the wafers of air between isentropic surfaces get thinner; this is helped by the divergence brought about by the pressure increase.

This divergence will lead to low level convergence and the system will propagate downward. We will discuss this later, but first we must overcome some formidable logical and psychological obstacles.

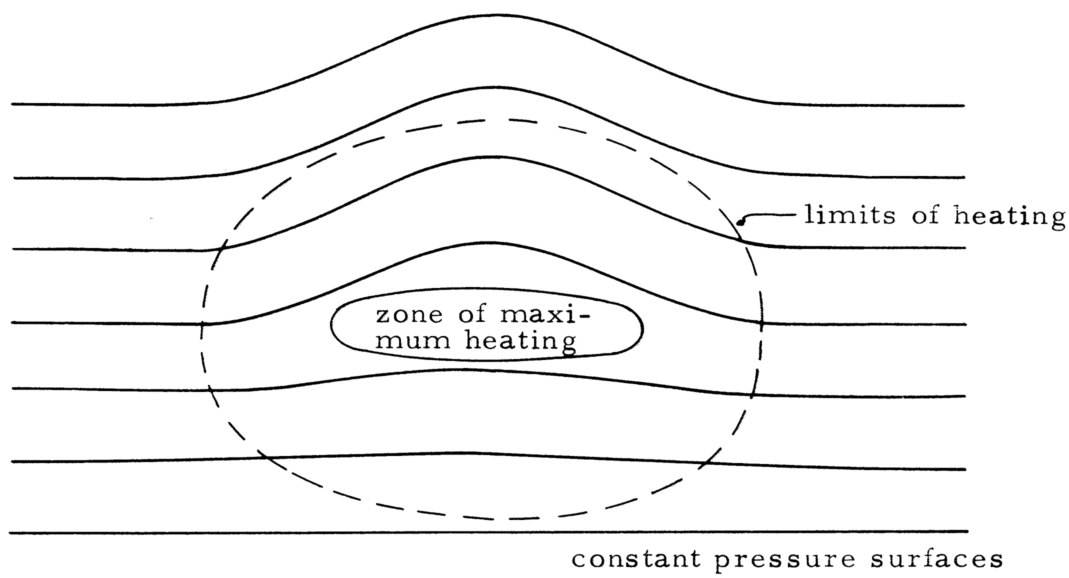

Heating in the upper atmosphere is assumed to cause a minimum disturbance at low levels so that all of the thickness change is manifest by increased height of the constant pressure surface above the level of heating.

Figure 2

Some Paper Tigers

There is now no doubt that solar disturbances or solar storms cause the magnetic disturbances or magnetic storms that interrupt and disturb electronic communications on the earth. This is a well documented fact based on experience and observation of simultaneous events and reasonably well explained by theory.

Weather events "simultaneous" with solar storms have been found by MacDonald and Roberts (1960) and by Shapiro and Ward (1962a). These are disturbances of the wind flow in the troposphere 3 to 10 days after the solar storm begins. In a study that follows this discussion, Portig shows that nearly every time there is a solar storm the same pressure change pattern occurs on a 10 mb chart. The existence of a simultaneous disturbance in the troposphere now seems to be established.

If the disturbances were unique (such as magnetic storms) or if they could be detected electronically and if they disturbed people in the quiet of their homes and offices, their effects might be more adequately recorded. With the possible exception of the pattern at 10 mb the disturbances are not unique, e.g. MacDonald and Roberts reported an increase and subsequent decrease in wind speed in a total system that fluctuates all the time.

This ambiguity in the data has hampered the acceptance of the above results in the face of what has always been assumed to be an overwhelming logical paradox. Paraphased in the language of the enthusiastic adherents of solar influence, this paradox is: "In spite of the overwhelming evidence of the influence of solar storms on tropospheric weather, there is no known way that sufficient energy (it is too small by powers of 10) can be shown to be available in the ionosphere to control the weather in the troposphere." To this paradox meteorologists have added another: "Even if enough energy were available there is no way to transmit it from the ionosphere to the troposphere."

In this report we attempt to resolve both of these. It is easier to dispose of the second because it simply is not true. It is an overblown assumption from a paper by Charney and Drazin (1961) and is not even supported by careful reading of their principle reference Ooyama (1958).

The paper by Ooyoma (1958) proves that if a disturbance at very high levels is sufficiently large in vertical and horizontal dimensions (this condition is satisfied by disturbances in the ionosphere), 10 to 15 per cent of its height contour change or wind speed change will be propagated downward as a combined gravity, inertial, and Rossby wave.

Charney and Drazin limited their discussion to smaller disturbances and quoted Ooyama (properly) as giving evidence that smaller disturbances had hardly any effect. The statement concerning downward propagating energy that led off this discussion is for the most part a second hand or third hand quotation (almost a rumor) that has been built up from their assumption.

The paradox concerning energy availability is real enough. There is so little kinetic energy (in the form of $\rho/2\, v^2$) in the ionosphere because of the very low density that if all of its very highest state of excitation were to be transmitted to the 500 mb level, it would not cause a 1 mph wind change. This hard fact has been the rock that sunk many fine and beautiful theories on solar influence on the weather.

We avoid this paradox in a rather unusual manner. We will endeavor to show that no significant energy is required to transmit a disturbance from upper layers to lower layers. We will discuss the possibility that there is sufficient energy in small scale flows at each level to bring about any required motion. Thus, we do not require energy from one level to bring about a change at another level. We need only demonstrate that there is a control mechanism. This approach to the problem actually opens the door to nearly every previously proposed model of transmission of effects from the ionosphere to the troposphere. We will suggest some models of changes that we feel are most appropriate and will explain how we think they develop.

A Model of the Atmosphere

The primary control mechanism that we propose is one that brings about the geostrophic or thermal wind relationship between wind, pressure and temperature. We do not really know what this mechanism is. We do know that in all rotating systems the motion becomes one in which the velocity vector is normal to the principal force vector. The most common popular example these days is the orbital velocity which is primarily perpendicular to the gravitational force vector. Meteorologists and oceanographers are all familiar with this idea in the form of the wind or current being along the lines of constant pressure, i.e., the geostrophic or gradient wind approximations.

In the case of an artificial orbit this condition is brought about by very careful and precise control of thrust rockets. We don't know what causes natural orbits. In meteorology and oceanography we postulate that the geostrophic balance is a result of mixing processes.*
Briefly we say:

1. Geostrophic balance is a result of mixing of air by small scale motions.
2. The mixing attempts to force linear profiles of momentum and density over large areas and depth of the atmosphere.
3. The non-linear property of the equations of motion and continuity are such that the change in the wind profile is not linear.
4. The mixing forces the new profile to be linear again. If the lines of constant zonal wind, lines of constant meridional wind, and lines of constant density are all parallel to the wind vectors, then the linear profiles can have linear changes and the mixing process is no longer needed. Thus, the parallel motion is a preferred motion because any time we are near it we stay in it.
5. If the lines of constant density are parallel to the winds and accelerations are zero, then the winds are geostrophic and the wind shears are thermal winds.
6. Thus, vertical and horizontal mixing bring about thermal winds.

---

*As found in NESCO's report, "The Effects of Internal Waves in the Easterlies on Mesoscale Weather Developments," Interim Report on Contract DA 28-043 AMC-00173(E).

Nearly all oceanographic work and most meteorological work (especially numerical weather prediction) is done under the assumption that the winds are always geostrophic. We will modify this slightly and say the winds strive to be geostrophic and that the mixing process brings this about. We need no further particular reference to the mixing process in this general discussion.

A few manipulations of the equations of motion or an appeal to the laws of conservation of angular momentum lead to a relation between the absolute vorticity in, or circulation of, a mass of air and the area covered by the mass of air.

If the air is of uniform thickness or has a known relation between thickness and area, then the thickness and the vorticity can have a known relationship.

The relation between thickness and vorticity is usually expressed in terms of the "conservation of potential vorticity equation," the primary action of which is summarized as follows:

(a) Decreased thickness results in decreased absolute vorticity which may even lead to anticyclonic relative vorticity.

(b) Increased thickness results in increased absolute vorticity which usually results in cyclonic relative vorticity.

We assume two major physical laws in our study of the atmosphere that follows.

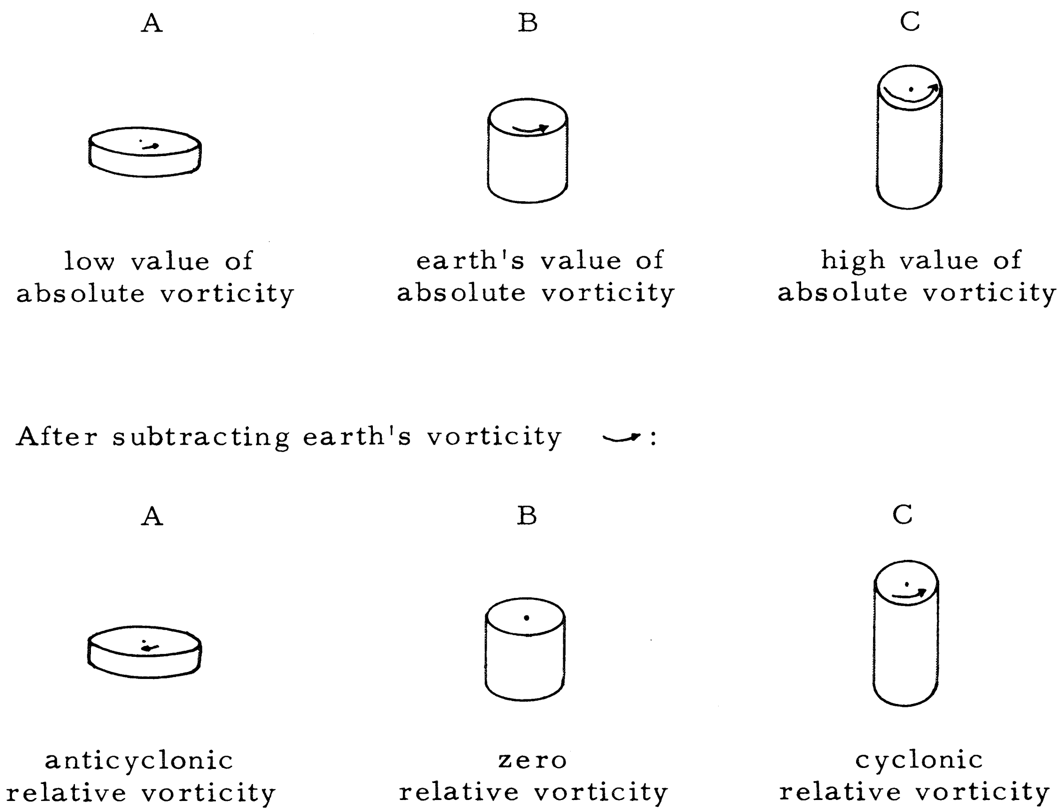

The air in cylinder B is at rest relative to the rotating earth. If the thickness of air is decreased, A results with anticyclonic relative vorticity. If the thickness of air is increased, C results with cyclonic relative vorticity. Absolute vorticities are shown at the top of the figure.

Figure 3

I The thermal wind relationship holds most of the time. The wind shear with height is parallel to the isotherms of virtual temperature with high temperature on the right (in the northern hemisphere; it is on the left in the southern hemisphere).

II The vorticity equation is true. As we follow a particular wafer of fluid, the absolute vorticity varies with the thickness of the wafer. Absolute vorticity is the sum of the wind shear, the angular velocity of the flow, and the earth's vorticity.

In Appendices A and B we have two papers concerned with the consequences of these two assumptions in the study of cross sections normal to a flow. The most significant result is that in a straight flow, the vorticity equation, the thermal wind equation, and the wind at two levels determine the whole cross section. Thus, a prediction at two levels is sufficient to determine a whole flow in the atmosphere following these assumptions. In fact, the wind at one level and the temperature distribution at two levels is sufficient.

There is a slight difference between our use of the geostrophic approximation and the usual approach in numerical weather prediction, where the geostrophic balance is assumed at all times. In our approach we assume that if there are deviations they are kept to a minimum, and the geostrophic balance is preferred. In other words, not only is the geostrophic or gradient approximation observed to be the true state of the winds but there is a quick acting process to being about balance in the atmosphere.

We assume the thermal wind and vorticity conservation hold from the lower ionosphere to the surface. We place the control for our model atmosphere in the lower ionosphere and there is significant modification of the vorticity relationship due to viscous like forces.

The Model Atmosphere to Study Solar Effects on the Weather

The Satellite Environment Handbook (1965) gives a description of the summer and winter conditions in the atmosphere. This description is summarized in Fig. 4. Note that there are three major layers in the lower atmosphere: troposphere, stratosphere, and mesosphere. They are capped by a very stable layer with most of the ionosphere above. The troposphere and mesosphere are relatively unstable and the stratosphere is stable. Also note that in the winter, at the pole, it can be considered that there is no mesosphere and no troposphere.

We make a model of the earth's atmosphere which emphasizes the gross features only and we concentrate on study of the model to emphasize solar effects. We have a system of rules that work best in a stable atmosphere and we have a stable "core" of the atmosphere from the ionosphere to the ground at the winter pole.

We postulate that this core allows solar effects to come from the ionosphere to the surface near the poles.

Very little modeling is required to account for the high pressure built up in the tropics on the 10 mb chart. The short waves heat the tropical stratosphere below the mesosphere. The immediate attempt to follow the thermal wind equation causes increased westerlies and these move downward at a rapid rate.

In the winter core of the stratosphere we can consider circular wafers of air trapped between material surfaces (when no heating occurs they can be considered as insentropic surfaces).

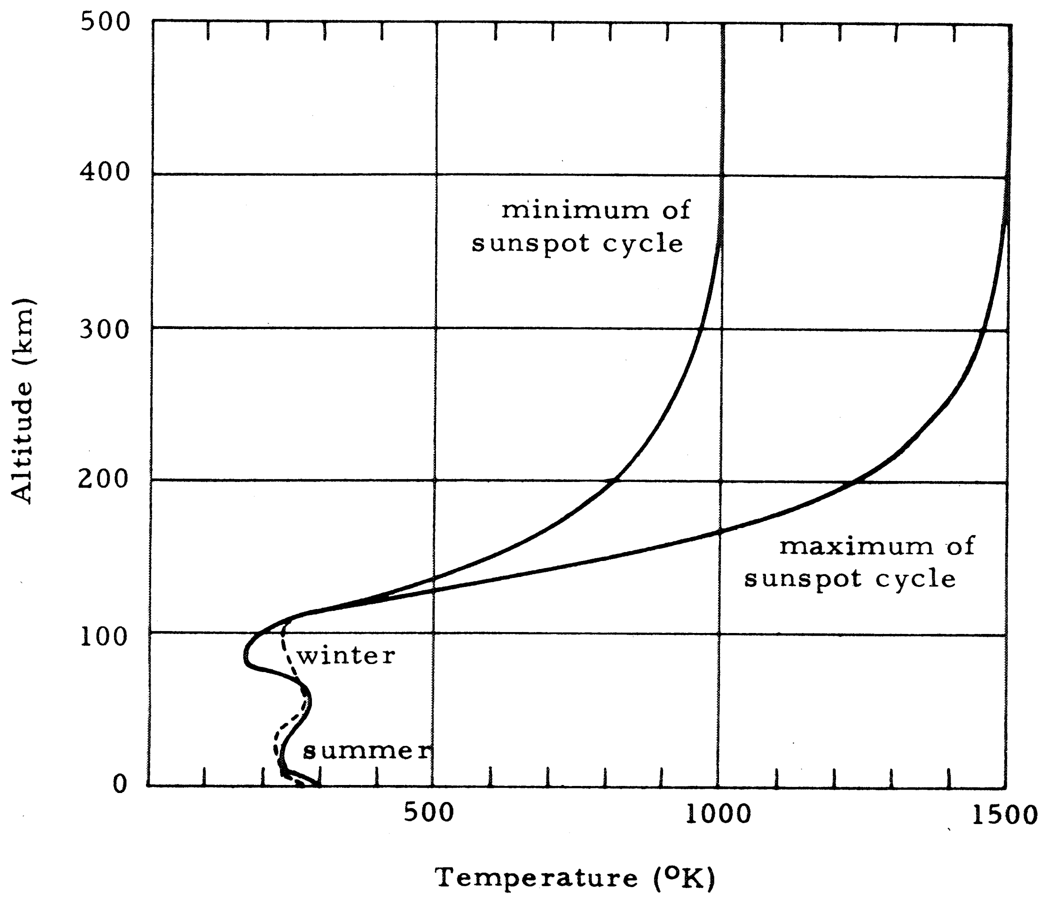

The vertical distribution of temperature showing changes with the season and with the sunspot cycle. Note the stability in the mesospheric region in the wintertime.

Figure 4

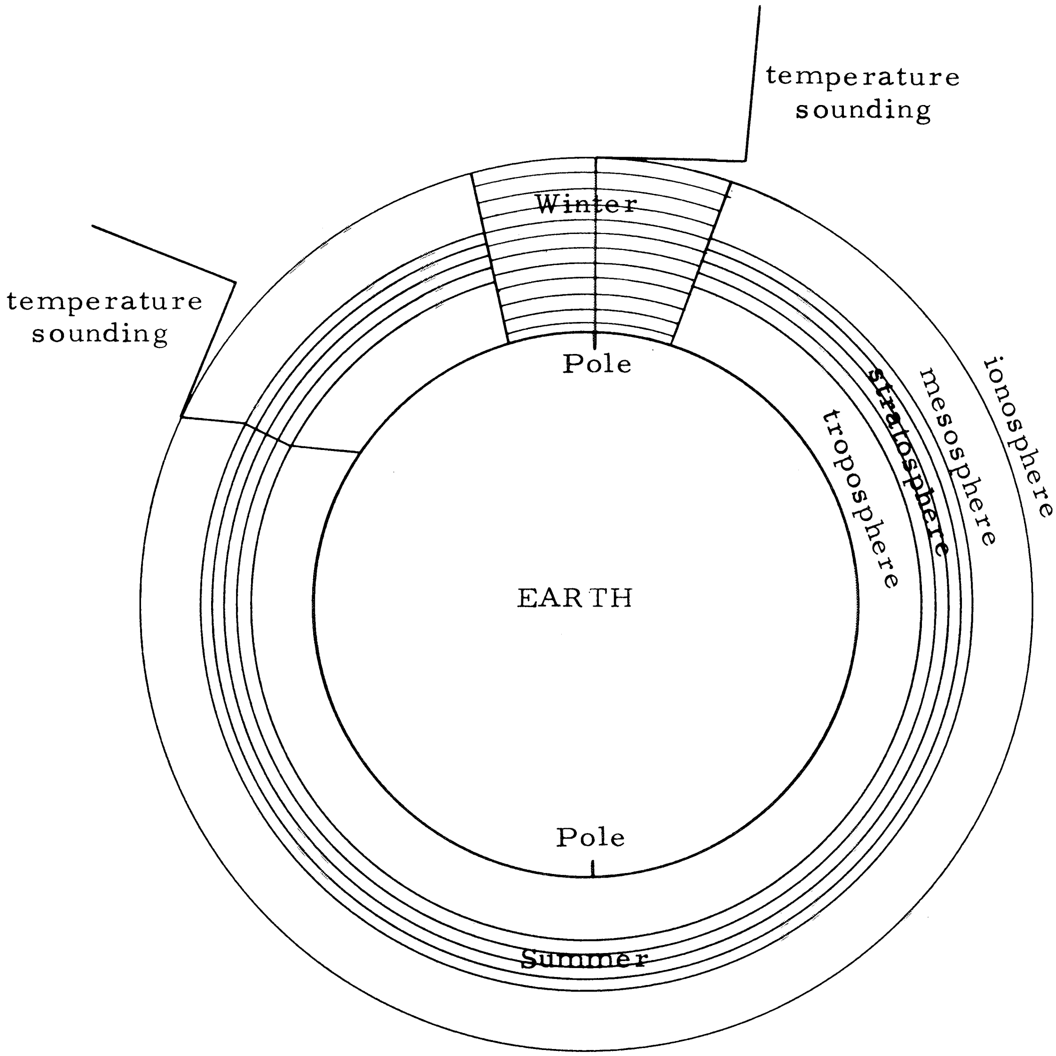

Cross section of the model of the earth's atmosphere which is envisioned as being affected by solar effects.

Figure 5

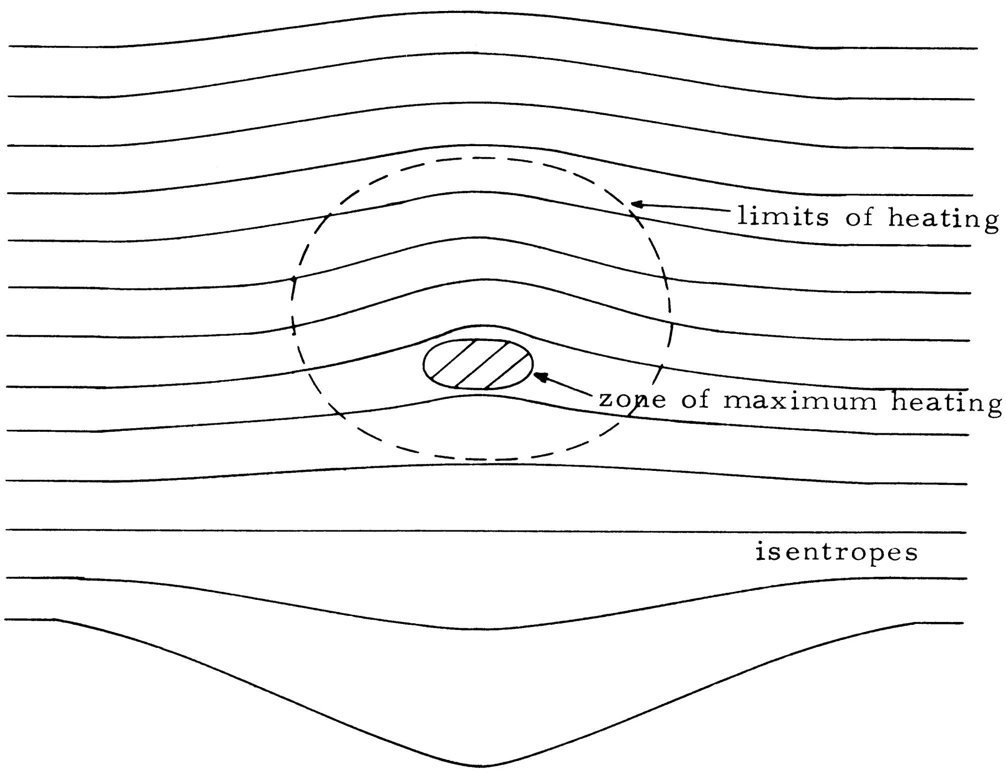

Isentropes showing divergence above the heating and convergence below the heating.

Figure 6

The circular wafers of air conserve absolute angular momentum. The thermal wind equation for the circular wafers calls for increasing angular momentum with altitude for a cold pole and decreasing angular momentum with altitude for a warm pole.

The students of upper air flow are careful to describe localized heating so that there is no disturbance of the system in the lower levels as a result of the relation between temperature and pressure. Thus, the lower limit of a heated surface shows no disturbance of the pressure surface. This is an application of the philosophy that it is much more likely that the upper atmosphere is disturbed by the high energy lower atmosphere than vice versa. Thus, if there is a heated area at some interior point in the stratosphere, the pressure surfaces above it will be raised and those below it will usually be undisturbed. (We do not think this is necessarily the way the atmosphere is heated but it is the way that it is usually said to be heated. We wish to show that even in this case the lower atmosphere is disturbed.) This is now an unbalanced flow and two simultaneous actions take place. The high pressure pushes the air from the poles and the air moves to achieve geostrophic balance. The geostrophic balance for the high pressure at the poles requires added anticyclonic circulation. In order to achieve the added anticyclonic circulation, divergence must take place in the upper levels to result in thinner layers of air. The divergence above the area of heating results in convergence below. The convergence results in cyclonic circulation and rising air. The rising stable air results in a cold zone with low pressure. This low pressure has cyclonic circulation.

This cyclone could utlimately result in an adjustment below it which will give divergence and anticylonic circulation. The values of the circulation, divergence, and temperature depend on the initial values of the heating. Some computations are shown in Section III that give the disturbances under various initial conditions. Note that even though the customary care to prevent low level disturbances due to upper air heating has been used, the disturbances affected the lower levels after all. The initial deviation from geostrophic balance was confined to the upper levels but it caused deviations to be propagated downward and the final disturbance was appreciable in the tropopause. These computations give the expected motion resulting from a sustained heating of the upper atmosphere. In Section II we describe the action of the stratospheric core and the nearby regions of the atmosphere when this heating occurs.

The first result is most striking at 10 mb, and it is the almost immediate appearance of a small region of isallobars of falling pressure over Greenland and rising pressure surrounding it. By 4 to 5 days after the event occurs, there is falling pressure over the pole and over a large area surrounding it. Thus, the cyclonic circulation has increased at 10 mb. There is some evidence that this pressure begins to rise at later times.

The time of falling pressure at 10 mb over the pole corresponds with the time of MacDonald's (1960) increase in cyclonic circulation and Shapiro's and Ward's (1962) increase in the westerlies.

The work of Shapiro and Ward led to the development of the table in Appendix C (p. 13) wherein "predictions" we have made, which were based on their results, and all of the predictions of increased westerlies and ultimate decreased westerlies turned out to be right. Thus we can summarize as follows:

1. There is solar influence on the ionosphere that leads to heating the stable polar core of the stratosphere.
2. There is sufficient energy available in small scale to bring about any large scale motion that a control requires.
3. A model that conserves potential vorticity and includes the atmosphere striving toward geostrophic balance controls the atmosphere so that disturbances can descend.
4. These disturbances call for an action of the stable polar core that has been observed by several workers, including the authors.
5. Thus we offer theoretical and descriptive evidence that solar storms cause weather changes on the earth.

II RESPONSE OF HIGH LEVEL CIRCULATION

A. Relationship Between the Solar Wind and 10 mb Contour Heights

Introduction

The model referred to in Section I requires increased cyclonic activity at 10 mb. This is shown in Figure 6 of this Section. During the last few years attempts have been made to relate cosmic events to weather developments on earth. There are basically two different methods of approach before physical reasoning can be applied.

One method consists in the search of terrestrial data for periodicities that are known to be periods of cosmic events. A large number of papers deal with relations between terrestrial events and the 11-year periodicity of the sunspots. More recently there have been increased numbers of papers that consider the effects of lunar phases and of the rotation of the sun. (Takahashi,1958) is among the few who have investigated the periodic effects the sun may have on our weather induced by the planetary tides of the sun's surface. After solar effects on the earth have been firmly established, Takahashi's ideas may serve as a basis to predict the events on the sun with the goal to foreshadow the solar effects on earth or on spacecraft. Another part of this report was stimulated by his ideas and contributes new facts. (See Appendix D.)

Another method of approach to the study of solar influences on our weather is the comparison of non-periodic time sequences of events on the sun with such sequences of events on the earth. Many years ago such studies led to the prediction of terrestrial magnetic storms. Recently the correlation between the solar wind and the magnetic behavior of the earth has been established (e.g. Snyder and Neugebauer; Snyder, Neugebauer, and Rao, 1963). Using the ΣK_p index for the geomagnetic activity, the correlation between ΣK_p and the speed of the solar wind is linear, or at least it seems to be so.

ΣK_p - Solar Wind Relationship

It seems reasonable to assume that an event on the sun, whose exact nature need not be specified here, produces an emission of electromagnetic waves reaching the earth in eight minutes, and the ejection of particles called the solar wind, which reach the earth after 3-1/2 days, assuming that their speed is near 500 km/sec. We used the graph published by Snyder, Neugebauer, and Rao and applied time corrections of the solar wind data which are due to the different locations of the Mariner II probe with respect to the earth. The solar wind data are presented in such a way that no correction can be applied. Instead we added the (published) correction with inverted sign to the ΣK_p index (which is published broken down into 3-hour periods). The correlation coefficient between the adjusted ΣK_p index and the speed of the solar wind was found to be $r_o = 0.71$ (Snyder, et al. found 0.73 for the unadjusted values).

This coefficient changes as follows when we introduce time lags between the variables:

K_p	forty-eight hours earlier than solar wind	$r_{-48} = 0.37$
K_p	twenty-four hours earlier than solar wind	$r_{-24} = 0.63$
K_p	nine hours earlier than solar wind	$r_{-9} = 0.77$
K_p	twenty-four hours later than solar wind	$r_{+24} = 0.22$

We deduce that on the average the K_p index is 8-10 hours earlier at its maximum than when the solar wind peak reaches the earth. Taking the mean solar wind to be 500 km/sec^{-1}, its maximum is still 1.8×10^8 km(= approx. 1/8 of the distance sun-earth) away when the geomagnetic activity is at its maximum.

The delay of the arrival of the solar wind maximum with respect to the maximum of geomagnetic activity can also be shown in another simple way. The time curve of the solar wind speed is sectioned into periods 25 days long each with a maximum on the 13th day and arranged such that all maxima, and also all other phases, are in line. Then we average them and obtain the curve S. W. in Fig. 1a. We do the same with the ΣK_p index such that the days of each period are identical to those of the solar wind. We obtain the curve K_p of Fig. 1a. The center of the curve was also computed for 3-hourly overlapping intervals and is shown with equal ordinate but enlarged time axis as Fig. 1b. It is seen that the K_p maximum is approximately 0.4 day earlier than the solar wind maximum.

The other features of both curves can be interpreted in at least two days. One can either conclude that a maximum is preceded and followed by abnormally low values of both S. W. and K_p, or that the phenomenon is periodic with a wave length of approximately seven days. It is difficult to decide without further computations which of

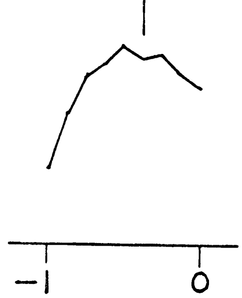

Fig. 1b 3-hourly plot of K_p

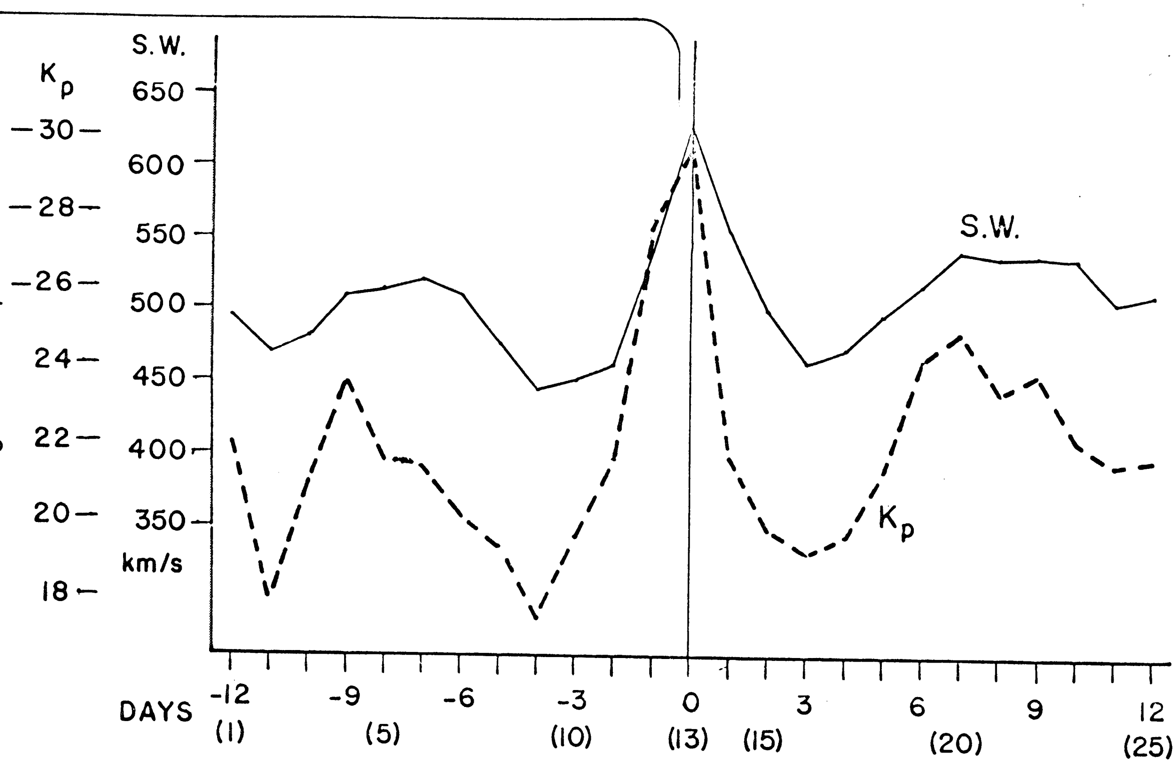

Fig. 1a Mean conditions of the solar wind and the K_p index before (minus) and after (plus) maxima of the solar wind speed

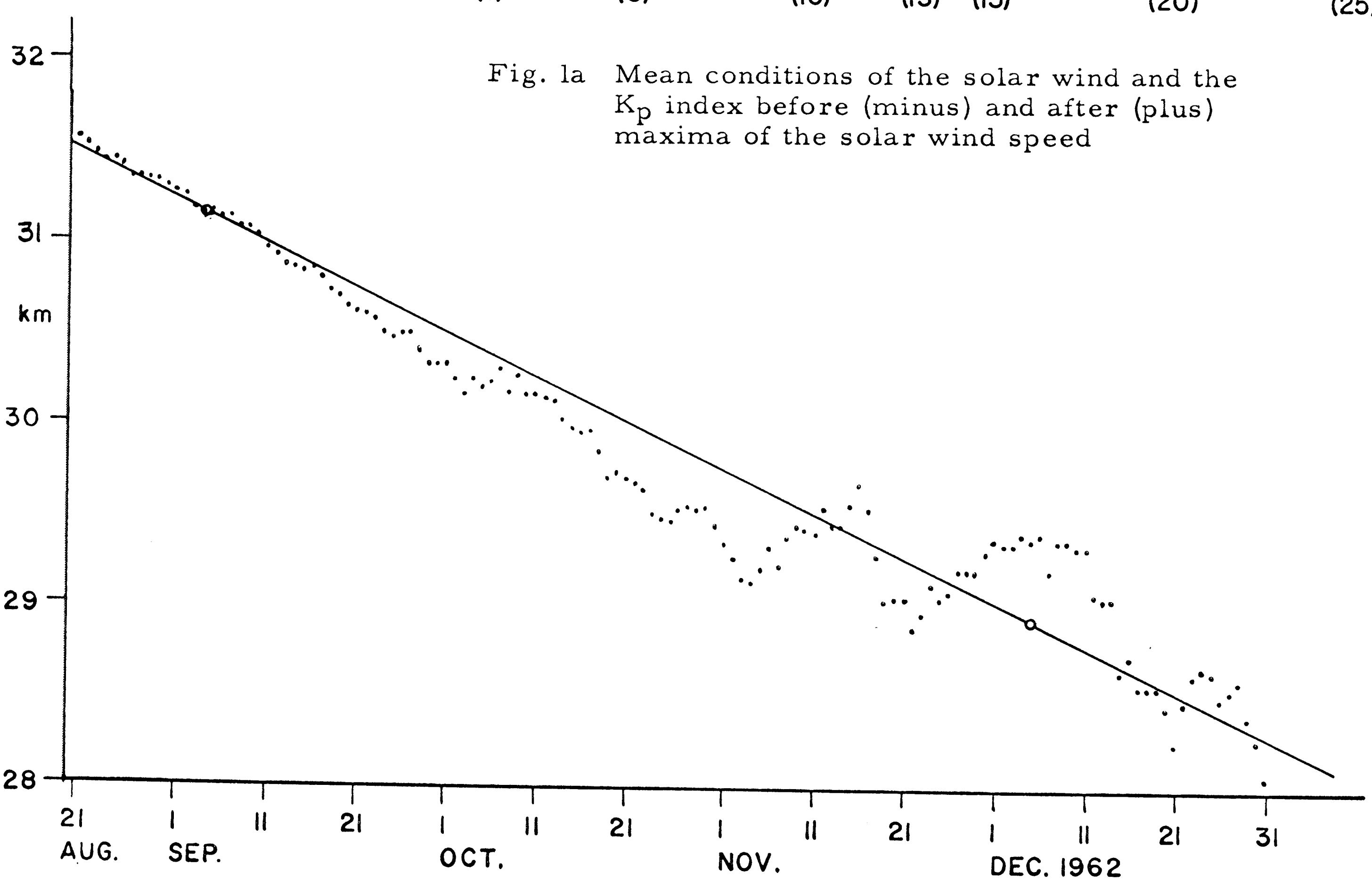

Fig. 2 10 mb contour height at the North Pole these, or perhaps even a third explanation, applies. Tentatively, one can compute from the Mariner II data a periodicity to be 6.7 ± 2.4 days.

Whatever the explanation may be, we have to deal with the fact that at least during the time Mariner II was relaying data, the average S.W. maximum and the average K_p maximum were preceded and followed by subnormal values. In particular, a marked minimum was found on the 3rd and/or 4th day before the maximum in 12 out of 15 cases, and on the 3rd and/or 4th day after the maximum in 11 out of 15.

The minimum preceding the K_p maximum has been described before by Wurlitzer (1958) who concludes that it is an essential part of the geophysical mechanism which culminates in the maximum. Data presented below support his hypothesis.

Although the second minimum is less conspicuous than the first, it does not preclude its possible importance.

ΣK_p Index and 10 mb Charts

The previous paragraphs showed that solar wind data and K_p index can be used almost interchangeably. Our studies began with the use of the solar wind data. However, it soon became obvious that in order to obtain conclusive results, it would be necessary to extend the studies into periods for which solar wind measurements are available. Consequently, the K_p index was taken as the indicator for the processes to be investigated.

Also the K_p data are more representative than the Mariner data since they stem from several observation sources which check each other.

Another reason to replace the S.W. with the ΣK_p data is the possibility to extend results obtained for the period of the Mariner II flight into other periods of time. The result described below in connection with a recent paper by Labitzke (1965) gives rise to the hope that an extension of these studies to other years may shed a new - perhaps the deciding - light on the nature of the 26-month periodicity.

Approach

The mere scanning of the 10 mb charts (Scherhag, et. al.) showed us the effect discussed below. There were, however, considerable difficulties to isolate it from the normal seasonal variations. Many attempts were made, only two of which will be presented here.

Seven cases were selected out of seventeen. The criterion was a sudden, strong rise of the K_p index rather than the occurrence of the maximum. The seven days are (date of S.W. max. in parentheses): Aug. 29 (S.W. unknown), Sept. 3 (3), Sept. 12(13), Oct. 1(1), Oct. 8 (9), Nov. 15 (16), and Dec. 17 (20). These days are called K, correspondingly the days before K-1, K-2, etc., and the days after K, K+1, K+2, etc.

The largest rise lies in each case between days K-1 and K. It should be mentioned, however, that the days can also be combined in slightly different ways. By shifting the time series for some very few days we can obtain that either all maxima or all preceding minima are in phase. Table 1 shows the different outcome of the three methods.

The heights of the 10 mb surface were read at 78 grid points for the days K-7 through K+7 and tabulated. The grid points lie along the meridians 0°, 30W, 60W, 90W, 120W, 150W, 180°, 135E, 90E, and 45E, and are spaced from 10°N to the North Pole. (See Figure 3.)

TABLE 1

Average K_p's Obtained Through Different Arrangements

I. Arranged for the strongest ascent of K_p (used in this Section)

K-7							K							K+7
20	20	21	21	18	18	17	33	30	25	24	21	20	21	25

II. Arranged for maximum K_p (as used on page II-31)

20	20	24	18	16	21	24	34	28	22	23	17	21	23	25

III. Arranged for minimum K_p (not used as yet)

20	18	19	16	13	25	29	32	29	24	22	17	22	23	23

There would be no differences between the three arrangements if the time difference from the minimum to the maximum were always the same and if the timing of the strongest rise between them were always equal.

It is contended that at the present stage of research a change from one arrangement to another would affect the results only in a negligible way. With increasing refinement of the research methods, re-arrangement may become in the future an essential tool in the study of the physical causes of the effects in the following paragraphs.

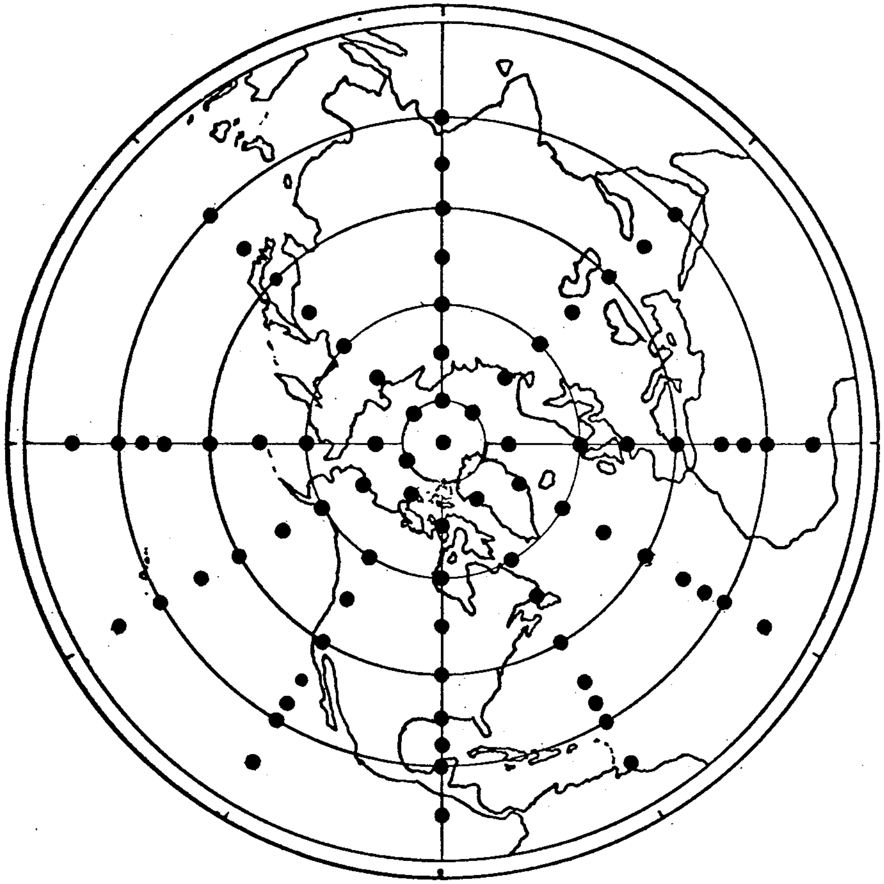

Fig. 3 The grid points

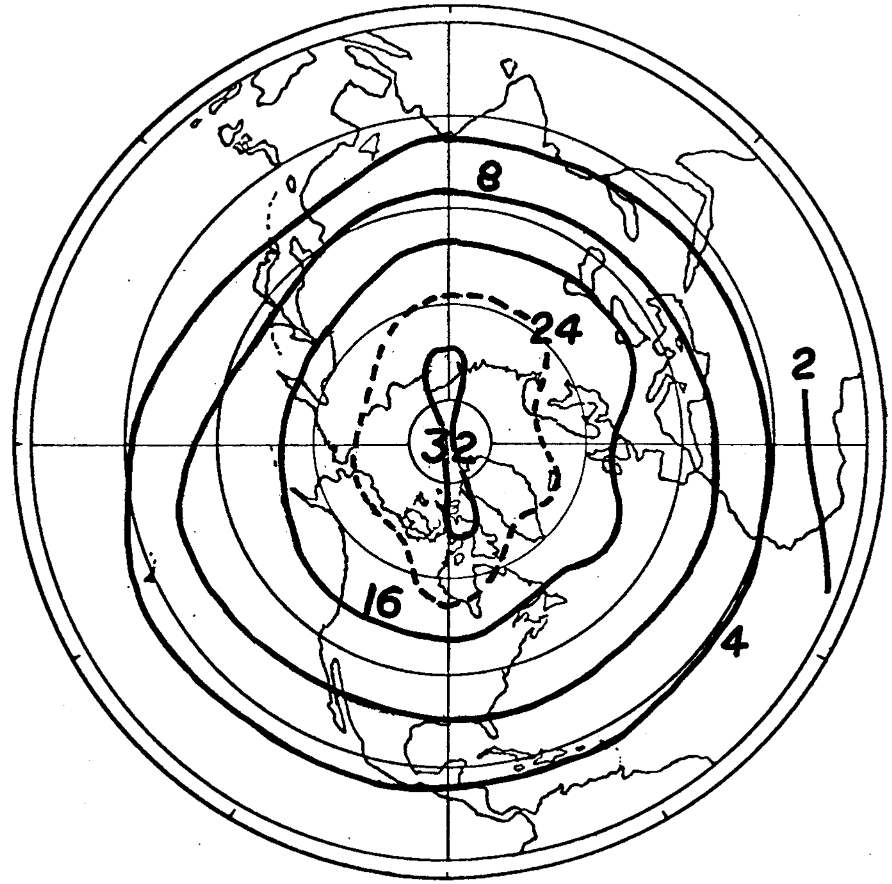

Fig. 4 Difference between the highest and lowest 10 mb contour height (in hundreds of meters)

The listed height values show a strong decrease with time. The North Pole, e.g., had on August 21 a 10 mb height of 31420 meters, which dropped to 28240 meters on December 31, 1962. (See Fig. 2.) It was assumed in the first investigation to be described here that the decrease of contour height is linear. The slope was found through the mean values of all days of the first two cases and of all days of the last two cases. Figure 2 shows for one grid point, the North Pole, the actual values, the two mentioned means, and the assumed slope for linear seasonal adjustment. The line of the Figure 2 indicates an adjustment of 2590 meters in 91 days equal to 28.5 meters per day. In the computations of the height at this grid point the values for the days K will be taken as given, the values for K+1 (K-1) will be increased (decreased) by 28.5, for K+2 (K-2) by 57.0, etc. The amount of adjustment changes from grid point to grid point, but does not change with time.

Figure 2 shows another obvious difficulty. The amount of interdiurnal variation increases drastically with time. The accuracy of the maps decreases in the same degree so that the large variations at the end of the year are neither more significant nor better established than the small ones in summer. This is also true for the changes of variability from latitude to latitude. Figure 4 shows, as an illustration of this fact, the difference between the largest and the smallest grid point values used in the computations of this paper. The spacing of the lines of Figure 4 is logarithmic (except the 2400 meter line).

The considerable time and space changes in interdiurnal variability are a severe handicap. In order to make differences of grid point data comparable, it would be necessary to apply a time-space system of corrections which would require the use of an electronic computer. The present stage of the work does not warrant the amount of work necessary for punching and programming. It is recommended that this problem be solved in future work by grouping cases of the same month from different years rather than different months of the same year.

Method A

In this stage of the project only the sign of differences with time was considered, i.e., all differences were set equal to -1, 0, or +1. In the following they are called "normalized." The maps are based on the arithmetic sum of these "normalized differences (changes)" for each grid point. It is pointed out that seven cases were considered so that the absolute maximum of such a sum can be not more than $|7|$. "Plus" means rises of contour height during the time period specified at the bottom of the charts.

Results of Method A

The strongest changes of the 10 mb contour heights, after freeing them from the seasonal trend, are found day K-1 to day K+3 (Fig. 6) and from K to K+3 (Fig. 10). These are the only parts of the time sequence where the maximum values of +7 and -7 are found. The seasonally-adjusted contour height dropped in all seven cases over

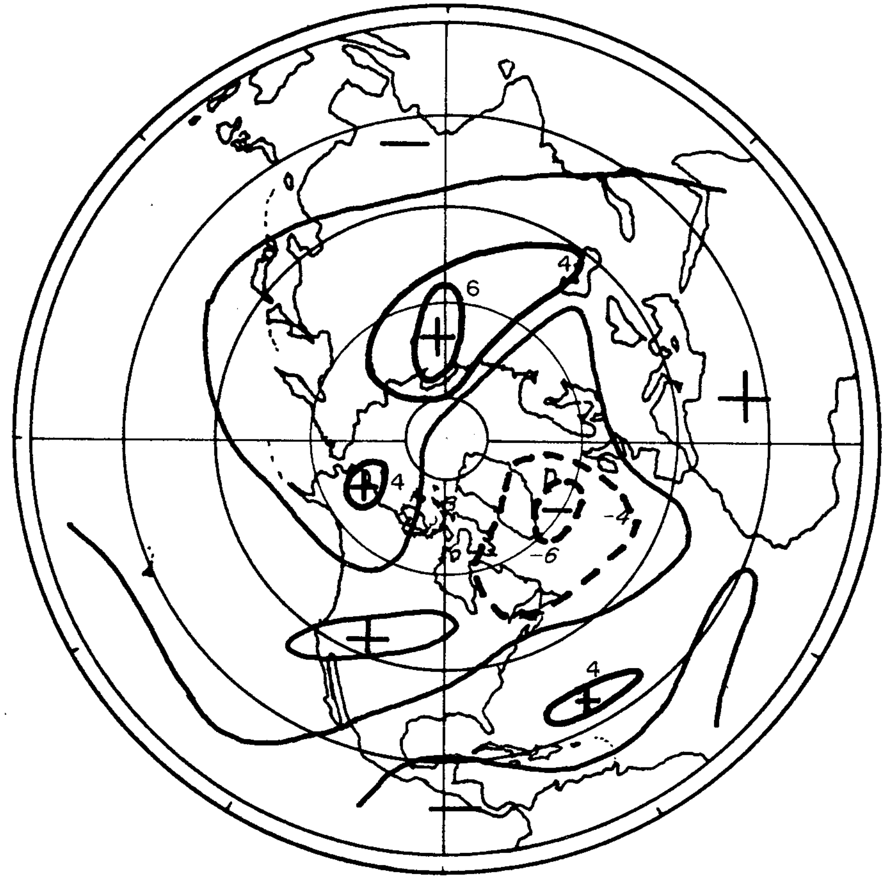

SUM OF THE "NORMALIZED" CHANGES OF THE 10MB HEIGHT (See text)

FIG. 5

From day K-4 to day K-1

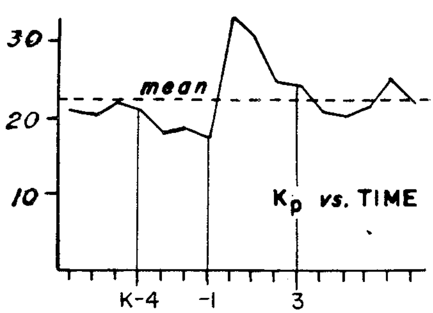

FIG. 6

From day K-1 to day K+3

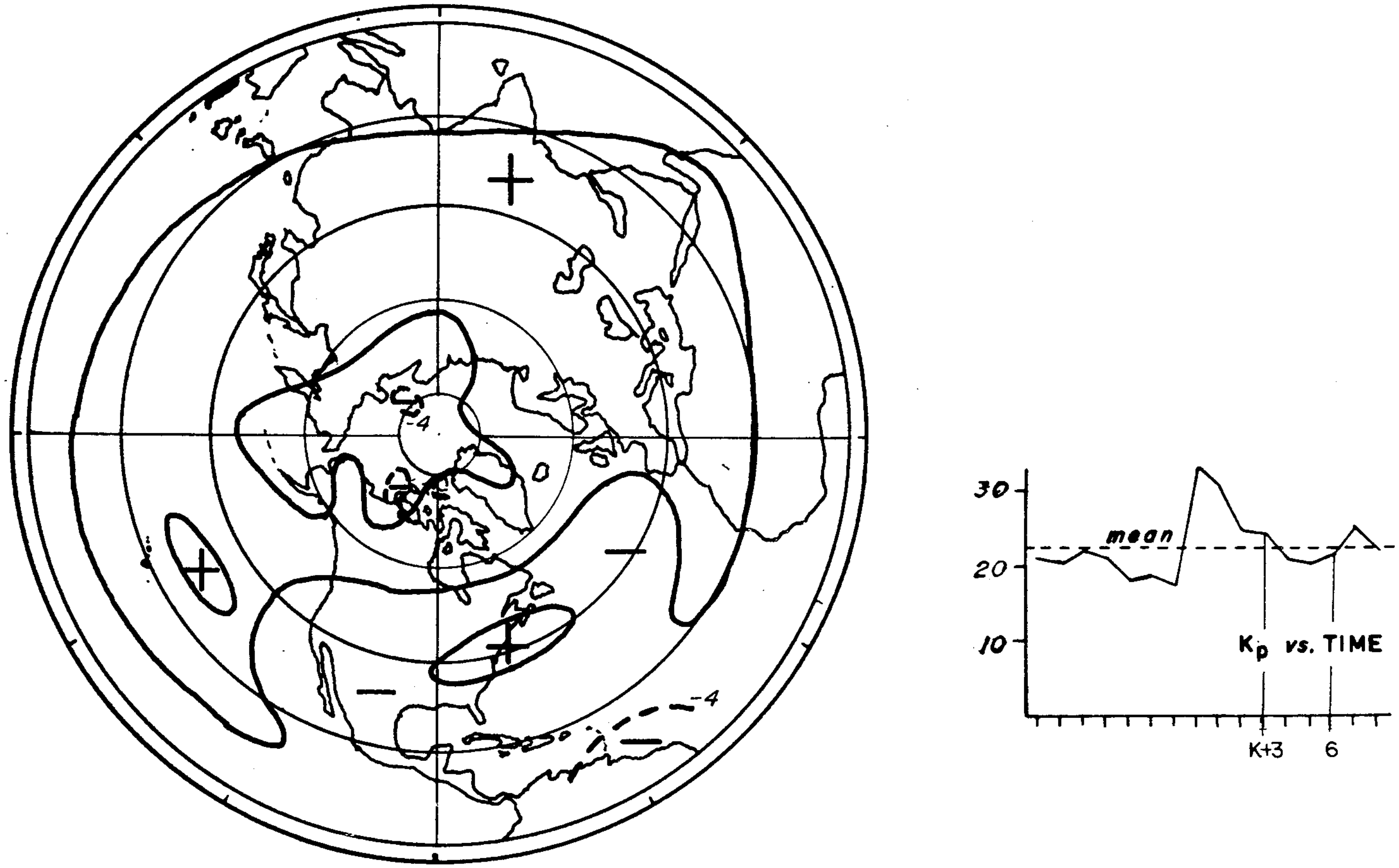

SUM OF THE "NORMALIZED" CHANGES OF THE 10MB HEIGHT (See text)

FIG. 7

From day K+3 to day K+6

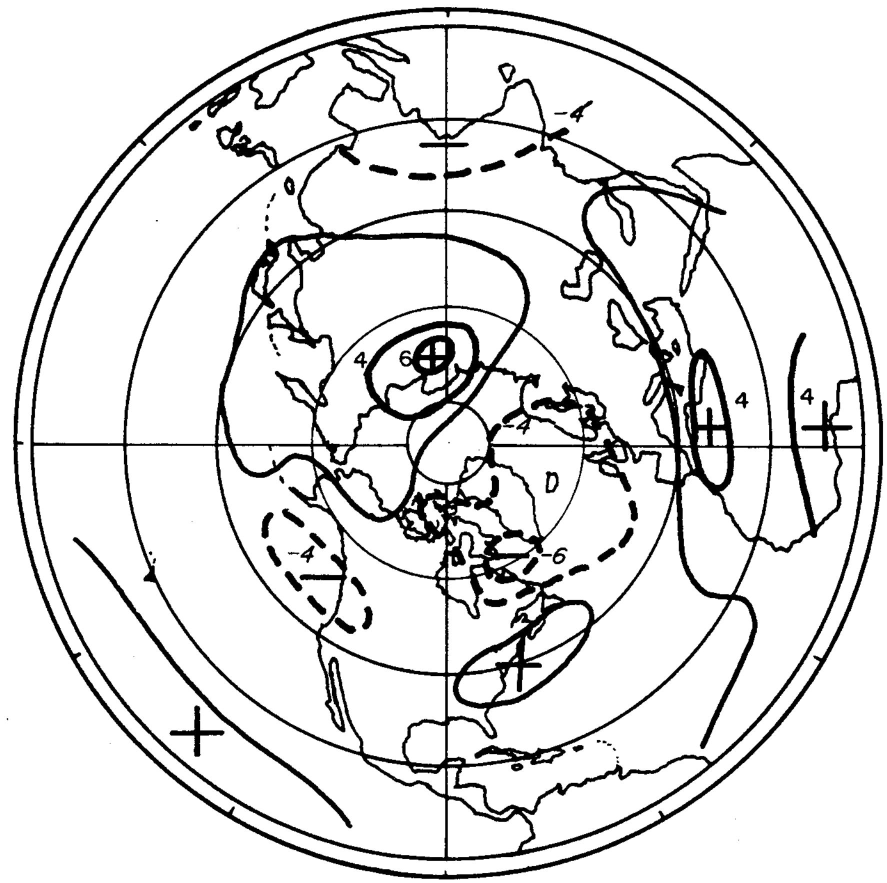

SUM OF THE "NORMALIZED" CHANGES OF THE 10MB HEIGHT (See text)

FIG. 8

From day K−2 to day K+1

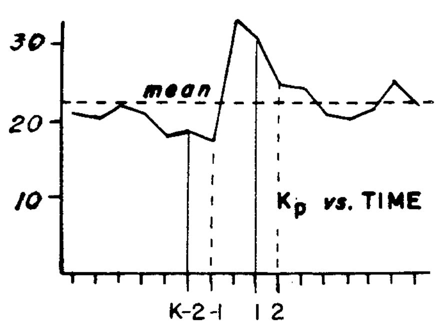

FIG. 9

From day K−1 to day K+2

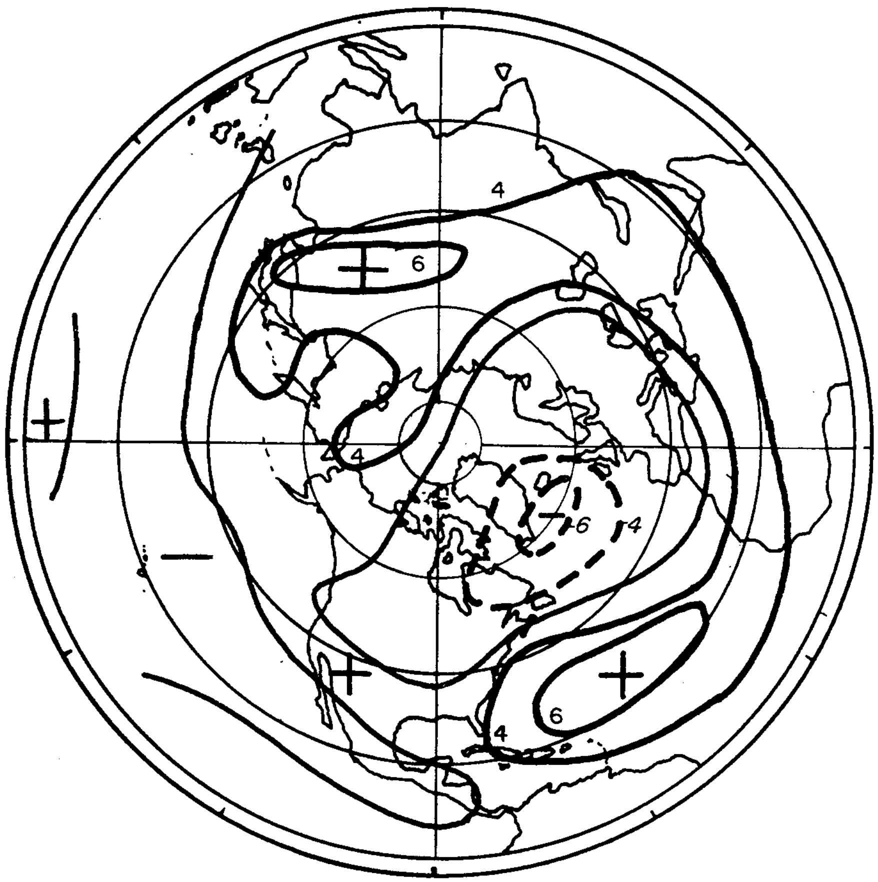

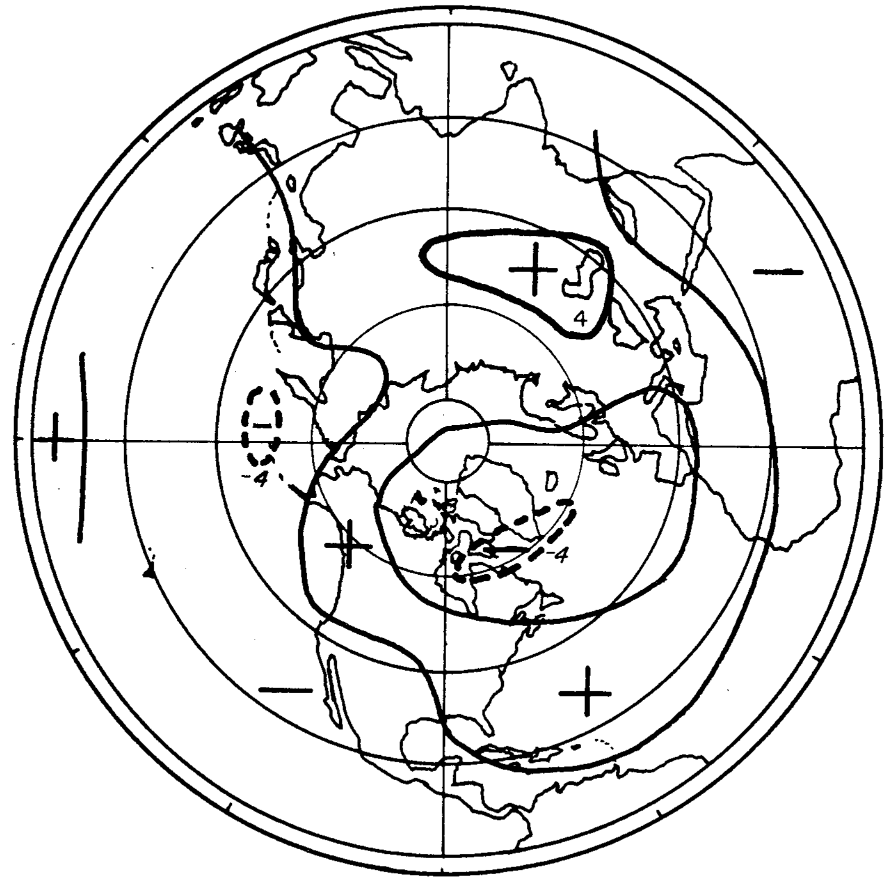

SUM OF THE "NORMALIZED" CHANGES OF THE 10MB HEIGHT (See text)

FIG. 10

From day K to day K+3

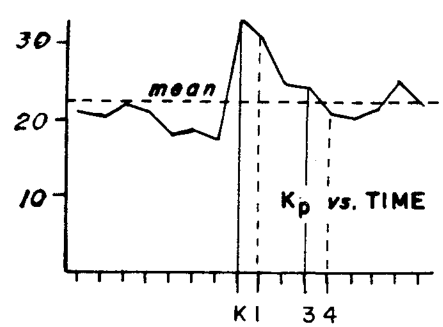

FIG. 11

From day K+1 to day K+4

the northern Atlantic in the time from immediately before the strong rise of the K_p index to three days after it. At the same time it increased in a ring around it with maxima near Bermuda, over the Mediterranean Sea over Japan, and over northern Siberia-Alaska.

The location where the 10 mb contour height drops is approximately the same which can be designated to be the center around which the "explosive warmings" of the stratosphere seem to circulate (Labitzke, 1965).

Figures 5 through 7 show the sums of normalized increases or decreases of the season-corrected contour heights during the indicated interval. The numbers do not exceed 4 for the time before the rise of K_p, i.e., the strongest effect - always in seven cases -, was: 5 rises, 1 fall, 1 even, 5-1+0 = 4. This picture changes when we proceed in time. With the rise of the K_p index (Insets of Figs. 5-9) the contour heights begin to rise and to fall more uniformly, and the lines labeled "6" comprise several "7"-points, i.e., points where the height change has had the same sign in all seven cases. After this the extreme values rapidly give way to statistically insignificant numbers (Fig. 7).

The Figures 8-11 break the critical interval down in order to make it more accurate. Comparison of the maps shows clearly that the peak of the atmospheric development is reached on the third day after the K_p maximum. At that time the depression discussed above is surrounded by a ring where the pressure had been rising through the previous days. If these changes of the pressure field would be cancelled by changes of the opposite sign, the subsequent change charts would be reversals of Figs. 6 and 10. Since this is not the case, we conclude that the change of pressure pattern has a certain persistence. This is similar to many other meteorological phenomena, especially to the explosive warmings, which begin with remarkable changes, are rapidly fully developed, and then diminish gradually in such a way that one cannot say when they have come to an end.

The amount of the contour height changes during the K_p maximum cannot be fully assessed because seven cases spread over four months are not sufficient. A rough estimate gives us as an order of magnitude 70 to 100 meters contour height change near the polar circle, counted from day K or K-1 to K+3, and freed from the seasonal trend. For the Tropic of Cancer we arrive at approximately half that amount.

Table 2 lists the contour heights averaged over the seven cases for two extreme grid points.

TABLE 2

Mean Contour Heights 10 mb at Selected Grid Points (in meters)

A: original; B: freed from seasonal trend

	K-4	K-3	K-2	K-1	K	K+1	K+2	K+3	K+4
					60N 30W				
A	30950	30984	30942	30914	30855	30835	30727	30722	30701
B	30900	30954	30922	30914	30875	30865	30777	30792	30781
					25N 60W				
A	31152	31148	31155	31121	31105	31120	31137	31142	31128
B	31142	31138	31155	31121	31105	31130	31147	31162	31148

One would be tempted to explain the belt of pressure rise through an intensification of the high pressure belt which separates the east from the west winds for most of the year at the 10 mb level. Figure 12 shows that such an interpretation would not be correct. The high pressure belt is non-existent in mid-summer because the highest pressure is at the North Pole at that time. With the advancing season it forms as soon as the polar vortex exists. With the increase of the latter, the belt moves further southward towards, and perhaps sometimes beyond, the equator. Figure 12 indicates by H's where the high pressure belt intersected the 50th meridian west on the seven days called "K". The dashed line is supposed to insinuate the approximate linear drop in latitude.

The same figure shows also as dots the latitudes near $50^{\circ}W$ at which the strongest pressure rise occurred while K_p had its maximum. The location where this unseasonal rise occurs does not obviously change as the high pressure belt does. Hence, the effects on the winds can be an enhancement as well as a slowing-down, depending on the considered latitude and the position of the highest pressure. In other words, the effect of the atmospheric changes connected with a maximum of the K_p index and of the solar wind is <u>primarily not a change of the kinetic energy of the air.</u> Such changes do occur, but only as a secondary effect. The change of atmospheric pressure, however, is a primary effect.

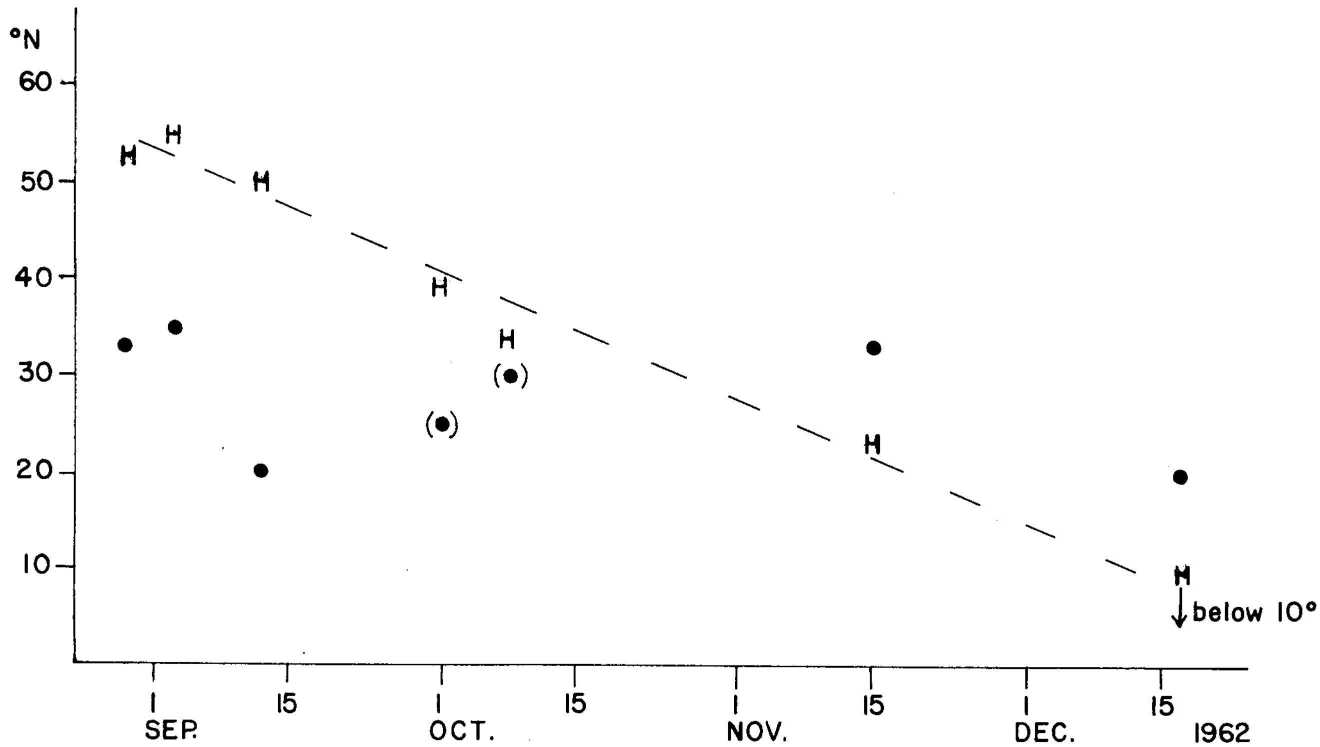

Fig. 12 Geographic latitude spread at 50°W longitude where the pressure rise after K_p maximum was strongest (heavy dots; dots in parenthesis mean that the <u>center</u> of the pressure rise area was at a different <u>latitude</u> and longitude.) The same for the high pressure belt (H).

Method B

A time difference chart may derive its features from the first of the days on which it is based, from the second of them, or from both. The change may occur in any portion of the time interval; and this portion is not known. Hence, attempts should be made to change from differences between two days to absolute values of particular days. But again we face the considerable seasonal and local changes as obstacles that tend to veil the effects we want to uncover. The local extremes of one day, December 17, 1962, e.g., were 31,150 and 28,160 meters with a difference of 2990 meters. The time extremes of one grid point, the North Pole, were for the K day 31,340 meters on August 29, and 28,560 on December 17, having a difference of 2780 meters. These differences compare with the previously mentioned 70-100 meters which is the order of magnitude of pressure height changes related to K_p extremes.

It becomes obvious from the foregoing that the computation of mean contour heights for certain K-days would mask the subtle effects we are after, in the "noise" of the data. Only anomalies can be expected to show the desired effects. It was decided that the linear interpolation between values at the beginning and at the end of the period was good enough for the computation of differences over a short period of time (Method A), but not for the computation of anomalies. Twenty-five running means were chosen to be the basis for anomalies. 13,104 contour heights had to be extracted from the 10 mb charts to compute the running means necessary to arrive at a relatively crude composite of only seven cases.

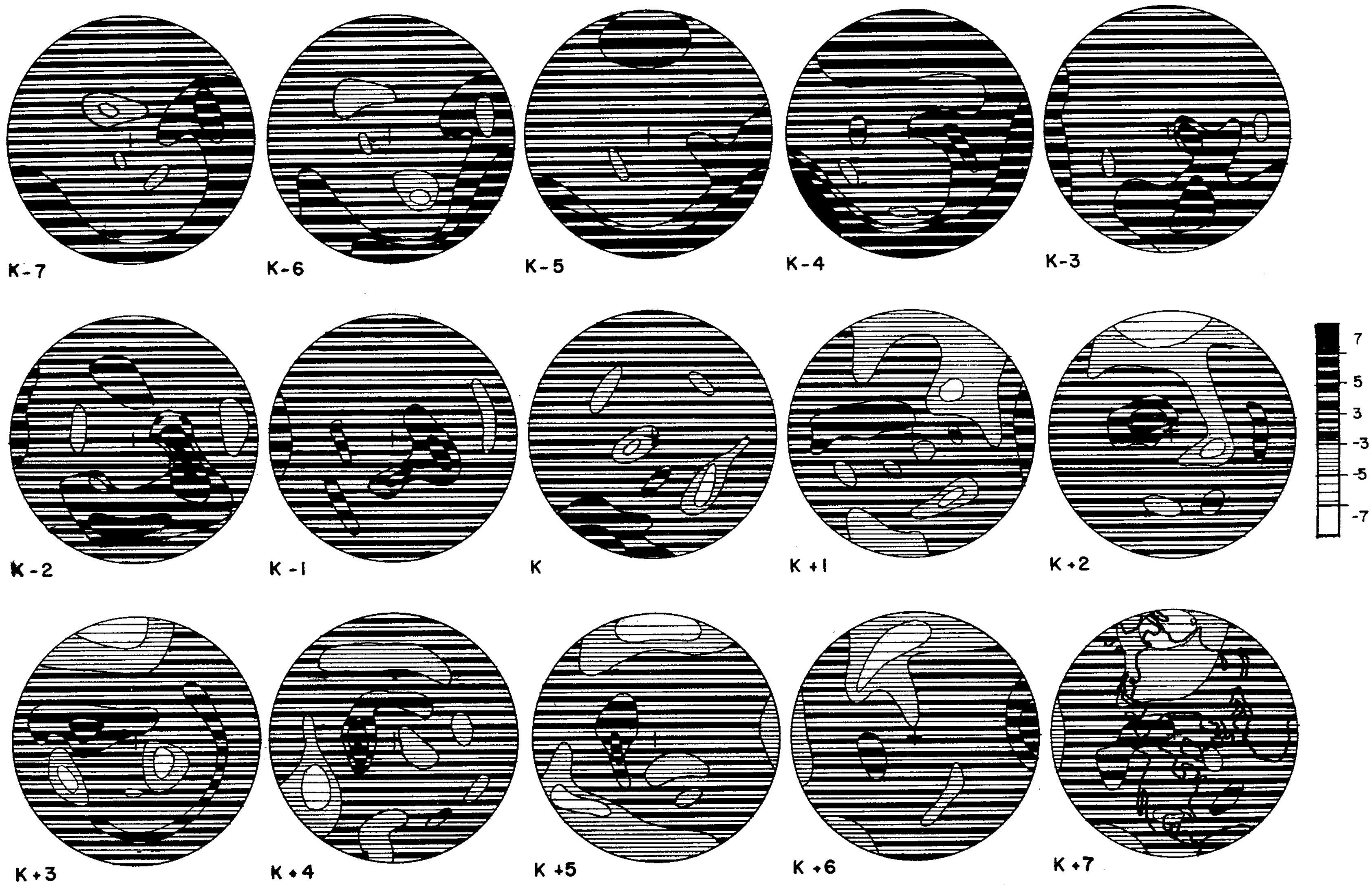

FIGURE 13 SUM OF "NORMALIZED CONTOUR ANOMALIES" OF THE 10MB LEVEL FOR THE NORTHERN HEMISPHERE.
(Chart K+7 shows land outlines)

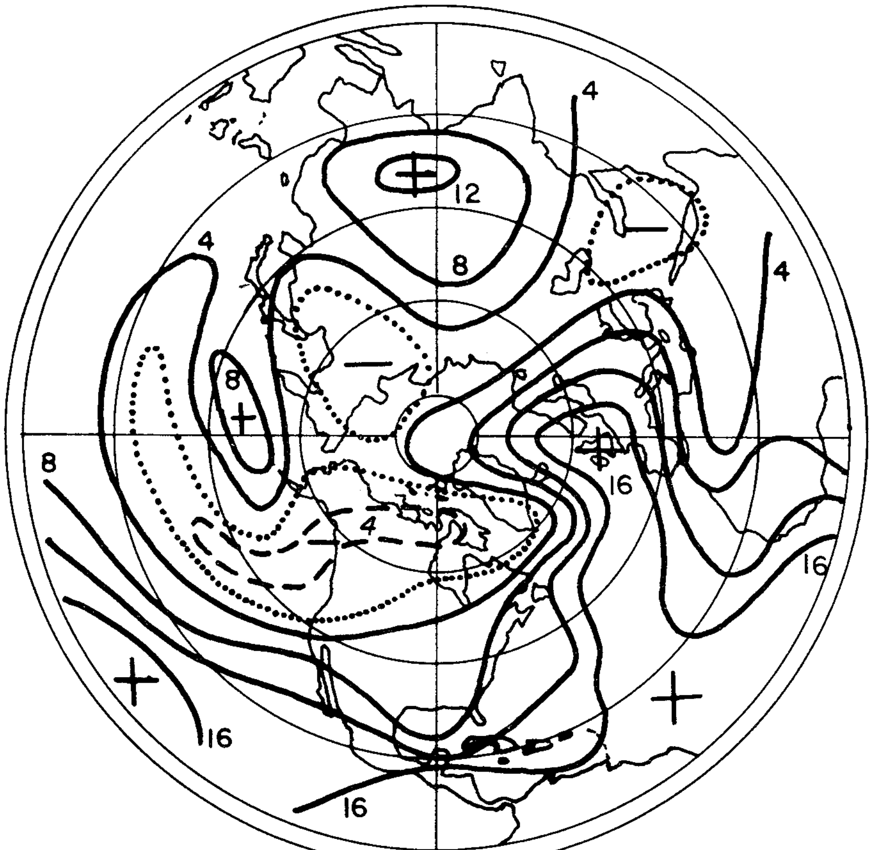

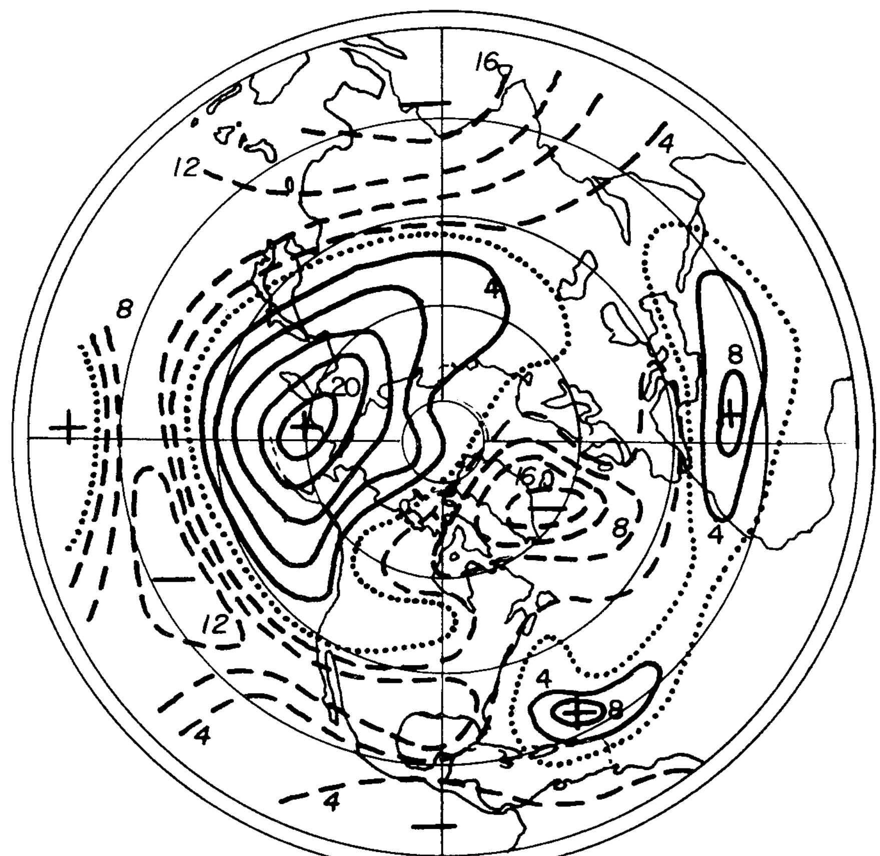

FOUR DAY SUMS OF "NORMALIZED CONTOUR ANOMALIES" OF THE 10 MB LEVEL

FIG. 14

DAYS K-5 THROUGH K-2

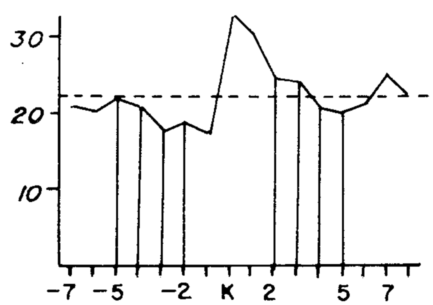

FIG. 15

DAYS K+2 THROUGH K+5

the days K-5 through K-2. Figure 15 does the same for K+2 through K+5. The small diagram below the figures presents - as before - the variation of ΣK_p index with time. The days from which the sums were computed are designated by vertical lines. It is remarkable that the area of negative anomalies in Figure 14 is much smaller than the area of positive ones. This makes us conclude that the influence of the solar event has already influenced our atmosphere before it becomes manifest in the magnetograms, and possibly even before it becomes visible on the solar disk. Figure 16 shows the time variation of the ΣK_p index, averaged over the seven cases, together with the average "normalized contour anomaly" of all grid points. (For better comparability the scale of the latter has been inverted.) It is quite apparent that the effect of the solar event on the earth begins before it shows up in the K_p index (or in the solar wind).

The change from the time before to the time after the solar event is presented as one chart in Fig. 17. For more legibility the lines are spaced at double the increments in Figs. 14 and 15. Without much imagination the following scheme becomes evident.

There is a center of positive anomalies near 65N 180 long. surrounded by a ring of negative anomalies stretching from the north Atlantic through the U.S., south of Hawaii to northern India and back to the north Atlantic. There is a center of negative anomaly on this ring near 57N 30W. This is surrounded by a circle of positive - or diminished negative - anomalies which goes through the positive center near Alaska, central Russia, west Africa, central Atlantic, and extreme western Canada. Figure 16 contains these two circles which

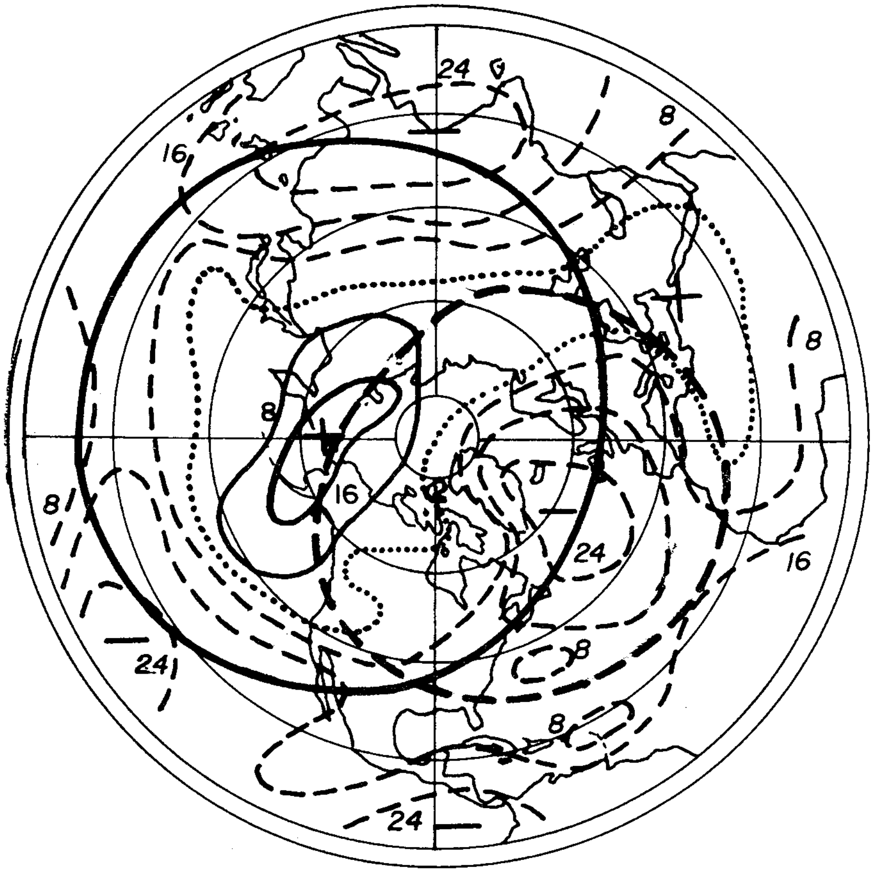

FIG.17 DIFFERENCE OF FIGURES 14 AND 15

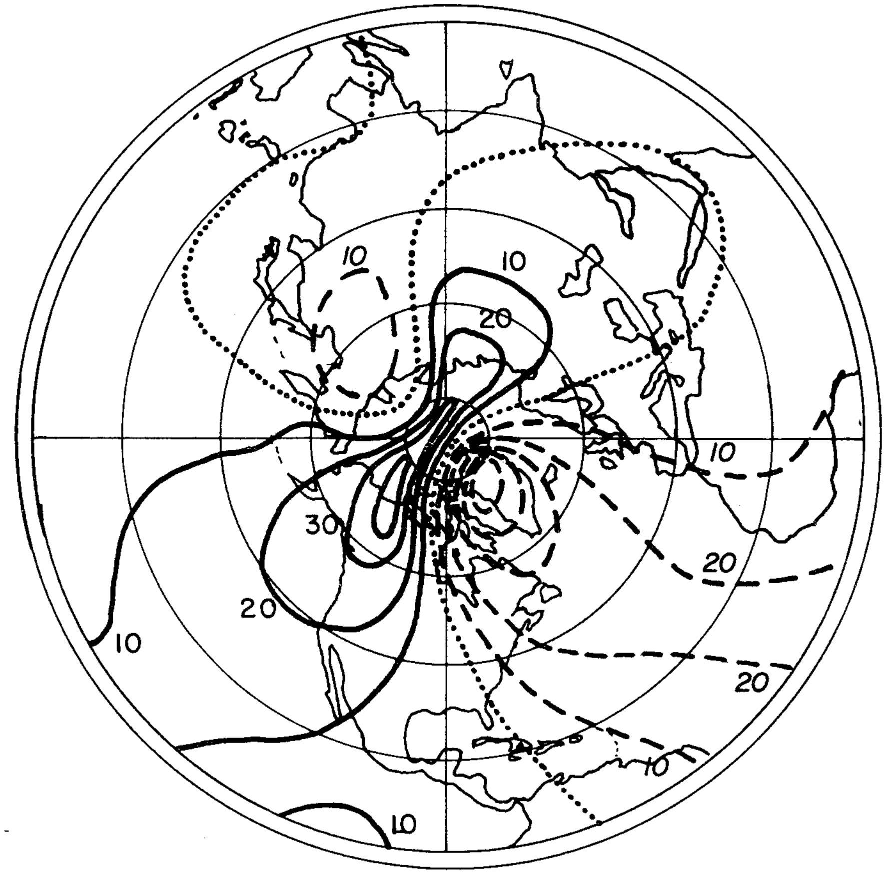

FIG. 18 GEOMAGNETIC DECLINATION

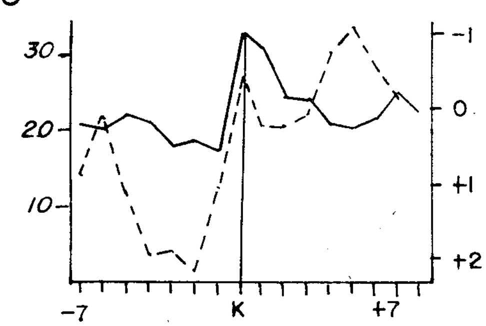

FIG. 16 K_p INDEX (——) AND MEAN DAILY ANOMALY (- - - -) vs. TIME to be compared with the K_p index. This is sufficient to group the cases for seasons so that the very disturbing change of variability during the course of the year would be eliminated, and "normalized anomalies" could be replaced by actual contour heights. Relating the contour heights of all eight years with the K_p index would enable us to assess quantitatively the response of the atmosphere to solar events.

Of course, after this has been done, the study should be extended to other, mostly lower, layers of the atmosphere (see also Part B of this section, on relations between cloud patterns and solar events). The extended study of the 10 mb level should precede (or parallel) that of other levels.

B. Satellite Cloud Features and Solar Events

In the course of the last year three attempts have been made by NESCO to relate cloud features, as they are seen by weather satellites, to the solar wind or to the K_p index. Two of them were inconclusive while the third one was a surprising success.

Before we describe the successful investigation it is appropriate to discuss the reasons why the previous attempts had no positive results. The philosophy was originally to combine as many pictures as possible for few days that have some time relationship to solar events. In order to draw conclusions it was necessary to have at least two different time relations. Expressed in the terms of Section II-A (Relationship Between the Solar Wind and 10 mb Contour Heights), we strived to have optimal TIROS coverage for a day K+i and a day K+j, $|i-j| > 2$. The first investigations aimed at the amount of clouds, the second at cloud shapes and patterns. Both studies suffered from the impossibility to have cloud pictures for the same large areas for two days or more, so that differences in the pictures could be ascribed to either solar effects or to local influences. Also, the number of usable days was too small to separate these two types of effects from synoptic developments originating from terrestrial dynamics.

The first of the investigations of TIROS pictures was part of a study in which, for the period August 29-September 12, 1961, as many atmospheric parameters as possible were compared. (See also Appendix C.) The second of the investigations was made after the work with the 10 mb data had revealed that a K_p maximum is likely to be in the middle between two different weather patterns. The selected event was supposed to be in the time when Mariner II made its measurements of the solar wind, i.e., between August 30 and December 30, 1962. It was not possible to find a single pair of suitable days because the probability is too small that the same large regions have a good TIROS coverage on two days which are typical for certain phases of a solar event, and in a certain part of a certain year.

After this had been recognized the conditions were relaxed. A search was made for days from four days before to four days after any K_p maximum when a sizable part of the area 10-30°N 70-100°W was viewed by a weather satellite. Seventy such days were investigated. They are distributed with respect to month and K_p index as follows. (See Table 4.)

TABLE 4

Distribution of Selected Days With TIROS Coverage of the Area 10-30°N 70-100°W

	Sum	K-4	K-3	K-2	K-1	K	K+1	K+2	K+3	K+4	b	a
Jan	3				1		1	1			1	2
Feb	8						2	1	3	2	0	6
Mar	19	2	3	2	3	2	2		2	3	8	4
Apr	8				1	3	1	2	1		1	4
May	4		1	1	1	1					3	0
June	4			1		1		1	1		1	2
July	2						1		1		0	2
Aug	11	1	2	2	1	1	1		2	1	5	3
Sept	18	1	1	2	2	3	2	1	4	2	5	7
Oct	2					1				1	0	1
Nov	4			2	1					1	3	0
Dec	3			1		1				1	1	0
Sum		4	7	11	10	13	10	6	15	10		

K is the day when the K_p index had a marked maximum. (This is in modification to Section II-A of this report where K is defined as the day after a strong rise of the K_p index.) The difference of the definitions affects the results only insignificantly.

Several days are counted twice because they belong simultaneously to the wake of one K_p maximum and to the introduction of the next.

It is obvious that there is a bias towards March and August-September which should be borne in mind when the meteorological side of the results is discussed. For the statistical significance it is essential that there is no bias between the K-days. The column b (before) presents the sum of the days K-3, K-2, K-1, and a (after) the sums of K+1, K+2, K+3. The series a and b coincide well. Both emphasize the times around the equinoxes and neglect the solstices. So that we conclude that there is no bias between the two periods which might invalidate the results. There are several periods with enough TIROS pictures to cover several K-days belonging to the same K_p maximum.

After preliminary studies 17 criteria were set up which are, in part, rather unconventional. For each day (case) it was decided which of the criteria were fulfilled. Then the data for each of the K-days were lumped together (i.e., seasonal differences were neglected) and it was computed how many (n) of the cases (N) showed a positive response: $p = 100 \frac{n}{N}$.

There are some criteria that do not show a variability of p with respect to K. Such criteria are of no use in our study (but may become of special value in future phases of investigation). In particular the following criteria were dropped: "outlines sharp on one side of cloud units, and fluffy on the other," "much cirrus," "clouds at more than one level," "cross patterns." Some other criteria were abandoned because their computed p-K relationship was too complicated to be significant, or because p stayed throughout too close to 0 or to 100. These criteria are "large areas with overcast skies", "streakiness of Ci, especially jet-associated," "streakiness of clouds other than Cu, Cb, Ci," "no obvious organization," "smooth, fluffy outlines (Ci)".

The eight remaining features are listed in Table 2. The values of p are slightly smoothed by combining two consecutive days.

Cloud shapes A and B, sharp or fibrous irregular outlines, have minimum frequencies shortly before a K_p maximum. One can also say that the cloud shapes tend to become smoother when the geomagnetic activity begins to rise to a maximum. This is also borne out by the (approximately) simultaneous rise of curve H, sharp smooth outlines.

There seems to be a change from more vertical cloud development to stratification, as the frequency of large areas with broken cloud cover (C) increases, and the numbers of plumes (F) and Cb cells (G) decreases.

From another point of view a stratified system seems to be more uniformly organized while vertical processes tend to be more individual developments. Under this premise, it seems logical that, during the evolution of a solar event, ill defined lines of Cu (E) become partly replaced by well defined such lines (D). The corresponding pictures (Fig. 19) show very well the difference between these two types. The cases of "no obvious organization," and "streakiness of clouds other than Cu, Cb, or Ci", which were excluded from Table 5 and Fig. 19 because of their small number, do not contradict the interpretation of increasing organization during a solar event.

If this concept is correct, it should also find its expression in the appearance of the weather map. For the same area and for the same days from which Table 5 was derived, some weather map features were counted.

Some of them showed a clear relationship to the evolution of a solar event, some of them did not.

Features that were discarded because of either erratic patterns ortoosmall numbers of occurrence are "several anticyclones," "easterly waves," "well defined front," and "wave development at a front."

FIG. 19 CLOUD SHAPES whose frequency of occurrence changes during periods in which the K_p index undergoes a maximum

A

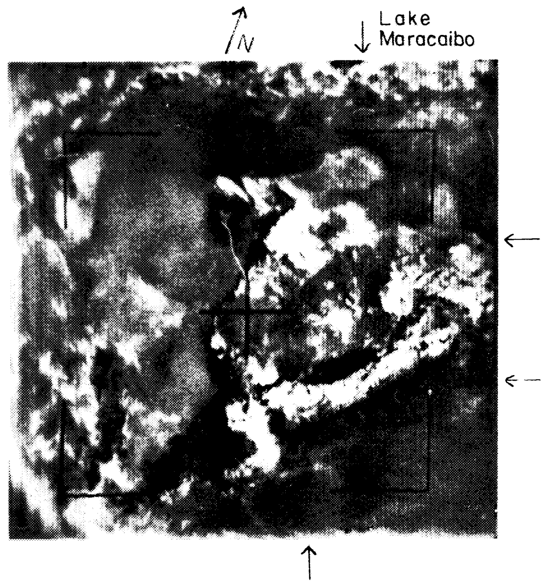

B

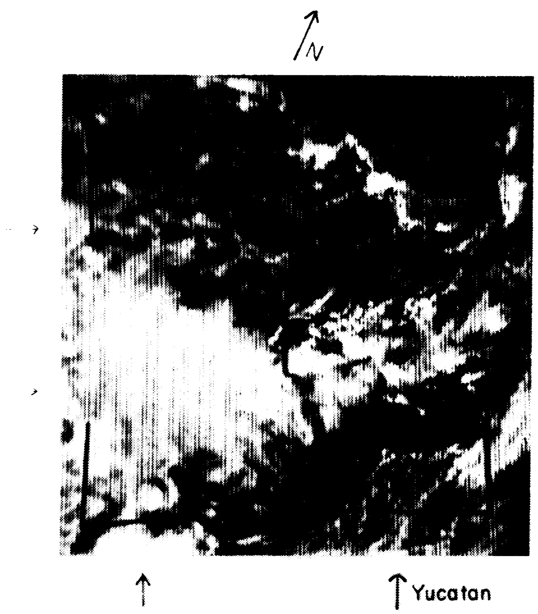

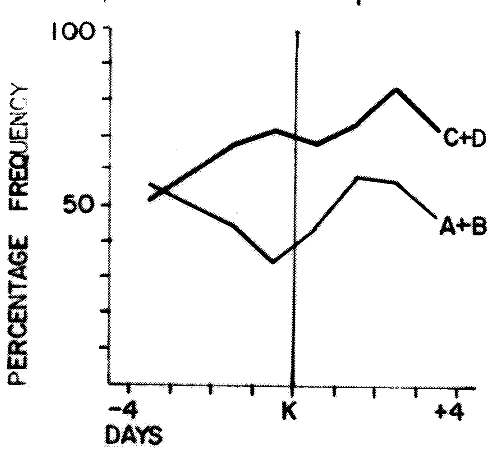

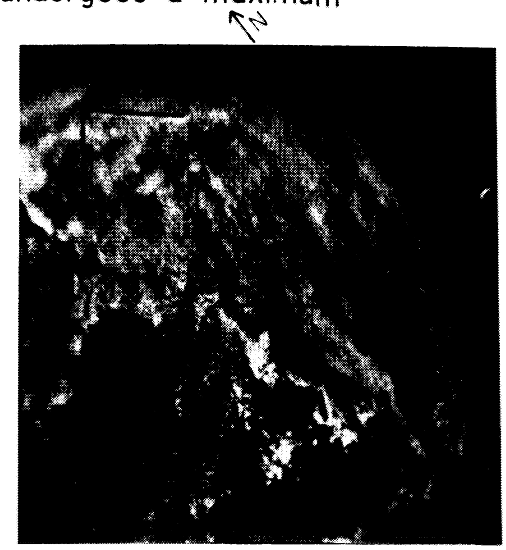

C

D

A. RUGGED OUTLINES, SHARP

B. RUGGED OUTLINES, FIBROUS

C. LARGE AREAS OF ◍

D. WELL DEFINED LINES OF CU

FIG. 19 CONT.

E

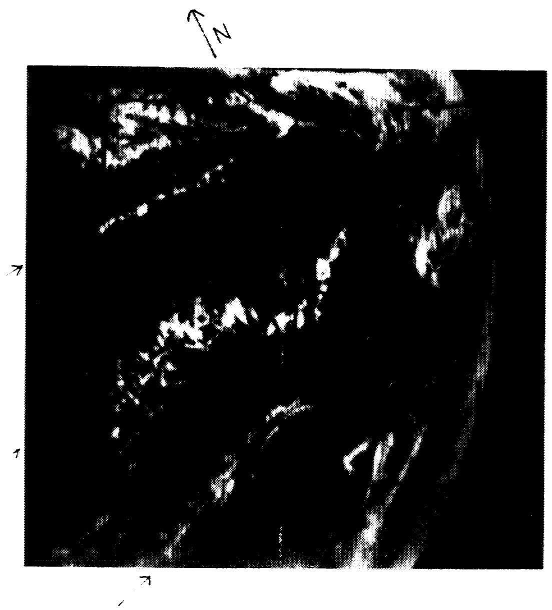

F

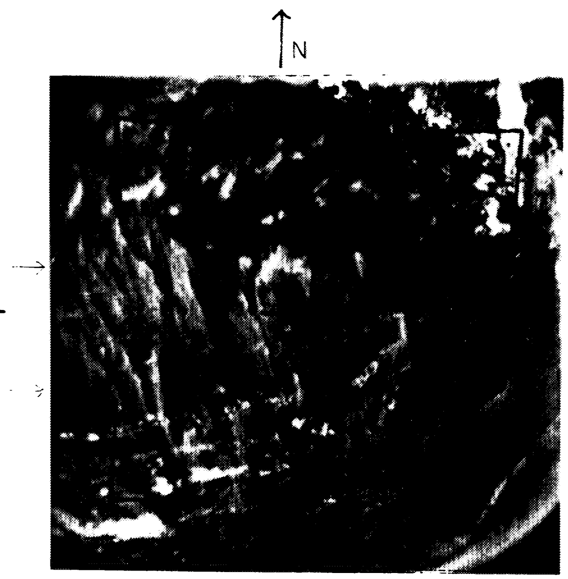

G

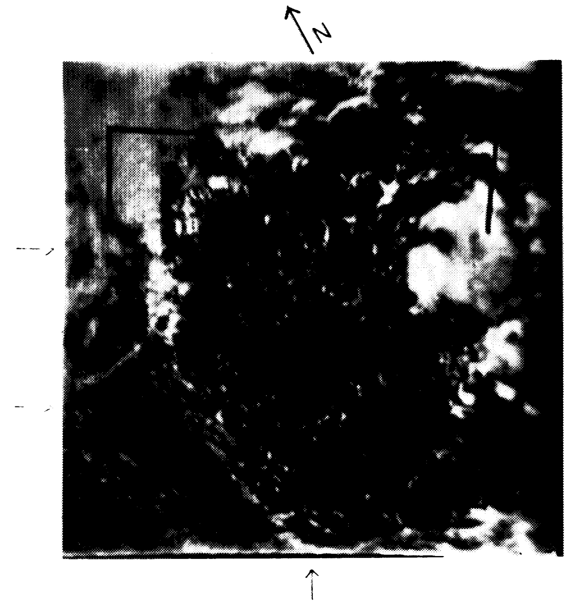

H
(G)

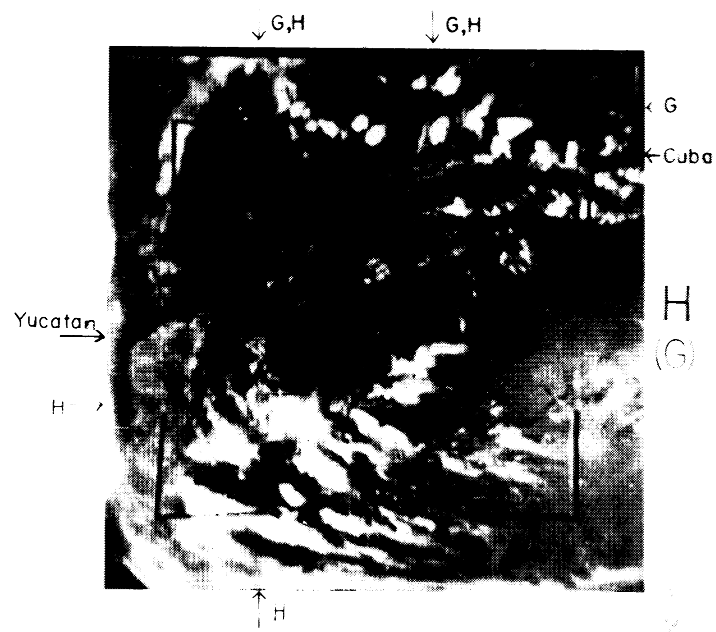

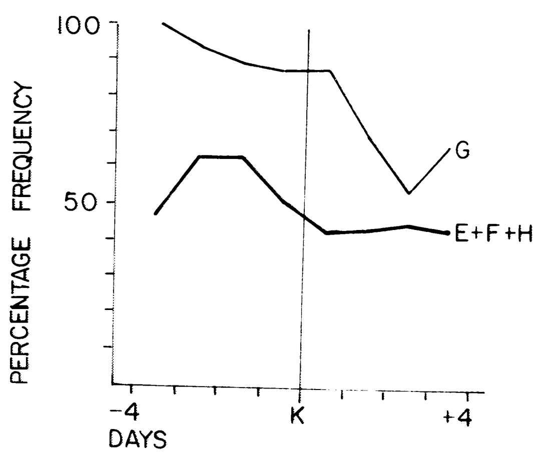

E. ILL DEFINED LINES OF CU

F. PLUMES

G. NUMEROUS CB CELLS

H. SHARP SMOOTH OUTLINES

TABLE 5

Percentages, p, of Cloud Features as a Function of Time Around a K_p Maximum

	K-3 K-4	K-2 K-3	K-1 K-2	K K-1	K K+1	K+1 K+2	K+2 K+3	K+3 K+4
A. Sharp, rugged outlines	$\underline{72}$	$\underline{50}$	33	29	41	38	53	52
B. Fibrous, rugged outlines	29	50	$\underline{56}$	41	47	$\underline{77}$	$\underline{59}$	43
C. Large areas with 5/10-9/10 cloud coverage	72	72	78	71	76	$\underline{92}$	94	81
D. Well defined lines of Cu	43	43	56	$\underline{71}$	$\underline{59}$	54	$\underline{71}$	$\underline{62}$
E. Ill defined lines of Cu	$\underline{43}$	$\underline{50}$	$\underline{44}$	29	29	31	35	29
F. Plumes	57	$\underline{71}$	$\underline{72}$	$\underline{59}$	47	54	53	48
G. Numerous Cb cells	$\underline{100}$	$\underline{93}$	$\underline{89}$	76	76	69	53	67
H. Sharp, smooth outlines	43	$\underline{71}$	$\underline{72}$	$\underline{65}$	52	46	47	52

Values larger than the line average are underlined

Figure 19 shows for each cloud shape a typical picture. In the left lower corner on both pages of the figure, we find diagrams depicting the variation of the percentage frequency with time. Though the absolute values are different, the shapes of some diagrams are so similar that they were combined, and the averages of A+B, C+D, and E+F+H are presented.

It was to be expected that several types of curves would be encountered, partly because of their definition (compare D with E), and partly because a parallel change of all types would mean a change in cloud amount which had not been found in previous work.

Table 6 presents weather map features that appear to show a relationship to processes manifested in a maximum of the K_p index.

TABLE 6

Percentage Frequency of Weather Map Features

(area and days the same as for Table 2)

		K-3 K-4	K-2 K-3	K-1 K-2	K K-1	K K+1	K+1 K+2	K+2 K+3	K+3 K+4
V	One well defined LOW	<u>44</u>	39	33	32	<u>50</u>	<u>50</u>	35	<u>44</u>
W	One well defined HIGH	33	39	33	<u>45</u>	<u>59</u>	<u>57</u>	<u>45</u>	40
X	Several LOW's	22	17	<u>29</u>	23	23	<u>36</u>	25	<u>32</u>
Y	Confused pressure distribution	<u>44</u>	<u>44</u>	<u>43</u>	<u>45</u>	<u>41</u>	29	30	36
Z	Dissolving front	<u>56</u>	<u>39</u>	24	23	23	21	30	24

Values larger than the average are underlined.

For the interpretation of Table 6 one should be aware that the considered area lies most of the year in the tradewinds where a closed isobar (depression) is a higher form of organization than the wave. Bearing this in mind we see that the concept developed from the analysis of the cloud shapes holds also here. The atmosphere becomes better organized during an increase of the K_p index. "Better" is to be understood as "regionally rather than locally."

The preliminary results presented here can be combined with the results described in Section II-A as set forth in Table 7.

Recommendations

Since the preliminary results offered here apparently open quite new aspects as to what is and what causes weather, more studies are needed to create the necessary heuristic, later statistical, basis on which the theorist can operate for the explanation of the mechanisms that relate processes on the sun to the forms of clouds and the appearance of weather charts. Studies should begin with an extension of the considered area, and with checks of whether better descriptive criteria for cloud features can be found. After this has been done attempts should be made to find numerical relations between the intensity of cloud-K_p relations and geomagnetic properties of the places where they occur.

TABLE 7

Summary of Preliminary Finds Concerning the Occurrence of Certain Weather

Features Before and After a Maximum of a Solar Wind

	2-4 days before the maximum	2-4 days after the maximum
Height of 10 mb level	General increase, especially over NW Europe.	Strong decrease, especially over North Atlantic. Increase over Bering Sea. Decrease predominates on a hemispheric basis.
Cloud shapes (10-30N, 70-100W)	High percentages of plumes, Cb cells, clouds systems with smooth, sharp outlines and ill defined lines of cumuliform clouds. Decreasing percentage of cloud systems with rugged outlines.	High percentage of cases where large areas are covered with broken cloudiness. High percentage of well defined lines of Cu. Increasing percentages of cloud systems with rugged outlines.
Weather map (10-30N, 70-100W)	High percentages of confused isobar patterns and of dissolving fronts.	High percentages of well defined LOWs (single or multiple) and single HIGHs.
In general (10-30N, 70-100W)	Tendency to local developments with emphasis vertical movements.	Tendency to regional weather systems, horizontally well organized.

III A DESCRIPTION OF THE PHYSICAL MODEL

The following is a physical discussion of a model of motion of the ionosphere and the subsequent effects to be expected in the troposphere. There is a basic underlying assumption to all of this discussion. This assumption can be summarized as follows:

1. There is always much more (by factors of 3 to 10) energy in the atmosphere in the small space scale and small time scale motions than in large scale motions.
2. The energy flow is usually from the large scale motion to the small scale motion, which follows turbulence theory, with at least one very important exception. The small scale motions force the large scale motions to be geostrophic. Thus the very large amount of energy of the small scale motion is available to bring about changes in the large scale motion that are required.
3. The problem of control of motions from one level to another is not a problem in transporting energy but rather a problem of requiring a certain change in the flow to bring about geostrophic winds. We will discuss point 3 first.

It is very interesting to note that the only theoreticians who make frank use of the geostrophic approximation are those involved in numerical weather prediction and related problems; but (in common with most descriptive meteorologists) when Webb* explained the diurnal and semi-diurnal pressure waves and their relation to very high altitude heating, he explained the tacit assumption that the winds become geostrophic from 30° latitude to the pole in less than two hours.

The importance of the atmosphere striving for geostrophic balance and the detail of the mechanism by which it strives for this balance has not been emphasized.

Since the establishment of Buys-Ballot Law in 1857, and probably before, those who have studied the winds have been aware of the atmosphere's tendency to flow parallel to lines of constant pressure. The geostrophic approximation is the foundation of weather map analysis and the thermal wind relation is a great aid in upper air analysis.

Charney (1951) and Thompson (1961) have established the geostrophic and thermal winds as being completely adequate approximations for numerical weather computation.

---

*Talk given to the Houston Chapter of the American Meteorological Society, Nov. 8, 1965 by Willis L. Webb entitled "Meteorological Rocket Exploration of the Stratospheric Circulation."

The overwhelming majority of oceanographic current estimates are obtained from a combination of density measurements and a geostrophic approximation. Because of this theorists in oceanography usually assume that the currents are very nearly geostrophic.

All of these statements have been made to emphasize that the geostrophic wind is accepted as being very nearly the actual wind.

The theoreticians in meteorology show in nearly every textbook, (see,for example,Hess (1959), Haurwitz (1941), and Brunt (1939)), that it is possible to have geostrophic winds in a rotating coordinate system. Experience shows us that the atmosphere is nearly always in geostrophic balance. This note is concerned with the question: "Why is the atmosphere nearly always in geostrophic balance?"

Later we will give a theoretical discussion. However, the reasoning can be outlined as follows:

(1) Turbulent transport of momentum from one layer to another brings about an acceleration in the direction of the wind difference.

(2) If we consider the middle of three layers and it is losing an amount of momentum M_L to the lower layer and gaining M_H from the upper layer then the net gain in momentum is $M_H - M_L$.

(3) Thus if $(\mathbb{V}_2 - \mathbb{V}_1)$ is the same across both boundaries of a layer (or if $\frac{\partial \mathbb{V}}{\partial z}$ = constant), the change in this layer due to momentum exchange is zero.

(4) If $\mathbb{V}_2 - \mathbb{V}_1$ differs from layer to layer, then the momentum changes but it changes in such a way that $\frac{\partial}{\partial t} \frac{\partial \mathbb{V}}{\partial z} \longrightarrow 0$.

This is the primary physical process that we plan to discuss as forcing the geostrophic approximation. So we will re-emphasize: If the coefficient of friction K is not a function of z then turbulent mixing of momentum serves to "straighten out" momentum profiles.

We illustrate below with typical layers in the free atmosphere.

Looking at A.

Momentum from M is lost to U and L so that a later profile is given by B.

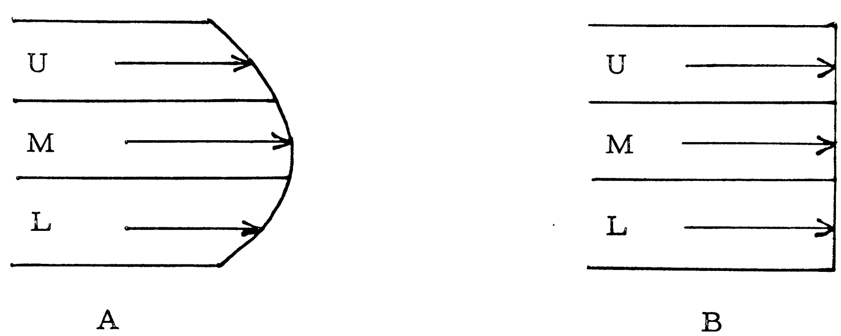

In C momentum is lost from M to L then from U to M to L and the profile D results.

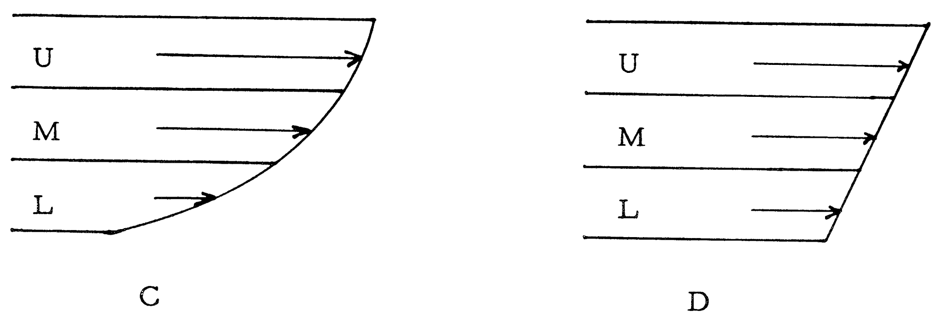

This is a perfectly straightforward physical result. When $\frac{\partial U}{\partial z}$ = constant the rate of loss and gain for a layer are equal and no change is expected.

(5) All of the reasoning above works the same for density in an incompressible fluid and for potential temperature in a compressible fluid. Thus $\frac{\partial \rho}{\partial z}$ = constant or $\frac{\partial \theta}{\partial z}$ = constant is forced by vertical mixing. For convenience of discussion we will treat incompressible fluids.

(6) If we integrate the equation for conservation of mass with a linear vertical density profile (and with a velocity profile a function of z) we find that the linear density profile will be destroyed except under very special conditions. Thus we have the paradox of vertical mixing forcing the profiles to be linear and the vertical distribution of velocity destroying the linearity.

(7) Our hypothesis is that nature solves this paradox by seeking a very special horizontal density distribution. Namely the lines of constant density are streamlines. Thus even though velocity is a function of z the advection is zero at every level.

(8) Thus there is a "bias" toward isotachs of the wind shear and isotherms being streamlines. The study of upper air maps shows a marked tendency for isotherms to be streamlines and a trend toward isotachs of the wind itself and, therefore, the wind shear to be streamlines.

(9) When the conditions of (6) exist, further investigation of the differential equations reveals the full thermal wind relationship including velocity inversely proportional to the distance between isotherms.

(10) Thus, it follows that vertical momentum transport forces linear wind profiles, maintenance of the linear profile forces isotherms and isotachs of wind shear to be streamlines. When they are streamlines, accelerations of the wind shear are very small and the thermal wind relation holds.

Vertical mixing of mass or momentum following* the same law with the same constants throughout the vertical will lead to velocity changes unless

$$\frac{\partial^2 M_x}{\partial z^2} = 0 , \quad \frac{\partial^2 M_y}{\partial z^2} = 0 , \quad \frac{\partial^2 \rho}{\partial z^2} = 0 \tag{1}$$

We assume incompressibility so $M_x \approx \rho u$ and $M_y \approx \rho v$.

*We recognize that there are many expressions for vertical momentum and mass transport. However, nearly all of them lead to a local condition $u = u(k_x, k_y)\, f(z)$ or $u = u(x_k, y_k)\ f(k\ (x, y)\ z)$, in particular $k = k(z)$ in the stratosphere.

Now let us assume that this process is at work and explore the consequences.

$$\frac{d}{dt}\frac{\partial u}{\partial z} + \frac{\partial u}{\partial z}\frac{\partial u}{\partial x} + \frac{\partial v}{\partial z}\frac{\partial u}{\partial y} = \frac{1}{\rho}\frac{\partial^2 p}{\partial z \partial x} + f\frac{\partial v}{\partial z} \tag{2}$$

for very small time*

$$\frac{d}{dt}\frac{\partial v}{\partial z} + \frac{\partial u}{\partial z}\frac{\partial v}{\partial x} + \frac{\partial v}{\partial z}\frac{\partial v}{\partial y} = -\frac{1}{\rho}\frac{\partial^2 p}{\partial z \partial y} - f\frac{\partial u}{\partial z} \tag{3}$$

for very small time*

Assume we have obtained

$$u = U(x, y, t)z \qquad v = V(x, y, t)z$$

From the hydrostatic relation we get

$$\frac{\partial p}{\partial z} = -g\rho, \qquad \frac{\partial^2 p}{\partial x \partial z} = -g\frac{\partial \rho}{\partial x}, \quad \frac{\partial^2 p}{\partial y \partial z} = -g\frac{\partial \rho}{\partial x} \tag{4}$$

Equation (2) becomes

$$\frac{dU}{dt} + Uz\frac{\partial U}{\partial x} + Vz\frac{\partial U}{\partial y} = -\frac{g}{\rho}\frac{\partial \rho}{\partial x} + fV \tag{5}$$

and Equation (3) becomes

$$\frac{dV}{dt} + Uz\frac{\partial V}{\partial x} + Vz\frac{\partial V}{\partial y} = -\frac{g}{\rho}\frac{\partial \rho}{\partial y} - fU \tag{6}$$

If we set

$$\frac{d_2 V}{dt} = \frac{\partial V}{\partial t} + 2u\frac{\partial V}{\partial x} + 2v\frac{\partial V}{\partial y}, \tag{7}$$

we can then write Equation (6) as follows:

$$\frac{d_2 V}{dt} = -\frac{g}{\rho}\frac{\partial \rho}{\partial y} - fU \tag{8}$$

---

*These include transport and vertical variation of density. Some of these terms will be significant near the ground.

This is a contradiction unless $\frac{d_1 V}{dt}$ is independent of z. The only way for the left-hand side of this equation to be a function of (x, y, t) and not of z is for $\frac{d_1 V}{dt} = \frac{\partial V}{\partial t}$.* We say that friction brings this about (especially in the troposphere). Thus we have

$$\frac{\partial V}{\partial t} = -\frac{g}{\rho}\frac{\partial \rho}{\partial x} - fU \tag{9}$$

and

$$\frac{\partial U}{\partial t} = -\frac{g}{\rho}\frac{\partial \rho}{\partial y} + fV \tag{10}$$

and if we can show $\frac{\partial V}{\partial t} << fU$ and $\frac{\partial U}{\partial t} << fV$

we have
$$-\frac{g}{\rho}\frac{\partial \rho}{\partial x} - fU = 0 \tag{11}$$

and

$$-\frac{g}{\rho}\frac{\partial \rho}{\partial y} + fV = 0 \tag{12}$$

which are equivalent to the thermal wind approximations.

Now we are only concerned with the reasoning that requires $\frac{\partial V}{\partial t} << fU$ and $\frac{\partial U}{\partial t} << fV$. Of course, we can appeal to observation but that is unfair since we hope we are explaining the observations.

We have been ignoring the equation

$$\frac{\partial \rho}{\partial t} + U_z \frac{\partial \rho}{\partial x} + V_z \frac{\partial \rho}{\partial y} = 0 \tag{13}$$

*This can be very nearly true if lines of constant U and lines of constant V are parallel to velocity vectors.

which is a very good approximation to the way ρ changes. So we have the following system of equations

$$\frac{\partial \rho}{\partial t} + U_z \frac{\partial \rho}{\partial x} + V_z \frac{\partial \rho}{\partial y} = 0$$

$$\frac{\partial V}{\partial t} = -\frac{g}{\rho} \frac{\partial \rho}{\partial x} - fU \tag{14}$$

$$\frac{\partial U}{\partial t} = -\frac{g}{\rho} \frac{\partial \rho}{\partial y} + fV$$

We say $-\frac{g}{\rho} \frac{\partial \rho}{\partial y}$ and $-\frac{g}{\rho} \frac{\partial \rho}{\partial x}$ are independent of height. If ρ is independent of height then U and V must be parallel to the lines of constant density so that $\frac{\partial \rho}{\partial t} = 0$.

Thus we have from Equation (13)

$$U \frac{\partial \rho}{\partial x} + V \frac{\partial \rho}{\partial y} = 0 \tag{15}$$

Multiplying Equation (10) by U and Equation (9) by V we have

$$U \frac{\partial U}{\partial t} = -\frac{g}{\rho} U \frac{\partial \rho}{\partial x} + fUV \tag{16}$$

$$V \frac{\partial V}{\partial t} = -\frac{g}{\rho} V \frac{\partial \rho}{\partial y} - fUV \tag{17}$$

and hence,

$$\frac{\partial}{\partial t} \left(U^2 + V^2\right) = -\frac{g}{\rho} \left(U \frac{\partial \rho}{\partial x} + V \frac{\partial \rho}{\partial y}\right) = 0 \tag{18}$$

In summary:

(1) Vertical transport of momentum gives an <u>active</u> tendency to linear wind shear U(x, y, t), V(x, y, t) at each point (x, y) on the earth.

(2) This leads to an equation for the wind shear in which there are terms implying that U could be a function of z, and V could be a function of z. We know the mixing forces these terms to be ineffective. This leaves U and V effectively functions of x, y, t only, and not functions of z. These terms are ineffective if the lines of constant U + V are parallel to the velocity vectors.

(3) When this condition is added to the equations for U and V the result is $\frac{\partial}{\partial t}(U^2 + V^2) = 0$

(4) The effective way for this to be true is

$$\frac{\partial U}{\partial t} \approx \frac{\partial V}{\partial t} \approx 0 \tag{19}$$

and thus,

$$-\frac{g}{\rho}\frac{\partial \rho}{\partial x} + fV = 0 \tag{20}$$

$$-\frac{g}{\rho}\frac{\partial \rho}{\partial y} - fU = 0 \tag{21}$$

i.e., we have thermal winds.

Note:

There is the possibility that $\frac{\partial (U^2)}{\partial t} = -\frac{\partial (V^2)}{\partial t} \neq 0$. But we are free to choose the axes, so we choose them parallel to the wind. Then

$$\frac{\partial U}{\partial t} = -\frac{g}{\rho}\frac{\partial \rho}{\partial x} = 0$$

because ρ = constant along streamlines, but then

$$\frac{\partial}{\partial t}\left(U^2 + V^2\right) = \frac{\partial (V^2)}{\partial t} = 0$$

Thus from Equation (9)

$$-\frac{g}{\rho}\frac{\partial \rho}{\partial y} - fU = 0 \tag{22}$$

The previous discussion* concerning the effect of mixing on curved profiles applies equally well to the horizontal on scales such that the coriolis parameter f = constant.

Thus on a small scale we find that $\frac{\partial *}{\partial x} \longrightarrow$ constant and $\frac{\partial *}{\partial y} \longrightarrow$ constant for all values.

Thus

$$\begin{aligned}
u(x,y,z,t) &\longrightarrow U_1(t)_x + U_2(t)_y + U_3(t)_z + U_4(t) \\
v(x,y,z,t) &\longrightarrow V_1(t)_x + V_2(t)_y + V_3(t)_z + V_4(t) \\
\rho(x,y,z,t) &\longrightarrow \rho_1(t)_x + \rho_2(t)_y + \rho_3(t)_z + \rho_4(t)
\end{aligned} \tag{23}$$

Because of non-linear terms the linear profiles have non-linear changes. The only way to get rid of the non-linear changes is to have the terms:

$$\begin{aligned}
u\frac{\partial u}{\partial x} + v\frac{\partial u}{\partial y} &\longrightarrow 0 \\
u\frac{\partial v}{\partial x} + v\frac{\partial v}{\partial y} &\longrightarrow 0 \\
u\frac{\partial \rho}{\partial x} + v\frac{\partial \rho}{\partial y} &\longrightarrow 0
\end{aligned} \tag{24}$$

or for lines of constant velocity to be nearly parallel to streamlines at all times.

Note then that horizontal on a small scale as well as vertical mixing can actively bring about quasi-geostrophic winds.

*The discussion of the geostrophic wind up to this point was accomplished under sponsorship of the U.S. Army Electronics Command on Contract No. DA 28-043 AMC-00173(E). The following discussion was developed for this contract.

It is interesting now to note that there is no need to worry about whether this geostrophic balance requires energy to be added or taken from the flow. If energy is needed it will come from the small scales; if it is lost, it can go into the smaller scale.

The routine computations of the Fleet Numerical Weather Facility* include computations of the total energy in three scales of motion. Less than half of the energy is in the very large scale motions. There is plenty of energy in the small scales to bring about changes in the large scale. The significance of this observation is that energy considerations do not control atmospheric motions. This is not because energy is not conserved, but it is because total energy is not calculated in the ordinary flow.

It is not a physical law that energy is conserved in large scale flow. The physical law is that energy is conserved in the total flow. This is exactly what happens when a gas is compressed. The work done in compressing the gas is used to add to the kinetic energy of the molecules in the gas. When the gas has an opportunity to expand the energy can show up as large scale kinetic energy.

In the study of the Carnot cycle of classical thermodynamics, we guide the flow of energy with a piston. In the study of the atmosphere the flow of energy is guided by the eternal seeking of geostrophic balance.

The significance of the discussion to the problem of solar influence on the weather in the troposphere cannot be overemphasized.

---

*Personal Communication, Dec. 1965, with Capt. Paul Wolff. In one example, (period: 26 Oct-30 Nov 1965) the small scale motions had an average value of 60, the medium, 41, and the large, 57.

There was a hint of this significance in our previous discussion of descending 26 month period wind waves (Freeman, Portig, et. al. 1963)). A hint is also contained in the essence of the attitude of Shapiro toward energy transfer: "An orientation and position of a 500 mb trough relative to a surface trough can release energy from the whole layer. A 250 to 500 mb system can release energy from that layer. A 125 to 250 mb system can release energy from that layer," etc.

Our present position concerning energy transport can be summarized as follows.

In the same sense that there is always energy in a gas in the form of molecular motion, there is always energy available in the atmosphere in the form of small scale motions. When a control on the atmosphere requires a change in the flow to achieve geostrophic balance in the very large scale flow, the energy of the small scale flow is available to bring about that change. Thus, we have removed the old "stumbling block" of a connection between ionospheric circulation and tropospheric circulation usually quoted as, "There is too little energy (by powers of ten) in the ionospheric motion to ever effect the tropospheric motion." We must now answer the question: "Does the flow in the ionosphere require a significant change in the troposphere in order to maintain total geostrophic balance?"

A rather complete discussion of steady state flow in atmospheric cross sections that show the dependence of one layer on another is given in Appendix A.

We extend this study to time dependence later in Appendix B. To study the flow in middle latitudes we can give an abbreviated discussion of this work. We expect this theory to be important in the study of the initial rise of pressure to the south discussed in Section II. There is a region of the atmosphere with nearly constant winds at all levels. We can draw a plane in this line from which we measure a distance y. (If we cannot draw such a plane we measure y from a nearly stationary surface of constant u or have a connection to u).

With this we can write a finite number of equations at each level of the form:

$$u_i = f_o Y_i + \frac{\beta Y_i^2}{2} - (i+1)\left(\frac{2L_o + i\Delta L}{2}\right) - M_o$$

Where β, f_o, L_o, ΔL, and M_o, are all constant for the whole flow, and thus we have an equation for u_i in terms of Y_i.

We devise the time dependent equation for cross sections in which the pressure gradient is measured by means of an estimate of the tipping of the surfaces of potential temperature and using the substitution above. The following several standard mathematical techniques result in an equation:

$$\frac{\partial^2 Y_i}{\partial t^2} = \frac{D_i f_o^2}{\ln \frac{\theta_{i+1}}{\theta_i}} \frac{\partial Y_i}{\partial z} + \left[f_o^2 - \left\{ \beta(i+1)\left(\frac{2L_o + i\Delta L}{2}\right) + M_o \right] Y_i\right.$$

We rewrite this equation in the form:

$$\frac{\partial Y_i}{\partial z} = k_i^2 \frac{\partial^2 Y_i}{\partial t^2} - k_2^2 Y_i$$

The solution to this equation is:

$$Y_i = C_+ Y_i + C_- Y_{i-}$$

where

$$Y_{i\pm} = e^{\left(\frac{1 \pm \sqrt{1+4b^2}}{2b^2}\right)\left(k^2 z + b \frac{k_2}{k_1} t\right)}$$

For all arbitrary constants b.

For the small values of b in which we are interested,

$$Y_{i+} = e^{\frac{1}{b^2}\left(k_2^2 z + b \frac{k_2}{k_1} t\right)}$$

$$Y_{i-} = e^{\left(k_2^2 z + b \frac{k_2}{k_1} t\right)}$$

For small b, the values Y_{i+} would decrease rapidly with z.

Thus a disturbance of shape A in the figure below would move slower than one with shape B.

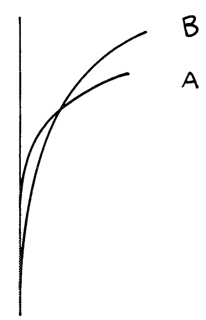

The important thing to keep in mind is that the changes in Y_i can propagate up or down and at many different speeds depending on the nature of the disturbance. Y_i can oscillate with free or forced oscillation.

The solar storm seems to be characterized by rapid heating and slow cooling so we would expect the effects (of heating) on Y_i to move down rapidly. We would assume that the early increase in pressure which would correspond to westerlies shown in Section II would result from this.

The following lower pressure in middle latitudes would be the slower moving effect of the cooling that results after the heating stops. Cooling, which depends on the radiative processes of particles in the high atmosphere for its action, is inherently slower than the heating which must absorb the energy during the brief period that is available.

A very simple model of the polar core leads to a reasonable imitation of possible solar influence through magnetic storms.

If we say the material layers are of thickness D_i, and we set R_m = distance from the pole, we then have a set of equations

$$\frac{\partial}{\partial t}\left(\frac{\Omega + \omega_{mi}}{D_{mi}}\right) = 0 \qquad \text{vorticity}$$

$$\frac{\partial}{\partial t}\left(R_{mi}^2 D_{mi}\right) = 0 \qquad \text{continuity}$$

$$\frac{\partial}{\partial z}\left[\frac{f}{2g}\frac{\Omega}{D_0} D_{mi} - \frac{1}{2D_{mi}}\frac{\partial D_{mi}}{\partial t}\right] = -\frac{D_{mi}}{K}\log\frac{\theta_{mi}}{\theta_{pmi}} \qquad \text{modified thermal wind equation}$$

with $U_n = 0$ when $D_{ni} = D_o$, controlling the method by which we chose D_o.

$u = (90° - y)\,\omega_{mi}$ is the wind velocity in the system and

$$u_m = R_{mi}\,\omega_{mi}$$

Note that when we have the true thermal wind equation we have reached a steady state and

$$\frac{\partial D_{mi}}{\partial t} = 0$$

We rewrite the modified theoretical wind equation into two equations: the first is

$$\frac{\partial M_{mi}}{\partial z} = -\frac{D_{mi}}{K}\log\frac{\theta_{mi}}{\theta_{pmi}}$$

If we assume $M_{n1} = \frac{f}{2g} \frac{\Omega}{D_0} D_{m1}$, then we can integrate this equation.

$$M_{mi} = M_{m1} - \sum_{k=1}^{i} \frac{D_{mk}^2}{K} \log \frac{\theta_{mk}}{\theta_{pmk}}$$

Now our other equation is

$$\frac{f}{2g} \frac{\Omega}{D_0} D_{mi} - \frac{1}{2D_{mi}} \frac{\partial D_{mi}}{\partial t} = M_{mi}$$

We can rewrite this equation in the form

$$\frac{\partial D_{mi}}{\partial t} = \frac{f}{g} \frac{\Omega}{D_0} D_{mi}^2 - 2 D_{mi} M_{mi}$$

If we substitute in this equation we get

$$\frac{\partial D_{mi}}{\partial t} = \frac{f}{g} \frac{\Omega}{D_0} D_{mi}^2 - \frac{f}{g} \frac{\Omega}{D_0} D_{mi} D_{m1} + 2 D_{mi} \sum_{k=1}^{i} \frac{D_{mk}^2}{K} \log \frac{\theta_{mk}}{\theta_{pmk}}$$

$$= \frac{f}{g} \frac{\Omega D_{mi}}{D_0} \left(D_{mi} - D_{m1} \right) + 2 D_{mi} \sum_{k=1}^{i} \frac{D_{mk}^2}{K} \log \frac{\theta_{mk}}{\theta_{pmk}}$$

This equation tells us immediately that $\frac{\partial D_{mi}}{\partial t}$ at one level is related to the D_{nk} at many other levels by means of an integration, so we need not be surprised at the interactions between layers.

The influence of the temperature is manifest in the term, $\log \frac{\theta_{mi}}{\theta_{pi}}$.

When the pole is warm, $\log \frac{\theta_{mi}}{\theta_{pi}} < 0$

When the pole is cold, $\log \frac{\theta_{mi}}{\theta_{pi}} > 0$

When we have a balance and no change taking place then

$$\frac{\partial}{\partial z} \left[\frac{f}{2g} \frac{\Omega}{D_0} D_{mi} \right] = - \frac{D_{mi}}{K} \log \frac{\theta_{mi}}{\theta_{pi}} .$$

In order to study the properties of these equations we can drop the i designation and we have

$$\frac{\partial}{\partial z} \left[\frac{f}{2g} \Omega \frac{D}{D_0} - \frac{1}{2D} \frac{\partial D}{\partial t} \right] = - \frac{D}{K} \log \frac{\theta}{\theta_p}$$

We postulate that we change $\log \frac{\theta}{\theta_p}$ from a balanced condition at some upper level. So that the initial condition is

$$\frac{\partial}{\partial z}\left[\frac{f}{2g}\Omega \frac{D_1}{D_0}\right] = -\frac{D_1}{K}\log\frac{\theta_1}{\theta_{p_1}} \quad \text{at} \quad t = 0,$$

which gives us D_1 at $t = 0$.

Now we write

$$\frac{\partial}{\partial z}\left[\frac{f}{2g}\Omega\frac{D}{D_0} - \frac{1}{2D}\frac{\partial D}{\partial t}\right] = -\frac{D}{K}\log\frac{\theta}{\theta_p}$$

with $-\frac{D}{K}\log\frac{\theta}{\theta_p} = \frac{D_1}{K}\log\frac{\theta_1}{\theta_{p_1}}$ below $z = z_o$.

This tells us immediately that the initial values of

$$\frac{\partial}{\partial z}\left(-\frac{1}{2D}\frac{\partial D}{\partial t}\right) = 0 \qquad \text{below } z = z_o .$$

Thus, whatever value of $\frac{\partial D}{\partial t}$ we had at $z = z_o$ is called $\left(\frac{1}{D}\frac{\partial D}{\partial t}\right)$. Below $z = z_o$ we have $\frac{1}{2D}\frac{\partial D}{\partial t} = \left(\frac{1}{2D}\frac{\partial D}{\partial t}\right)$.

Thus, if we have convergence at the bottom of the heated level, we have convergence below it.

Also, initially above $z = z_o$ we have

$$\frac{\partial}{\partial z}\left(-\frac{1}{2D}\frac{\partial D}{\partial t}\right) = HD \qquad \text{with } H > 0.$$

Thus, we have divergence in the upper levels of the heating. The amount of divergence decreases downward and we can have either convergence or divergence below the heating.

If the upper divergence continues, the equations change so that the low level convergence disappears. This is shown by

$$\frac{\partial}{\partial z}\left[-\frac{1}{2D}\frac{\partial D}{\partial t}\right] = HD .$$

As D gets smaller, $\frac{\partial}{\partial z}\left[-\frac{1}{2D}\frac{\partial D}{\partial t}\right] = HD$ gets smaller and soon the divergence reaches the bottom of the heated layer. Probably more important, the unbalanced portion of $-\frac{D}{K}\log\frac{\theta}{\theta_p}$ gets smaller and results in the upper and lower level motions being about the same.

APPENDIX A

A THEORY FOR ATMOSPHERIC CROSS SECTIONS

by

John C. Freeman, Jr.*

*Dr. Glenn H. Jung helped with the preparation of a discussion in 1958 which formed the basis of this paper.

Objectives and Conclusions

It is our purpose here to describe the flow in the upper troposphere by means of a simple mechanism. We postulate that the upper troposphere acts in accord with two very basic principles - the conservation of vorticity and the thermal wind approximation - which permit explanation of the gross features.

The concept to be developed here will show that: (1) a concentration of isentropes and isotachs results as a natural process of the atmosphere responding to the vorticity conservation and the thermal wind relationship when a disturbance in the initial flow arises from an outside cause; (2) on cross sections, the process in (1) can continue until a complete discontinuity is obtained in the isentropic and isotach fields; this discontinuity appears in the middle of a region of increasing anticyclonic vorticity in accord with the vorticity conservation law.

The discontinuity itself, appearing as a line on weather charts and cross sections, represents an actual finite zone within the atmosphere where strong gradients of potential temperature are developed and continued as long as the flow concentrates isentropes and isotachs in the region.

Mixing across the concentration region then transforms the cyclonic wind shear across the discontinuity (usually situated in a zone of anticyclonic vorticity) into large cyclonic relative vorticities which results in much larger values of potential vorticity than had previously existed in the system.[1] This vorticity creation involves the generation of new values of $\frac{\zeta + f}{D}$, a process which violates the potential vorticity conservation law. Thus the conservation law holds completely within the regions adjacent to the discontinuity and, indeed, up to the discontinuity itself. It does not hold, however, in the discontinuity and it is suggested that, here, large values of the potential vorticity are actually created.

Meridional cross sections showing the vertical distribution of potential temperature and wind speed are used as analysis tools throughout the discussion. Various cross sections from earlier studies as well as model diagrams are used to illustrate the mechanism described here.

The premise that the upper troposphere follows vorticity conservation and the thermal wind relation is not new; the appearance of new high values of potential vorticity in the jet stream vicinity has been noted as well (Reed, 1955).

Having stated the conclusions which will be shown, let us now develop the argument in detail.

---

1. The term $\frac{\zeta + f}{D}$, represents the vertical component of the potential vorticity of a fluid particle; ζ represents the relative vertical vorticity component (expressed as $\frac{\delta v}{\delta x} - \frac{\delta u}{\delta y}$ in rectangular coordinates), f is the vorticity due to the earth's motion, and D is the vertical distance between material surfaces. The conservation equation for this component may be written $\frac{d}{dt}\left(\frac{\zeta + f}{D}\right) = 0$. Thus when D changes, the quantity $(\zeta + f)$ changes in the same sense in accord with the conservation law. Potential vorticity thus is distinguished from absolute vorticity, $(\zeta + f)$, representing the sum of relative and earth-derived vorticities.

Cross Sections and a Paradox

In upper level shear zones where isentropic surfaces are closely spaced in the vertical (D is small), potential vorticity conservation requires that absolute vorticity, $(\zeta + f)$, also be small. However, very large values of ζ or $(\zeta + f)$ are observed on cross sections within these zones. Several detailed synoptic studies within recent years have demonstrated this last statement. Hsieh (1950) notes that ζ increases within such zones, while a study by Reed and Sanders (1953) shows that $(\zeta + f)$ is generated within a mid-tropospheric frontal zone; Petterssen (1955) shows a similar, more pronounced, generation of absolute vorticity.

In an outstanding case of shear line formation in the upper atmosphere, Hsieh (1950) illustrates the hypothesis that upper troposphere shear lines can be extensions of surface frontal surfaces. In the example, there is pronounced downward motion of isentropic surfaces below 350 mb during the entire study, which leads to a packing of isentropes between 600 and 700 mb. Hsieh notes this observed so-called "direct" solenoidal circulation is a necessary, but not sufficient, condition for formation of a shear line in the upper atmosphere. Hsieh also remarks on the observed (horizontal) divergence below about 400 mb, recalling that the vorticity equation requires a <u>decrease</u> of originally-existing relative cyclonic vorticity, ζ, in the absence of meridional motion (f remains constant). Then, he goes on, the <u>observed increase</u> of ζ near the trough line at the 500 and 700 mb surfaces must be due to downward transport of ζ

from upper levels, in excess of the decrease accompanying the lower-level divergence.

We note that Reed and Sanders (1953) do not agree with Hsieh in regard to the origin of the relative cyclonic vorticity present here. Reed and Sanders describe the generation of absolute vorticity ($\zeta + f$) in a mid-tropospheric frontal zone, and demonstrate that the observed increase of cyclonic ($\zeta + f$) is primarily generated locally, rather than being pre-existing cyclonic vorticity that is transported downward into the shear line region.

Austin (1954) states, in a case of strong upper level trough development, that a large amount of absolute vorticity is created in the upper troposphere, and that this arises from subsidence in the vicinity of the upper trough where horizontal divergence is small. He notes that the shear vorticity varies rapidly in the horizontal, requiring a close network of values to portray the actual relative vorticity distribution.

Petterssen (1955) illustrates the same view with a case history showing a situation where ($\zeta + f$), from the surface to 200 mb, increases more than fourfold in a 24-hour period; he shows that vast amounts of ζ were created and dispersed over large areas surrounding a developing cyclone center. He further shows that ζ was created in a subsiding region to the west of an approaching upper trough; thus when this newly-created mid-troposphere moved over a surface disturbance, very rapid cyclogenesis was initiated. The storm developed was then made self-perpetuating by the thermal advection. Newton (1954) also illustrates these points with a different synoptic study.

The paradox is recognized by Reed (1955) leading to these statements regarding the validity of vorticity conservation within certain tropospheric zones: p. 233: "... the equation expressing the conservation of partial potential vorticity[2], which has provided the basis of numerous studies, including recent work on numerical prediction ... does not adequately describe developments within a highly baroclinic region." p. 236: "... The potential vorticity on pressure surfaces (partial potential vorticity) is poorly conserved in strong baroclinic zones."

Reed notes as well that the observed increase of horizontal temperature gradient (on isentropic surfaces in upper-level frontogenetic regions) is due to a steepening of the slope of isentropic surfaces as a result of an "indirect"[3] solenoidal circulation. He finds the upper-level frontal zone is a dynamically-produced phenomenon which intensifies as the storm intensifies, and the circulation within it is the reverse of that required for energy release in the classical sense. Further, the frontal zone does not separate air of immediate polar and tropical origin.

---

2. Reed defines this as $(\zeta_p + f)\,{}_p/\partial\theta$, where $\zeta_p = \left(\frac{\partial u}{\partial x} - \frac{\partial u}{\partial y}\right)_p$ is measured on a constant pressure surface.

3. Murray and Daniels (1953) show cross stream velocities in a jet which indicate a direct thermal circulation above or below the jet at the jet "entrance" (looking downstream) and an indirect thermal circulation at a jet "exit." Newton (1955) discusses this also.

A Model that Resolves the Paradox

A basic tool for this discussion will be the meridional cross section showing the vertical distribution (z-direction) of wind speed and potential temperature with latitude. It is assumed that such a section, oriented perpendicular to the latitude circles (y-direction) is also perpendicular to the jet stream flowing in the westerlies belt of winds at mid-latitudes (in the x-direction). Having assumed the flow is essentially west-east, it follows that v, the north-south wind velocity, is much smaller than u, the west-east velocity. We also assume $\frac{\partial u}{\partial x}$ is much smaller than $\frac{\partial u}{\partial y}$. The cross sections studied here will be a time series occurring along a single meridian. The flow is assumed to be isentropic, so that surfaces of constant potential temperature (isentropes in cross section) will be material surfaces. Thus in the vorticity equation

$$\frac{d}{dt}\left(\frac{\zeta + f}{D}\right) = 0 \tag{1}$$

D refers to the normal distance between two adjacent surfaces of potential temperature. In the equation above, the relative vorticity is given by

$$\zeta = -\frac{\partial u}{\partial y} \tag{2}$$

and f is the Coriolis parameter which is assumed constant. The derivative in (1) is the material derivative.

We also assume that the thermal wind equation holds[4]

$$\frac{\partial u}{\partial z} = -K(z)\frac{\partial T}{\partial y} \tag{3}$$

where T represents temperature and z represents height.

For simplicity we assume

$$\frac{\partial u}{\partial z} = -K\left(\frac{\partial \theta}{\partial y}\right) \tag{4}$$

where K is a constant and θ is potential temperature. As an initial assumption, when $D = D_o$, $\zeta = 0$. This is equivalent to an initial or boundary condition where all isentropes are a distance D_o apart in the vertical, and the velocity is constant in the horizontal at a particular level. Thus Eq. (1) becomes

$$\frac{\zeta + f}{D} = \frac{f}{D_o} \tag{5}$$

The following quantities will be used in the further development:

H	vertical distance between isotachs, lines of constant wind speed.
W	horizontal distance between isotachs.
L	horizontal distance between isentropes.
Δu	constant increment between isotachs.
$\Delta \theta$	constant increment between isentropes.

---

4. This is essentially the geostrophic approximation. The paper, "The Bathystrophic Storm Tide," by Freeman, Baer, and Jung (1957) shows that fluid systems seek geostrophic flow. Experience in meteorology shows the same thing.

Eq. (5) becomes

$$\frac{\frac{-\Delta u}{W} + f}{D} = \frac{f}{D_o} \qquad (6)$$

and Eq. (4) becomes

$$\frac{\Delta u}{H} = -K \frac{\Delta \theta}{L} \qquad (7)$$

Rewriting (6) and (7) ,

$$D = D_o \left(1 - \frac{\Delta u}{f W}\right) \qquad (8)$$

$$H = -\frac{1}{K} \frac{\Delta u}{\theta} L \qquad (9)$$

Eqs. (8) and (9) indicate that when the horizontal gradients of wind and potential temperature (W and L) are known in a plane, then it is possible to determine the vertical gradients of wind and potential temperature (D and H) across the plane. Thus additional horizontal surfaces, above and below the original, can be drawn, and the horizontal distribution of wind and potential temperature can be determined for the new surfaces. The "chain" can be continued indefinitely, as long as it is valid to assume the vorticity equation and the thermal wind relationship.

To demonstrate this relationship, the initial conditions of the air are shown in Figure 1. Figure 5 has been prepared by use of a nomogram, shown in Figures 3 and 4, which is based on Eqs. (8) and (9) . The values in Figure 2 represent the boundary conditions, while the remaining values in Figure 5 are

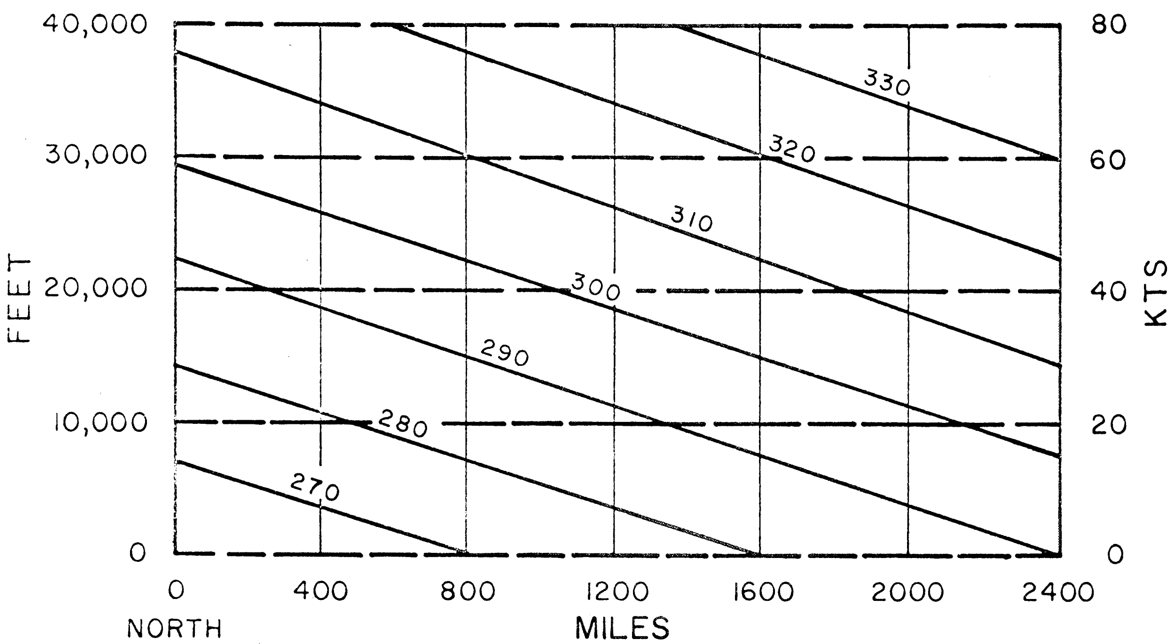

LEGEND

Isentropes and isotachs in a cross section in middle latitudes. The horizontal scale is in miles.

FIGURE 1

ISOTACHS AND ISENTROPES

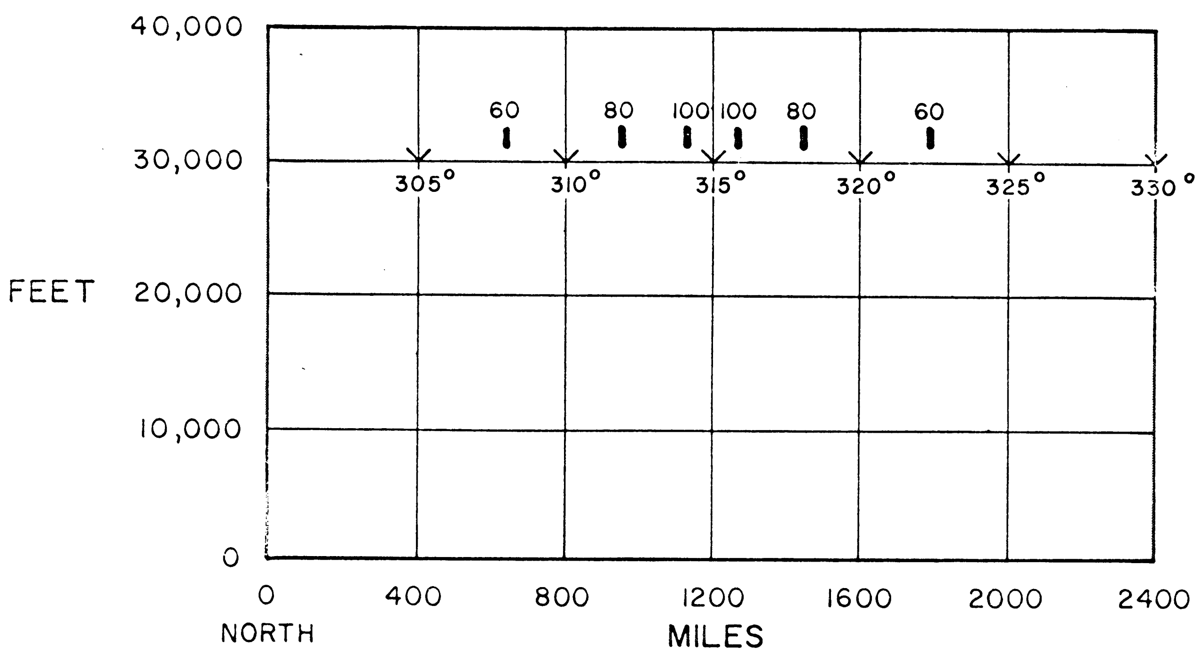

LEGEND

The winds and temperatures at one level are given and it is assumed that the same air as the original is at that level.

FIGURE 2

THE DISTURBED WIND FIELD

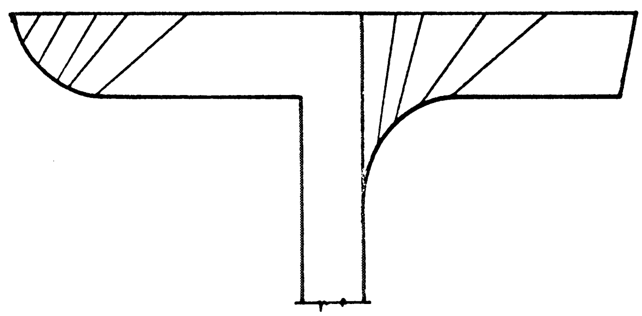

LEGEND

The scale for relating vertical distance of isentropic surfaces to horizontal wind gradients.

FIGURE 3

THE GRAPHICAL COMPUTER

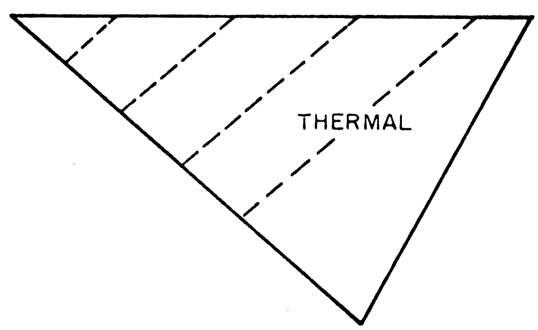

LEGEND

The scale for relating horizontal temperature gradients to vertical wind gradients.

FIGURE 4

THE GRAPHICAL COMPUTER

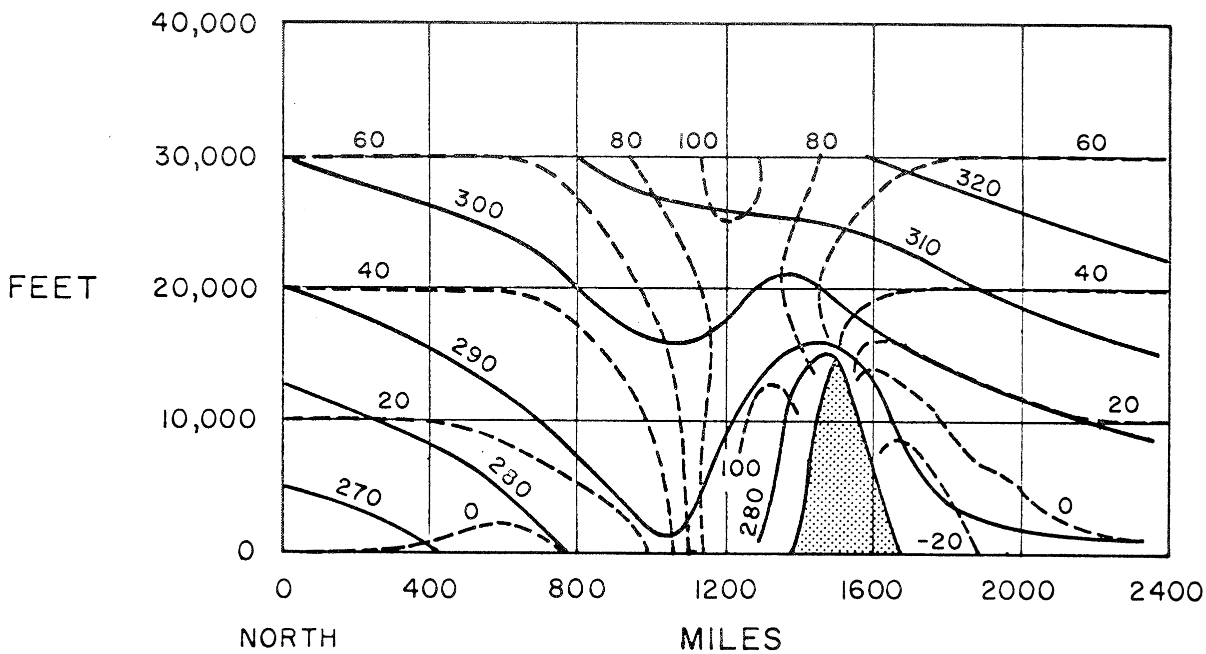

LEGEND

The results of the computation indicated in Figure 2. Note bulges in the isentropic surfaces and the shaded are where the computation must be adjusted with a new physical assumption. The discontinuities can be avoided by limiting the study to the upper 15,000 feet.

FIGURE 5

THE NEW STEADY STATE

computed values.

The initial and boundary conditions in Figure 1 were carefully selected to avoid discontinuities in the flow. However, the wind speed increase has resulted in cold air moving to a position under the axis of the jet stream. This indicates that, in actual synoptic examples, one can expect limited southward motion of cold air at the surface to be related to increased wind speeds aloft. In Figure 5 , there is even a hint of a cut-off dome of cold air to the right of the jet stream axis.

The discontinuity of Figures 6 , 10 and 11 may be explained through the following considerations. The thermal wind equation requires, for the normal tropospheric temperature gradient across mid-latitudes, that the wind speeds increase with height. Such a localized increase in wind speeds result in an anticyclonic wind speed shear and a decrease in cyclonic vorticity. Correspondingly, a decrease in spacing between isentropic surfaces must occur, thus strengthening the potential temperature gradient (horizontally as well as vertically); a stronger temperature gradient requires an increase in the vertical wind shear so that the process is self-perpetuating. Eventually, the thickness, D, between isentropes becomes zero so that a discontinuity in potential temperature has been formed which corresponds to the shear line formation process of Hsieh, or the mid-trospheric frontal zones described by Reed and Sanders. This could be the vortex sheet formation process which, in a theory of Rossby, must somehow be a source of new potential vorticity[5].

---

5. Verbal communication, 1952.

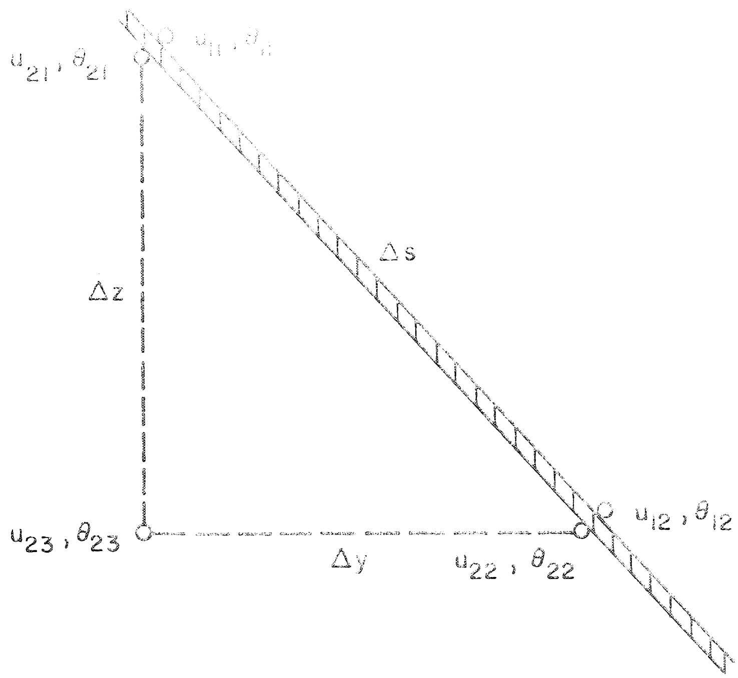

LEGEND

The new physical assumption is that an interface is created which is a vortex sheet and a temperature discontinuity.

FIGURE 6

INTERFACE CONDITIONS

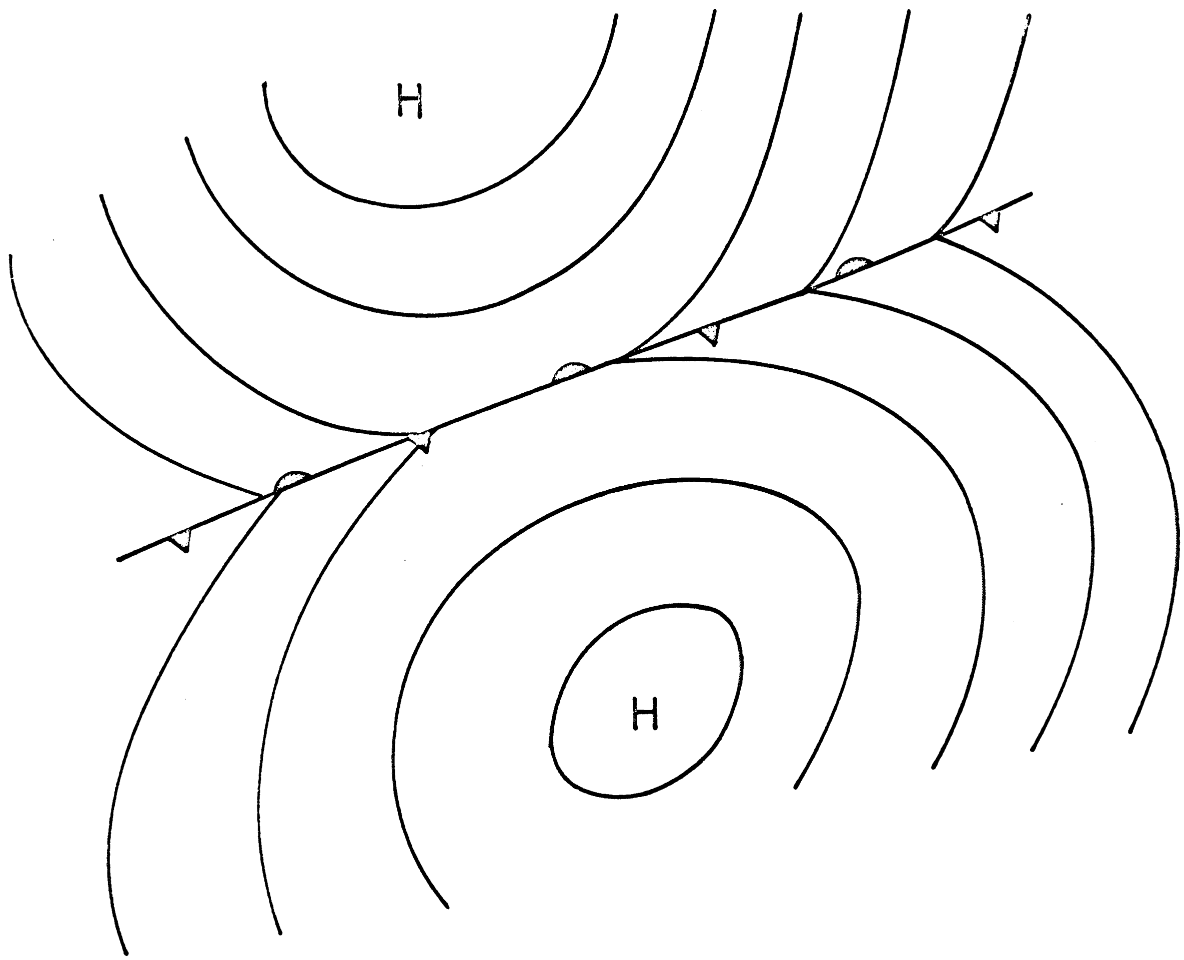

LEGEND

Temperature and wind discontinuities in regions of maximum anticyclonic vorticity in two fluids is not really a new meteorological concept. This is typical of a very common analysis of surface pressure.

FIGURE 7

FRONT IN ANTICYCLONIC VORTICITY

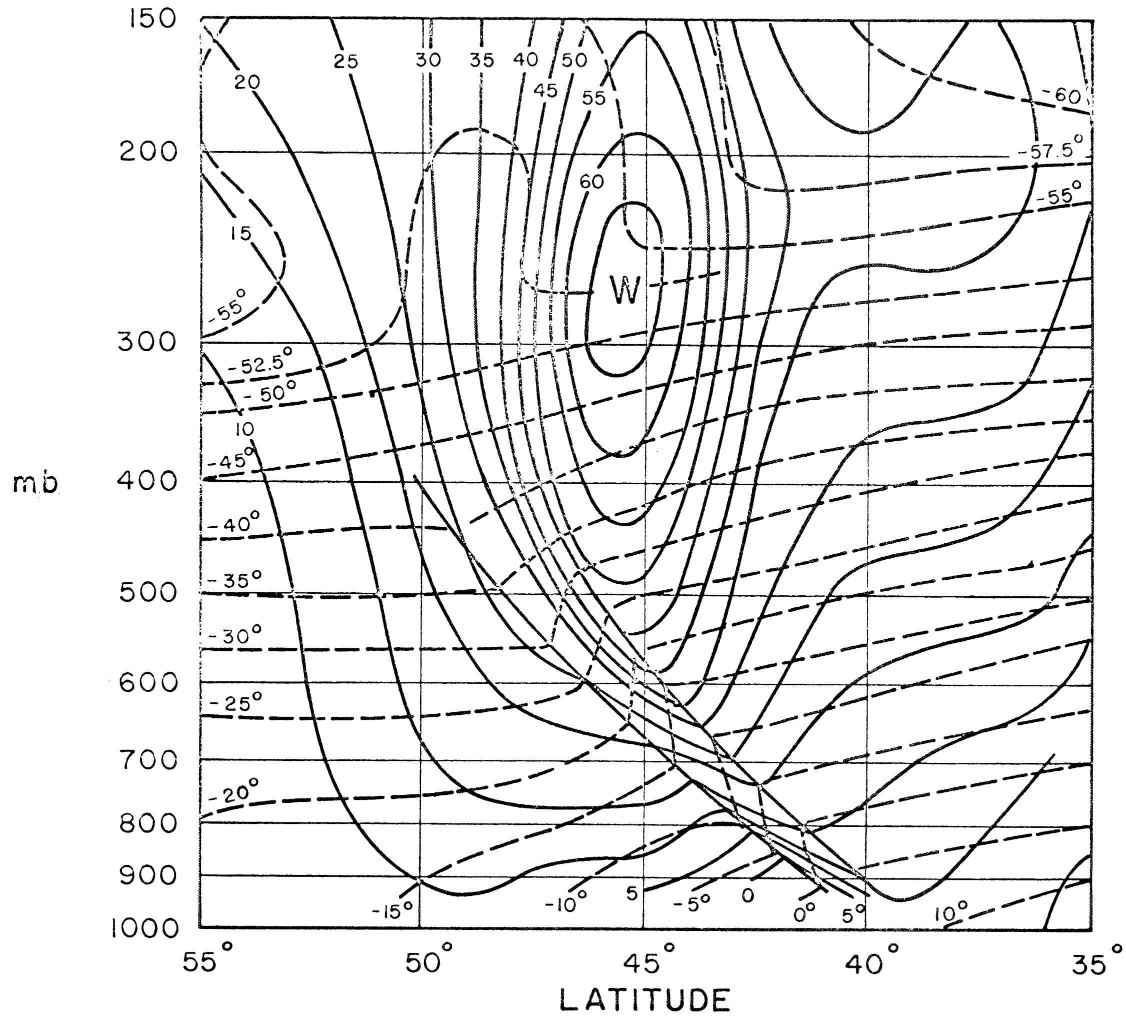

LEGEND

Bjerknes (1951) analysis of a frontal surface. Note that the maximum discontinuity is in a region of anti-cyclonic wind shear.

FIGURE 8
JET STREAM AND FRONT

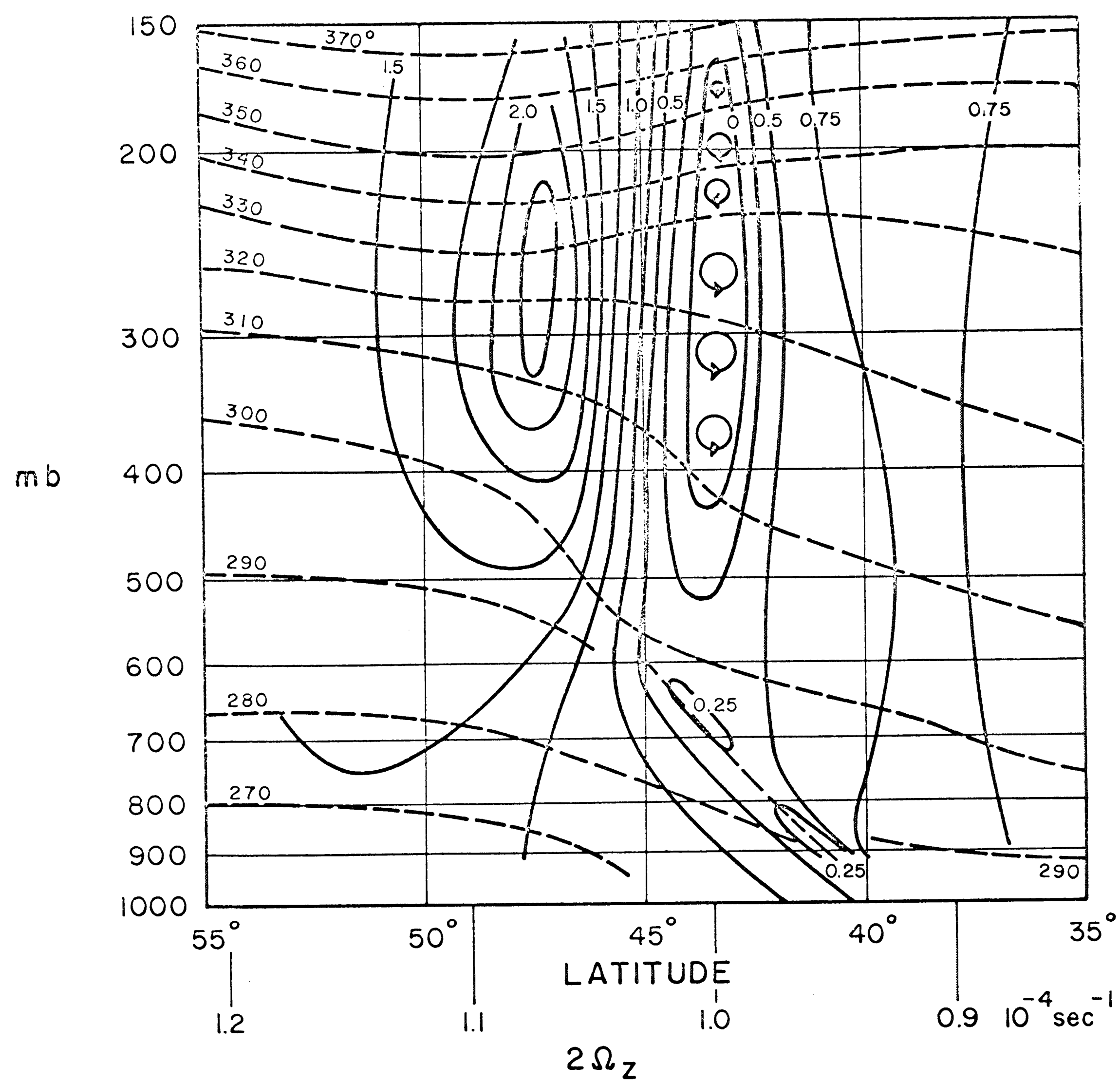

LEGEND

Absolute vorticity chart for Figure 8, also from Bjerknes (1951), confirming that anticyclonic (i.e., values less than value plotted on bottom) vorticity is found near the front.

FIGURE 9

VORTICITY DISTRIBUTION

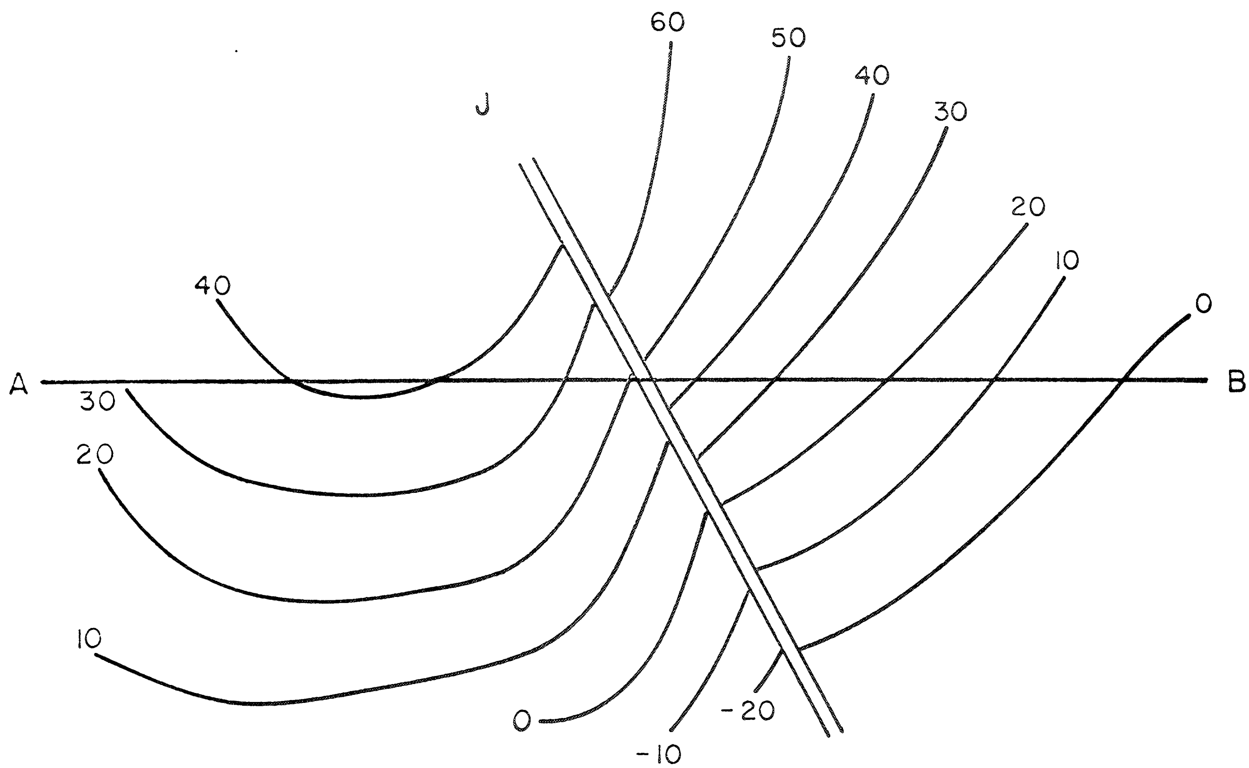

LEGEND

A model of a front similar to the actual case outlined in Figure 8.

FIGURE 10

MODEL JET STREAM AND FRONT

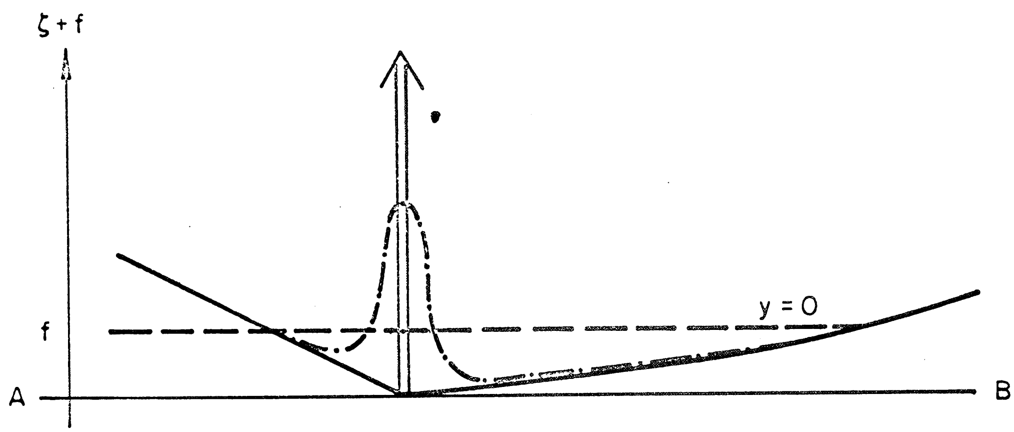

LEGEND

The delta-function type vorticity distribution at the discontinuity with an indication of the result of diffusion of vorticity from the finite circulation per unit length.

FIGURE 11
DIFFUSION OF VORTICITY

Through the mutual interaction of vorticity conservation and the thermal wind relationship it has been demonstrated that vortex sheets are forced by the pinching out of isentropic layers, and that the velocity distribution thus becomes discontinuous. This discontinuity region is surrounded by closely-spaced isentropic surfaces, and is imbedded in a region of anticyclonic vorticity. There can be <u>cyclonic wind shear</u> across the discontinuity, but no cyclonic vorticity.

The nature of this discontinuous wind velocity distribution should be considered. The magnitude of the discontinuity depends on the scale of the chart or cross section on which data are entered. Thus very sharp discontinuities drawn on weather charts or sections of usual scale become less sharp when drawn to larger scale. These discontinuities, when considered in the actual atmosphere represent zones of finite thickness over which the given change in wind occurs. The same applies for temperature discontinuities. Figure 7 serves as a reminder that fronts in regions of maximum anti-cyclonic vorticity are not complete physical paradoxes.

Intense mixing within these zones of discontinuity is commonly observed; it is postulated here that this mixing represents the agency whose action creates cyclonic potential vorticity within the zone. In the gross picture then, potential vorticity is essentially conserved while the model developed here explains the observed generation of new cyclonic vorticity in regions of discontinuous wind and temperature, which represent small finite portions of the gross picture. The final conditions will be much like those shown in Figure 8 and 9 which were taken from Bjerknes (1951).

The Model and the Atmosphere

This model can be shown in actual operation in the atmosphere by referring to actual synoptic situations which have been investigated in detail and the results published by various authors as cited below.

Let us examine the basic premises of the model in the light of previous investigations:

(1) The atmosphere must satisfy both the conservation of vorticity and the thermal wind relation:

The success of current numerical weather prediction techniques is evidence that the atmosphere behaves roughly in accord with the absolute vorticity conservation principles advocated by Rossby and adopted as the basis for the NWP models.

There is need for considering the thermal wind relation along with the vorticity conservation principle; however, as shown by Sawyer and Bushby (1953), for example, who point out that a baroclinic model of the atmosphere which includes the thermal wind (restricted, however, to a single direction) appears to remedy prediction discrepancies of NWP barotropic models without thermal wind considerations.

Another example of the approach to the atmosphere from a dynamic point of view is given by Newton, et al (1951). They describe pressure trough deepening which was accompanied by baroclinicity in the upper troposphere increased with time in the shear line region, indicating the thermal wind relation was in operation.

Reed and Sanders (1953) describe vertical shear terms in their dynamic analysis of a synoptic situation. These terms act to transform vorticity about a horizontal axis to vorticity about a vertical axis. Thus they illustrate a horizontal gradient of vertical velocity (i. e. sinking motion) that gives rise to a changing (intensified) horizontal temperature gradient leading to a marked change (increase) in vorticity, as in our model.

Austin (1954) notes that upper trough development, such as described by Reed and Sanders (1953), is accompanied by the creation of an upper-level zone (400 - 600 mb) of strong temperature contrast just upstream from the developing trough or shear line. The thermal gradient decreases markedly toward the earth's surface.

Petterssen (1955), concerned only indirectly with upper troposphere development, considers both dynamic and thermal aspects in his analysis of cyclogenesis.

Reed (1955) notes that air particles acquired greater thermal stability in order to conserve potential vorticity during development of an upper-level region of frontogenesis. Reed clearly calls for the simultaneous operation of vorticity conservation and the thermal wind relation.

In starting from purely thermodynamic considerations, on the other hand, McIntyre (1953) takes up the problem of converting potential into kinetic energy in the atmosphere originally investigated by Margules and Normand, and concludes that dynamic, as well as thermodynamic factors must be taken into account. Because of the earth's rotation, final equilibrium will not be attained when the enthalpy is at a minimum, but rather when the newly-created kinetic energy has organized itself in such a way that the thermal wind equation is satisfied.

(2) The compaction of isentropic layers underneath and to the left of the jet stream (facing downstream) during development of upper tropospheric shear line:

Rossby (1951) has shown that in order to achieve the observed vertical concentration of momentum in oceanic and atmospheric jet streams, currents tend to approach the "critical" velocity which leads to a minimum transfer of momentum and in many cases must shrink vertically to develop a sharp velocity maximum at or below the free surface (in this case the tropopause), for the general case of a continuous fluid density distribution. Reed and Sanders (1953) demonstrate that the underlying mechanism for their case of intense frontogenesis at 500 mb involves a cross stream gradient of sinking motion with strongest subsidence at the warm edge of the frontal zone. Austin (1954) calls attention to the importance of this region in which subsiding motion initiates the frontogenesis. Reed (1955) presents an outstanding example of subsidence in such a region. Pothecary (1956) provides evidence for descending motion of air as it approaches the jet stream from the left (looking downstream) in the form of moisture records on flights in this region. The extremely dry air here indicates subsidence is occurring. Newton (1954), p. 458-459, discusses other evidence of this feature as well. His Figure 13a, when adopted for frontogenesis conditions, illustrates this condition, as does Figure 10 of Reed (1955).

(3) The "self-perpetuating" feature brought about through interaction of vorticity-conservation and the thermal wind effect:

Petterssen (1955) considers upper tropospheric processes affecting surface cyclogenesis. He suggests that advection of vorticity over an incipient system initiates the development; at this time the thermal advection is very small. However, once initiated, the developing cyclone distorts the temperature field so that temperature advection becomes a prominent factor in the cyclogenesis, and "in Sutcliffe's terminology, the system has become self-developing." Since the upper tropospheric process we are describing is connected with surface frontogenesis or cyclogenesis (see Austin, 1954; Reed, 1955), Petterssen's observations support the self-perpetuating feature of our proposed model. The confluence mechanism of Namias and Clapp, which accounts partly for concentrating the temperature field in the middle troposphere, is necessary for frontogenesis according to Newton (1954). This is an essential feature linked with vertical as well as horizontal variations in the wind field. It acts in addition to those factors which are significant in bringing about changes in vertical shear and stability.

(4) The weather chart or cross section discontinuity is actually a finite zone where wind and temperature have very large, although finite, gradients:

Hurst (1952, 1953) describes the microstructure of winds across a strong jet stream at 300 mb. The winds shown here present a continuous distribution when drawn in large-scale; in weather-chart scale, however, this would have been a pronounced discontinuity.

(5) <u>Mixing occurs across the zones of high wind shear</u>:

In the papers presented at the February 20, 1952 meeting of the Royal Meteorological Society, the topic of "Meteorology and the Operation of Jet Aircraft" was discussed. The remarks by several authors concerning the occurrence of clear air turbulence, as well as observations given relating place of occurrence to the jet stream axis, lends support to the hypothesis that clear air turbulence is the sensible manifestation of the mixing process across wind shear zones as postulated in our model. An article by Bannon (1952) illustrates that observed clear air turbulence occurs in the regions anticipated by our model's mixing region. The second of two possible mechanisms to explain clear air turbulence proposed by Scorer (1952) involves folding of stratospheric air beneath tropospheric air, producing static instability causing the turbulence. This folding process is similar to the process postulated by Reed (1955) in explaining upper level frontogenesis. Scorer continues that this "folding process" may continue for a long time so that new instability is continuously generated.

Arakawa (1953) notes the work of Bannon in clear air turbulence, who concluded that clear air turbulence is associated with wind shear in the vertical. Arakawa notes that cases of clear air turbulence also occur with wind shear in the horizontal, and sets up an equation for critical cyclonic shear to produce such turbulence. Values of critical shear which Arakawa thus determines compare favorably with those of Bannon's diagram, where the tropopause is discontinuous near the jet stream. In almost every case of observed turbulence the isentropic shear or horizontal (wind) shear was large, occurring mostly on the low-pressure side of the jet stream where the shear is cyclonic in sense and excessive. He concludes, like Scorer, that such turbulence can occur in mixing of tropospheric and stratospheric air across "breaks" in the tropopause.

We do not concur with the view that the stratosphere is folded down into the troposphere; we maintain that the continued self-perpetuation of our model leads to vortex sheet formation which resembles the situation described by Scorer and Reed. We postulate that clear air turbulence is the mixing which occurs in the process of vorticity creation observed in the several cases described and permitted in our model.

In a brief discussion to be submitted in the near future, the effects of non-adiabatic heating on the model behavior will be illustrated and discussed. It will be shown that the model is capable of incorporating these effects while retaining its basic approach. Thus the model permits such outside influences to enter into consideration, which adds a very desirable feature to the model in its application to the actual atmospheric behavior.

Including Heating Effects in the Model

Up to this point the discussion has centered on how a cross section of atmospheric particles can change in response to basic physical laws. The hypothesized mechanics are shown to fit results of detailed synoptic studies published previously.

Now let us consider <u>why</u> the changes occur; if this can be answered to satisfaction, a potentially powerful forecasting technique has been developed.

From this point on in our discussion one previous assumption is dropped. Non-adiabatic effects are now considered, so that the resulting motion is no longer adiabatic. It will be necessary, then to follow the motion of material surfaces which may initially coincide with particular isentropic surfaces; however, these material surfaces later move through the isentropic surfaces and become deformed as the result of the non-adiabatic disturbing effects. The only such effects to be considered here will be those arising from non-adiabatic heating of the atmosphere.

If we think of the atmosphere as a dynamic system, non-adiabatic heating then resembles a forcing function. It is fairly well established in the study of dynamic systems that the long-term changes are closely related to the forcing function - more than to the details of the system dynamics. For example, in mechanical vibrations the particular phase of free vibration that was in effect at the initial time is less important than the history of the forcing function in determining future vibration behavior.

In the atmosphere, the long waves in the westerlies correspond to the free vibrations of the mechanical system. The analogy suggests that the initial phase or longitudinal positioning of the particular set of long waves enters into future long-term behavior only incidentally as is the case with initial phase of mechanical vibrations. Thus a mean atmospheric cross section in a sense filters out such incidental initial detail over an interval of time, in which many long waves have passed through the section. Heat added to the atmosphere during this time should exercise control over the changes in the cross section. In order to facilitate discussion of heating we need some new definition of layers.

The Mixed Layer

The model proposed here is a multilayered model of the atmosphere. In order to approximate known conditions in the atmosphere and various theories of local winds, it seems desirable to describe another distinct type of layer.

Mixing is the primary property of this layer and the temperature and momentum are functions of the height of the bottom and top of the layer, of the boundary conditions and of the vertical transport function of the layer. The whole layer must be considered as an entity. The upper and lower boundaries of the layer are easy to follow but the surfaces of constant potential temperature show very little organization.

Except in special cases a vertical description of the atmosphere will include both types of layer, usually more than one of each. Mixed layers are to be expected near the ground and in wind shear zones, and isentropic layers in the stratosphere.

The writer is quite aware of some of the troubles inherent in the study of mixed layers with a stable lid (as illustrated in "The Solution of Nonlinear Meteorological Problems by the Method of Characteristics," Freeman, 1951) and in geostrophic isentropic layers, as indicated in the contents of this paper. The jumps and roll waves behind a mountain and the vortex sheets formed when a jet is squeezed are very real physical phenomena.

The boundary between stable and mixed layers can be of several types and we consider two of them here.

(1) A lower layer of height $H(x, y, t)$ with $\Theta(x, y, t)$, $C_m(x, y, t)$ forms a boundary as shown in Figure 12. On this kind of boundary we have:

$$\frac{du_m}{dt} = -\frac{1}{\rho}\frac{\partial p}{\partial x} + fv + K\frac{\partial}{\partial z} u_m \left| u_m^2 + v_m^2 \right| - \frac{g(h_{m+1} - h_m)\frac{\partial \theta}{\partial z}}{\theta}\frac{\partial H}{\partial x}$$

$$\frac{dv_m}{dt} = -\frac{1}{\rho}\frac{\partial p}{\partial y} + fv + K\frac{\partial}{\partial z} v_m \left| u_m^2 + v_m^2 \right| - \frac{g(h_{m+1} - h_m)\frac{\partial}{\partial z}}{\theta}\frac{\partial H}{\partial y}$$

(2) Several isentropic layers meet a mixed layer, or two mixed layers meet (see Figure 13). This type of boundary results in mutual determination of boundary conditions and the mixed layer may possibly grow at the expense of the isentropic layers and occasionally vice versa (especially near discontinuities).

In dealing with a mixed layer from h_m to h_{m+1} we consider the following:

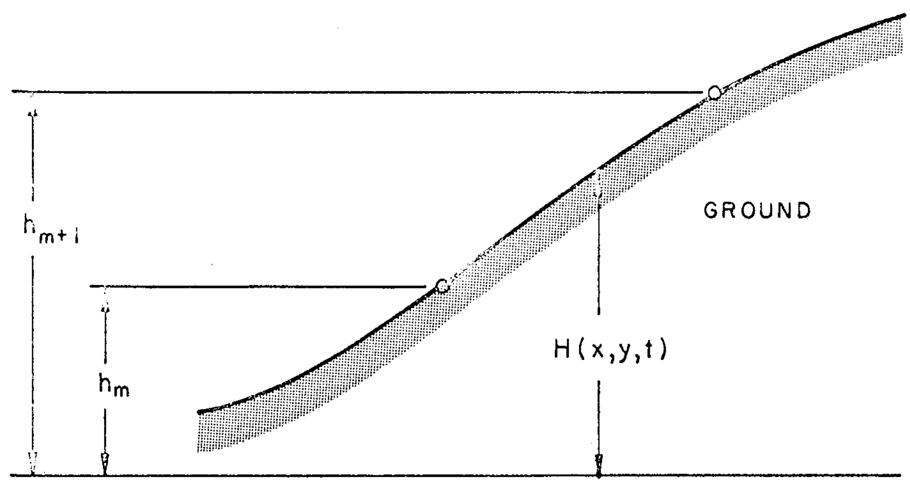

LEGEND

Isentropic layers meeting the ground.

FIGURE 12

LAYERS ON A SLOPING GROUND

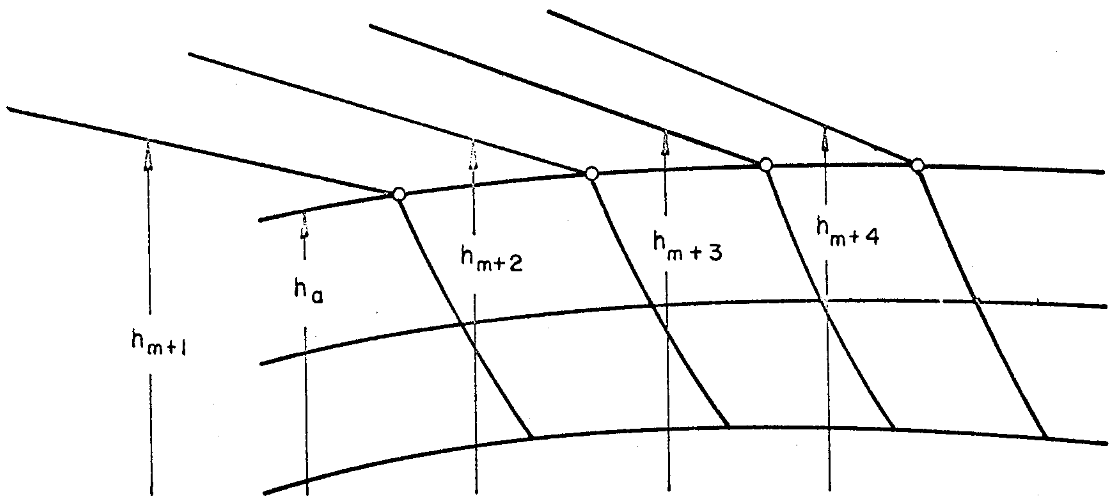

LEGEND

Different kinds of layers meeting. A mixed layer of height h_m and stable layers h_{m+1} to h_{m+4} .

FIGURE 13

STABLE AND ADIABATIC LAYERS

$\theta(Z) = H\ (h_m, h_{m+1}, \theta_m, \theta_{m+1},\ flux_m\theta, flux_{m+1}\theta, u_m, u_{m+1}, v_m, v_{m+1})$

$u(Z) = U\ (h_m, h_{m+1}, \theta_m, \theta_{m+1}, flux_m u,\ flux_{m+1}u, u_m, u_{m+1}, v_m, v_{m+1})$

$v(Z) = V$ (similar function)

Of course, this will usually be a relatively simple function like a linear or exponential θ and an Ekman spiral for u and v.

In this case we use integrated momentum and temperature equations as well as integrated continuity equations to find u_m, h_m, θ_m, etc. and to compute the needed Θ, U, V.

For example, the problems in the paper by Freeman (1951) are degenerate forms of these equations in which $h_m = 0$, $h_m = h$, $u_m = u_{m+1} = u$, $v_m = v_{m+1} = v$, and $\Theta = \theta_1 = \theta_m$.

In order to work with mixed layers and with thick stable layers it is handy to have an analytic form of the solution of the equation we have been discussing.

We rewrite the equations:

$$\frac{\partial \theta}{\partial y} = -K_1 \frac{\partial u}{\partial z} \qquad \text{(Thermal Wind)}$$

$$\frac{\partial \theta}{\partial z}\left(-\frac{\partial u}{\partial y} + f\right) = K_2 \qquad \text{(Vorticity Equation)}$$

If we differentiate the first equation with respect to y and the second with respect to x we get

$$\frac{\partial^2 \theta}{\partial y^2} = -K_1 \frac{\partial^2 u}{\partial z \partial y}$$

$$-\frac{\partial^2 u}{\partial z \partial y} = \frac{K_2 \Big/ \frac{\partial^2 \theta}{\partial z^2}}{\left(\frac{\partial \theta}{\partial z}\right)^2}$$

$$\frac{\partial^2 \theta}{\partial y^2} = \frac{K_1 K_2 \Big/ \frac{\partial^2 \theta}{\partial z^2}}{\left(\frac{\partial \theta}{\partial z}\right)^2}$$

If we set

$$\theta = F(y)\,G(z) + K_3 y + K_4$$

$$\frac{\partial^2 \theta}{\partial\ ^2} = F''G, \quad \frac{\partial \theta}{\partial} = FG', \quad \frac{\partial^2 \theta}{\partial\ ^2} = FG''$$

and our equation becomes

$$F''G = K_1 K_2 \frac{FG''}{(FG')^2}$$

$$F''F = \frac{K_1 K_2 G''}{G G'^2} = K_5$$

We have now succeeded in separating the variables in this equation and we can say

$$F''(y)\,F(y) = K_5$$

Or, if we multiply by F'

$$F''F' = \frac{K_5 F}{F}$$

$$\frac{F'^2}{2} = K_5 \log F + \frac{K_6}{2}$$

$$F' = \sqrt{2K_5 \log F + K_6}$$

We make a simple substitution

$$\log F = \overline{H}$$

$$\frac{F'}{F} = \overline{H}'$$

$$H' C^{H} = \sqrt{2 K_5 \overline{H} + K_6}$$

Now we set $w = \sqrt{2 K_6 \overline{H} + K_6}$ and find

$$\overline{H} = \frac{w^2 - K_6}{2 K_5}$$

$$\overline{H}' = \frac{2 \dot{w} w' - K_6}{2 K_6}$$

$$\frac{2 w w'}{2 K_5} C \frac{w^2 - K_6}{2 K_5} = w$$

The solution of this equation is the probability integral.

$$\int_{w_0}^{w} C \frac{w^2 - K_6}{2 K_5} = K_5 (y - y_0)$$

Returning to the equation in z we find

$$\frac{K_1 K_2 G''}{G'} = K_5 G G'$$

Or integrating we get

$$K_1 K_2 \log G' = \frac{K_5}{2} G^2 \log K_6$$

Simple transformation gives

$$\frac{G^{I} K_{1} K_{2}}{K_{6}} = C \frac{K_{5}}{2} G^{2} \text{ and } G^{I} = K \frac{1}{K_{1} K_{2}} C \frac{K_{5}}{2 K_{1} K_{2}} G^{2}$$

The solution to the equation is then:

$$\int_{G_0}^{G} C \frac{K_5}{2K_1 K_2} \eta^2 \, d\eta = z - z_0$$

Thus we have closed form equations giving the values of z and y for certain values of θ from these equations.

REFERENCES

Arakawa, H., 1953: Clear air turbulence near the jet stream. Quart. J. R. Meteor. Soc., 79, 162-163.

Austin, J. M., 1954: The forecasting significance of the Reed-Sanders article. J. Meteor., 11, 253-254.

Bannon, J. K., 1952: Weather systems associated with some occasions of severe turbulence at high altitude. Meteor. Magazine, London, 81, 97-101. (His Figure 3 appears in Quart. J. R. Meteor. Soc., 78, 441.)

Bjerknes, J., 1951: Extratropical cyclones. Compendium of Meteorology, Boston, American Meteorological Society, 577-598.

Freeman, Jr., J. C., 1951: The solution of nonlinear meteorological problems by the method of characteristics. Compendium of Meteorology, Boston, American Meteorological Society, 421-433.

Freeman, Jr., J. C., L. Baer, and G. H. Jung, 1957: The bathystrophic storm tide. J. Marine Res., 16, 12-22.

Hsieh, U., 1950: On the formation of shear lines in the upper atmosphere. J. Meteor., 7, 382-387.

Hurst, G. W., 1952: The profile of a jet stream observed 18 January 1952. Quart. J. R. Meteor. Soc., 78, 613-615.

Hurst, G. W., 1953: The profile of a jet stream observed 1 September 1952. Quart. J. R. Meteor. Soc., 79, 407-411.

McIntyre, D. P., 1955: On the baroclinic structure of the westerlies. J. Meteor., 12, 201-210.

Murray, R., and S. M. Daniels, 1953: Transverse flow at entrance and exit to jet streams. Quart. J. R. Meteor. Soc., 79, 236-241.

Newton, C. W., 1954: Frontogenesis and frontolysis as a three-dimensional process. J. Meteor., 11, 449-461.

Newton, C. W., 1955: An investigation of cyclone development. Storm No. 5. University of Chicago Technical Report 5, Contract AF 19(604)-1293, 45 pp.

Newton, C. W., N. A. Phillips, J. E. Carson and D. L. Bradbury, 1951: Structure of shear lines near the tropopause in summer. Tellus, 3, 154-171.

Newton, C. W., and J. E. Carson, 1953: Structure of wind field and variations of vorticity in a summer situation. Tellus, 5, 321-339.

Petterssen, S., 1955: A general survey of factors influencing development at sea level. J. Meteor., 12, 36-42.

Pothecary, I. J. W., 1956: Comments on "A study of characteristic type of upper-level frontogenesis." J. Meteor., 13, 316-317.

Reed, R. J., 1955: A study of a characteristic type of upper-level frontogenesis. J. Meteor., 12, 226-237.

Reed, R. J., and F. Sanders, 1953: An investigation of the development of a mid-tropospheric frontal zone and its associated vorticity field. J. Meteor., 10, 338-349.

Roberts, G. S., et al, 1952: Meteorology and the operation of jet aircraft. Quart. J. R. Meteor. Soc., 78, 427-456.

Rossby, C.G., 1951: On the vertical and horizontal concentration of momentum in air and ocean currents. 1. Introductory comments and basic principles with particular reference to the vertical concentration of momentum in ocean currents. Tellus, 3, 15-27.

Sawyer, J. S., and F. H. Bushby, 1953: A baroclinic model atmosphere suitable for numerical integration. J. Meteor., 10, 54-59.

Scorer, R. S., 1952: Comments on two possible explanations of clear-air turbulence. Quart. J. R. Meteor. Soc., 78, 449-450.

University of Chicago, Staff Members, Department of Meteorology, 1947: On the general circulation of the atmosphere in middle latitudes. Bull. Amer. Meteor. Soc., 28, 255-280.

APPENDIX B

THEORETICAL CONSIDERATIONS RELATED TO VERY HIGH ALTITUDE ATMOSPHERIC MOTION

by

John C. Freeman, Jr. and Peter Hanna

Introduction

The major supporting theory for our premise that energy need not be transported downward is given in the main body of our report. The different theoretical considerations reported in this Appendix support the theory and to some extent the observations reported.

First, we remind all meteorologists that response of a fluid system to a sustained pressure gradient is multiplied as you descend in the fluid and it is only complete de-coupling that allows complete compensation such as between ocean and atmosphere.

Next we give some theoretical support to the 26 month equatorial wind cycle.

The third theoretical consideration involves a theory of flow in the ionosphere with a mixture of ions and neutral particles.

The final discussion adds the theory for unsteady motions of atmospheric cross sections.

All of these theories lend support to the interaction between the higher and lower atmosphere and to each other. For example, at the equator the equation for time dependent motion in a cross section changes to a wave equation for vertical motion of wind. The ion-neutral flow equation is compatible with the theory of heating and subsequent slow-down postulated as the primary effect of short wave radiation on the atmosphere.

A New Look at Low Level Response

The work of Wexler (1950) considers the motion of a lower layer of fluid when there are density and height changes in an upper layer. He draws the conclusion that a large wind change in a layer of very low mass will not lead to a significant change in wind or pressure in a lower layer of large mass. The difference between Wexler's and this work is that we consider the ionosphere heated and the density "increased" while Wexler considers it heated and the pressure decreased.

It is common to upper air studies to assume that low energy supply and small pressure changes must result from high layers. If we consider adiabatic layers then we have a paradox. The top of an adiabatic layer near zero pressure has a much smaller density than the bottom. A sustained pressure gradient above the surface results in a height gradient of a constant pressure surface. This height gradient is the same throughout the fluid and the change in wind will be the same at every level. Thus a very small pressure gradient at upper levels can result in a very large pressure gradient in the lower levels in anadiabatic (barotropic) layer.

The usual argument against adiabatic layers in the atmosphere is based on the fact that they reach zero density and pressure at too low a level (about 10 km) if you start from temperatures between -50° and $50^{\circ}C$ at any tropospheric level. However, if we investigate the atmosphere starting from the top we do not meet the same paradox.

We begin with a strongly distorted atmosphere of two adiabiatic layers, one with the potential temperature representative of 100 km and one with the potential temperature representative of the surface layer.

This model results in a potential temperature difference of 900° at the interface with the air in the lower layer at 200°.

Thus a height contour gradient in the upper fluid at this interface would be reduced by a factor of $\frac{200}{1100}$. This is a significant decrease in the height contour gradient but it is not small enough to back claims that there is no effect of a very small pressure change in the upper levels.

The unreality of the model can be modified extensively by consideration of many layers.

If we had three layers (for instance) we could have a 450° temperature change at the middle of the upper layer. Then we would have*

$$\frac{\partial h}{\partial x} \text{ middle } = \frac{650}{1100} \frac{\partial h}{\partial x} \text{ upper}$$

Then at the bottom of the middle layer we would have

$$\frac{\partial h}{\partial x} \text{ lower } = \frac{200}{650} \frac{\partial h}{\partial x} \text{ middle } = \frac{200}{1100} \frac{\partial h}{\partial x} \text{ upper}$$

Thus there would still be the same 17% of the 100 km height change at the troposphere. During solar disturbance contour height changes of several thousand feet in a few hours are not uncommon at 100 km; thus we can expect significant height changes in the stratosphere as a result of solar disturbances.

This is a statement of sweeping generality similar to those previous statements that effects cannot be expected in lower levels as a result of solar disturbances. Here, however, we have a theoretical development that predicts very large changes. We now have a problem of discovering why the changes are as small as they are.

The idea of horizontal dissipation of energy through vertically propagating sound or gravity waves must be viewed in light of the large geographic distribution of the disturbances being considered. Any dissipation mechanism could be in itself a significant source of solar effects on weather.

---

* $\frac{\partial h}{\partial x}$ is the slope of a surface of constant pressure.

Theory of the 26 Month Cycle

The alternating, descending westerlies and easterlies at the equator have been discovered by McCreary and discussed, and their longitudinal extension verified by Ebdon and Veryard (1961) and by Reed, Campbell, Rasmussen and Rogers (1961). These winds are a striking physical phenomenon and cry for a theoretical explanation as simple as the relation between the tilt of the earth's axis and the annual temperature cycle in middle latitudes. However, the theoretical evidence in this paper points to an explanation bearing a family resemblance to that for the semi-diurnal pressure wave in the tropics.

Near the equator (within about 10°) and all around the earth there is a region in which alternating bands of westerlies and easterlies overlie each other and move down. Each band is about 200 km wide and 10 km thick. They form descending waves with a period of 24 to 27 months. At the present time (and based on 56 months of data) 26 months is the accepted period.

There has been some difficulty in devising a physical mechanism that can bring about these bands or anything similar to them and most of the efforts toward explanation have centered on searches for forcing functions of 24 to 27 months period.

The present paper presents a model of the equatorial winds in which alternating easterlies and westerlies are possible. The model is very dependent on the equatorial environment and as a bonus the period of the oscillation between easterlies and westerlies is of the right order of magnitude.

We postulate a very stable and therefore nearly flat layer of the atmosphere at the equator. The stability is approximated by discontinuities in the potential temperature with differences $\Delta\theta$ above and below the layer of thickness 2D. We will make the gross (and probably unnecessary) assumption that the middle of this layer remains level.

All of the air of this layer has absolute vorticity $\zeta + \beta y = 0$ where $\beta = \frac{2\Omega}{R_E}$. In our case $\zeta = -\frac{\partial u}{\partial y}$. Thus the potential vorticity equation becomes $\frac{-\frac{\partial u}{\partial y} + \beta y}{2D} = 0$. In other words, convergence and divergence will not change the vorticity.

We can write

$$\frac{\partial}{\partial y}\left(-u + \frac{\beta y^2}{2}\right) = 0$$

or

$$-u + \frac{\beta y^2}{2} = \text{const.} = -u(a) + \frac{\beta a^2}{2}$$

where $u(a)$ is the wind velocity at $y = a$.

If we assume there is a moving boundary at $y = a(t)$ (and $y = -a(t)$) of our layer and that $u(a) = \text{const.} > 0$ (or is a west wind) then we have

$$u(y) = u(a) - \frac{\beta a^2}{2} + \frac{\beta y^2}{2}$$

In particular we are interested in u when $y = 0$ or at the equator.

$$u(o) = u(a) - \frac{\beta a^2}{2}$$

We can see from this equation when a is small then $u(o) \approx u(a)$ (a west wind) and when a is large then $\frac{\beta a^2}{2}$ is large and $u(o) < 0$ (or we have east winds).

The "physical" appearance of the bands in east winds and west winds is symbolized in Figure " 1.

A "map" of the winds is given in Figure 2.

The stability is important in this discussion as a restoring force. This can be seen roughly by the high values of D at the equator. Actually, the stability is more important as a link between the pressure and the height of a potential temperature surface. Thus we have a mechanism for alternating west winds and east winds. We also can see that there is some reason to think it will oscillate.

In order to investigate the period of oscillation we need a little previous philosophical and mathematical discussion.

The theoreticians in oceanography have had a distinct advantage over their counterparts in meteorology. The only significant measure they have had of deep ocean currents has been a result of density measurement and the geostrophic approximation. Thus in oceanography

$$fu = -\frac{1}{\rho}\frac{\partial P}{\partial y} \qquad \text{and} \qquad fv = +\frac{1}{\rho}\frac{\partial P}{\partial x}$$

have always been acceptable approximations. The numerical weather prediction group led by Charney has also given the geostrophic

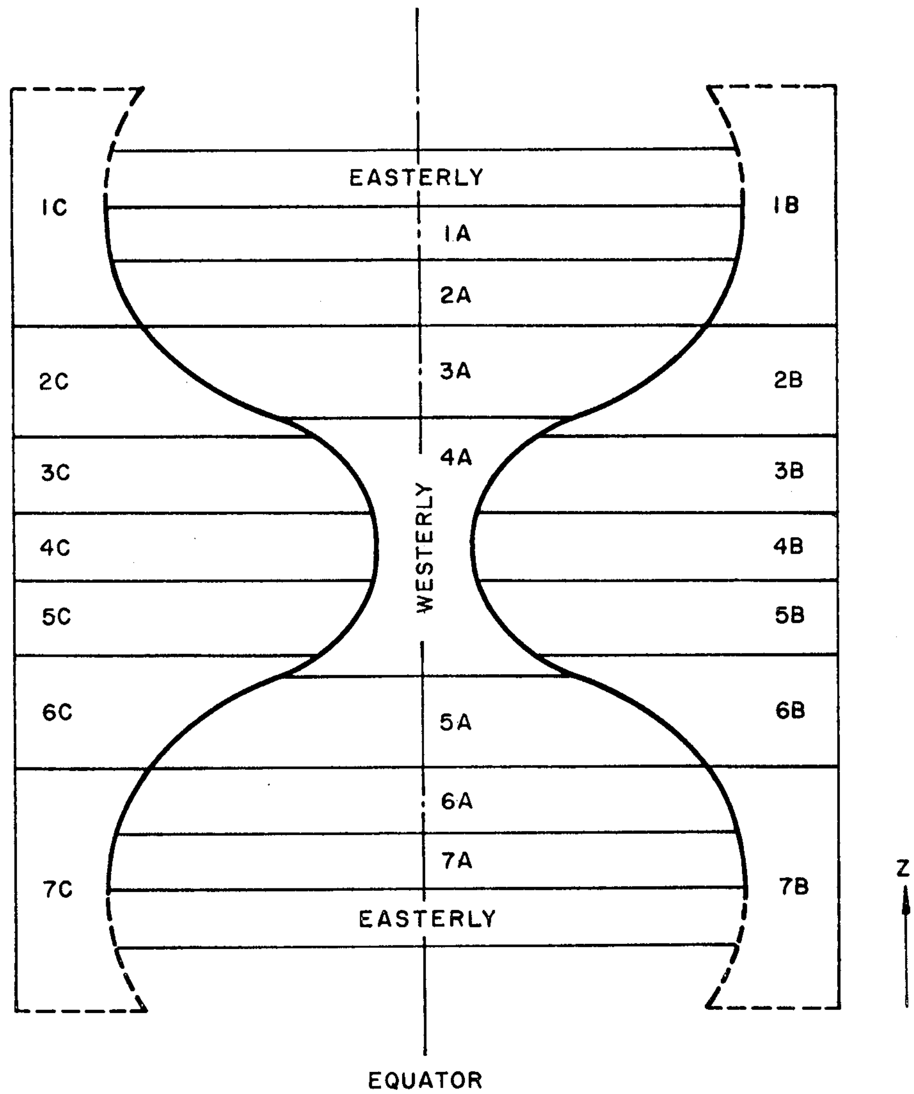

LEGEND

The bands or ribbons of stable air that undulate in width and thickness with the frequencies discussed in the model.

FIGURE 1

VERTICAL WAVE MODEL

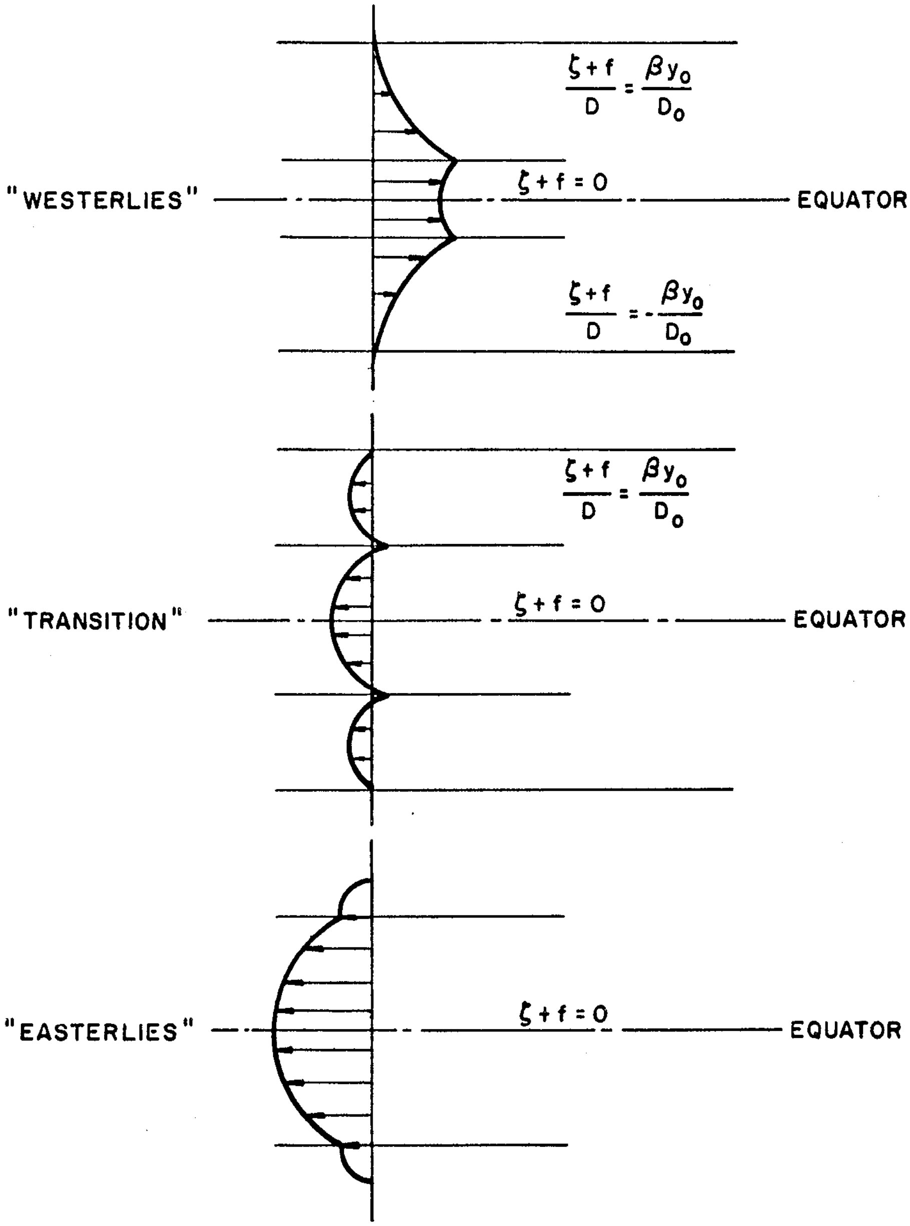

LEGEND

Horizontal drawings of the wind profiles in the model discussed in this paper. The boundary bands of $\frac{\zeta+f}{D}=\frac{\beta y_0}{D_0}$ are important in defining the westerlies, and the central band of $\zeta + f = 0$ is important in defining the easterlies.

FIGURE 2

BANDS OF VORTICITY

approximation an aura of respectability in meteorology. Freeman, Baer and Jung (1957) have shown that flow becomes nearly geostrophic rapidly when it is free to do so and, in addition, theories supporting it are given earlier in this paper. We are going to study a problem in which we can find u when the boundary a is known. Thus it will be to our advantage to use the approximation in the sense, "given the wind we use the geostrophic approximation to find the pressure."

Exactly on the equator this results in the statement

$$\frac{\partial p}{\partial z} = -2\Omega \rho g \tag{1}$$

This is a modification of the hydrostatic equation. This statement should also be true for several degrees of latitude away from the equator.

Near the equator we have

$$\frac{1}{\rho} \frac{\partial \rho}{\partial y} = - \beta y u \tag{2}$$

We are going to be considering a system in which alternating values of positive and negative u overlie each other so the best geostrophic approximation in the horizontal is

$$\frac{1}{\rho} \frac{\partial p \text{ hydrostatic}}{\partial y} = - \beta y u$$

In order to follow the north south motion of the boundary a we write

$$\frac{\partial a}{\partial t} = V$$

and

$$\frac{d}{dt} \frac{\partial a}{\partial t} = \frac{\partial^2 a}{\partial t^2} = - \frac{1}{\rho} \frac{\partial p}{\partial y} - \beta y u \tag{3}$$

Now we want to use a changed value of g.

$$gu = g + 2\Omega u$$

With our stable layer and no value of u we had

$$-\frac{1}{\rho}\frac{\partial p}{\partial y} = -\gamma\frac{\partial D}{\partial y} = -g\frac{\Delta\rho}{\rho}\frac{\partial D}{\partial y} = \text{hydrostatic pressure gradient}$$

Now with u having a value we can say

$$-\frac{1}{\rho}\frac{\partial p}{\partial y} = \gamma u\frac{\partial D}{\partial y} = -g\frac{\Delta\rho}{\rho}\frac{\partial D}{\partial y} - 2\Omega u\frac{\Delta\rho}{\rho}\frac{\partial D}{\partial y}$$

$$= -\frac{1}{\rho}\frac{\partial p\ \text{hydrostatic}}{\partial y} - 2\Omega u\frac{\Delta\rho}{\rho}\frac{\partial D}{\partial y}$$

$$= \beta yu - 2\Omega u\frac{\beta yu}{g}$$

Substituting this in Eq. (3) and putting a for y we get

$$\frac{\partial^2 a}{\partial t^2} = -\frac{2\Omega\beta u^2}{g}a$$

If we set

$$a = a_o \sin.\frac{2\pi t}{T}$$

$$\frac{\partial u}{\partial t} = \frac{2\pi a_o}{T}\cos\frac{2\pi t}{T}$$

$$\frac{\partial^2 a}{\partial t^2} = -\frac{4\pi^2 a_o}{T}\sin\frac{2\pi t}{T}$$

and we get

$$\frac{4\pi^2}{T^2} = -\frac{2\Omega\beta u^2}{g}$$

this gives

$$T^2 = \frac{4\pi^2 g}{2\Omega\beta u^2} \qquad\qquad T = \frac{2\pi}{|u|} \cdot \sqrt{\frac{g}{2\Omega\beta}}$$

Let us evaluate these terms:

$$1 \text{ day} = 8.64 \times 10^4 \text{ sec.}$$

$$1 \text{ yr.} = 3.153 \times 10^7 \text{ sec.}$$

$$\Omega = \frac{2\pi}{8.64} \times 10^{-4}/\text{sec.}$$

$$\beta = \frac{2\pi}{8.64 \times 3} \times 10^{-10}/\text{m. sec.}$$

$$g = 10 \text{ m/sec}^2$$

$$T = \frac{2\pi}{|u|}\sqrt{\frac{10 \times 10^{14}}{\frac{2 \times 2\pi \times 2\pi}{3 \times 8.64 \times 8.64}}}$$

$$= \frac{8.64}{|u|} \times 10^7 \sqrt{\frac{10 \times 3}{2}}$$

$$3.15 \times 2.16 = \frac{3.9 \times 8.64}{|u|}$$

$$|u| = \frac{3.9 \times 8.64}{3.15 \times 2.16} = \frac{33.69}{6.80} = 4.95$$

$$|u| = 5 \text{ m/sec. when } T = 26 \text{ mos.}$$

Our previous analysis has resulted in a reasonable frequency of vibration for the atmosphere and a mode of vibration that will allow alternate easterly and westerly winds at the equator.

The frequency was found to be in the range of interest resulting from the observed 24 to 27 month period of vibration of the equatorial winds.

We now need some way of arriving at a vertical wave length for the waves. The first analysis (for the period) has assumed that the stability is so great that no vertical motion is possible. Since we have an organized vertical motion resulting from the expansion and contraction of ribbons of fluid it is not surprising that in order to find the vertical motion of the waves we must give some vertical motion to the fluid.

We assume $w = \frac{\partial(h-h_o)}{\partial t}$ where h_o is the fixed height for a fluid ribbon at which some variable has a fixed value. Now h_{o2} and h_{o1} can be subtracted to give D_o and $h_2 - h_1 = D$. This can be expressed in differential form as $D \frac{\partial w}{\partial z} = D \frac{\partial^2 h}{\partial z \partial t} = \frac{\partial D}{\partial t}$.
The continuity equation for narrow levels is already sufficient to give us

$$\frac{\partial a D}{\partial t} = 0$$

The geostrophic approximation and previous considerations in the first equation of motion is sufficient to give us

$$\frac{\partial u}{\partial t} = -\left(2\Omega + \frac{\partial u}{\partial z}\right) w$$

We differentiate with respect z and get

$$\frac{\partial}{\partial z} \frac{\partial u}{\partial t} = -\left(2\Omega + \frac{\partial u}{\partial z}\right)\frac{\partial w}{\partial z} = -\left(2\Omega + \frac{\partial u}{\partial z}\right)\frac{1}{D}\frac{\partial D}{\partial t}$$

We know from continuity that $\frac{1}{a}\frac{\partial u}{\partial t} = -\frac{1}{D}\frac{\partial D}{\partial t}$ so we can write

$$\frac{\partial}{\partial t}\frac{\partial u}{\partial z} = +\frac{\left(2\Omega + \frac{\partial u}{\partial z}\right)}{a}\frac{\partial a}{\partial t}$$

We assume max $\frac{\partial u}{\partial z} >> 2\Omega$ so we can say $\dfrac{\frac{\partial}{\partial t}\frac{\partial u}{\partial z}}{\frac{\partial u}{\partial z}} = \dfrac{\frac{\partial a}{\partial t}}{a}$

This tells us that log $\frac{\partial u}{\partial z}$ - log a = const. in time

or $\frac{\partial}{\partial t}\log \frac{\partial u}{\partial z}/a$ = const.

or $\frac{\partial u}{\partial z}/a$ = const. $= \dfrac{\frac{\partial u}{\partial z}/max.}{a_{max.}}$

This equation can be written

$$\frac{\partial u}{\partial z} = \frac{\frac{\partial u}{\partial z\ min.}}{a_{max.}}\, a$$

If $u = u_0 \cos\left(\frac{2\pi z}{2} - \frac{2\pi z}{T}\right), \quad a = a_0 \sin\left(\frac{2\pi z}{2} - \frac{2\pi t}{T}\right).$

We find that this condition is compatible with any set of waves moving near the equator. In other words the vertical waves can have any speed depending on max $\frac{\partial u}{\partial z}$. Apparently the condition on $\frac{\partial u}{\partial z}$ is inherent in the driving function.

Earlier we presented a model of equatorial winds in which alternating easterlies and westerlies are possible. In addition, we found that frequency of vibration for reasonable values of $|u|$ was in the range of interest (i.e., 24 to 27 months observed).

Now we will apply the same techniques to the wind below a layer in which geostrophic balance has been reached in the equatorial atmosphere (near the equator, not at the equator) and also develop a relationship for the vertical wave length.

We make the same assumptions as before, i. e., a very stable flat layer of atmosphere near the equator. Also, as before absolute vorticity $\zeta + \beta y = 0$ for this layer.

Assume $u = u_A + \Delta u$ where u is the wind speed at the bottom layer, Δ u is the change through the layers, and u_A is the wind speed at the lower part of the top layer and geostrophic balance has been reached with hydrostatic pressure.*

From the hydrostatic relationship, we have

$$-\frac{1}{\rho}\frac{\partial p}{\partial y} = -g_u \frac{\Delta\rho}{\rho}\frac{\partial D}{\partial y} - \frac{1}{\rho}\frac{\partial p_A}{\partial y}$$

as in Ebdon and Veryard (1961) we have

$$\frac{\partial^2 a}{\partial t^2} = -g_u\left(\frac{\Delta\rho}{\rho}\frac{\partial D}{\partial y}\right) - \frac{1}{\rho}\frac{\partial p_A}{\partial y} - \beta y(u_A + \Delta u)$$

$$= -g_u\left(\frac{\Delta\rho}{\rho}\frac{\partial D}{\partial y}\right) - \beta y\,\Delta u$$

*This means that the east-west velocities have balanced each other down to this point.

by use of the geostrophic approximation, $-\frac{1}{\rho}\frac{\partial p_A}{\partial y} = \beta y\, u_A$,

and setting $g_u = g - 2\Omega u$, we obtain

$$\frac{\partial^2 a}{\partial t^2} = -\frac{(g-2\Omega u)}{2}\frac{\Delta\rho}{\rho}\frac{\partial D}{\partial y} - \beta y\,\Delta u$$

$$= -\frac{g}{2}\frac{\Delta\rho}{\rho}\frac{\partial D}{\partial y} - \beta y\,\Delta u + 2\Omega(u_A + \Delta u)\frac{\Delta\rho}{2\rho}\frac{\partial D}{\partial y}$$

By use of the geostrophic approximation for Δu , $-\frac{g}{2}\frac{\Delta\rho}{\rho}\frac{\partial D}{\partial y} = \beta y\,\Delta u$,

we have $\frac{\partial^2 a}{\partial t^2} = -\frac{2\Omega(u_A+\Delta u)}{g}\Delta u\,\beta y$

Setting $y = a$,

$$\frac{\partial^2 a}{\partial t^2} = -\frac{2\Omega(u_A+\Delta u)}{g}\Delta u\,\beta a$$

Let $a = a_o \sin\frac{2\pi t}{T}$

then $\frac{\partial a}{\partial t} = \frac{2\pi a_o}{T}\cos\frac{2\pi t}{T}$

$$\frac{\partial^2 a}{\partial t^2} = -\frac{4\pi^2 a_o}{T^2}\sin\frac{2\pi t}{T}$$

Hence $\frac{4\pi^2}{T^2} = \frac{2\Omega\beta}{g}(u_A+\Delta u)(\Delta u)$

For $u_A = 0$

$$\Omega = \frac{2\pi}{8.64} \times 10^{-4}/\text{sec.}$$

$$\beta = \frac{2\pi}{8.64\times 3} \times 10^{-10}/\text{m. sec.}$$

$$g = 10\ \text{m/sec}^2$$

$$T = 26\ \text{mos.}\ ,$$

we have

$$|\Delta u| = 5\ \text{m/sec.}$$

which is reasonable.

We assume that we have two surfaces of constant potential temperature with relationships as in the following diagram.

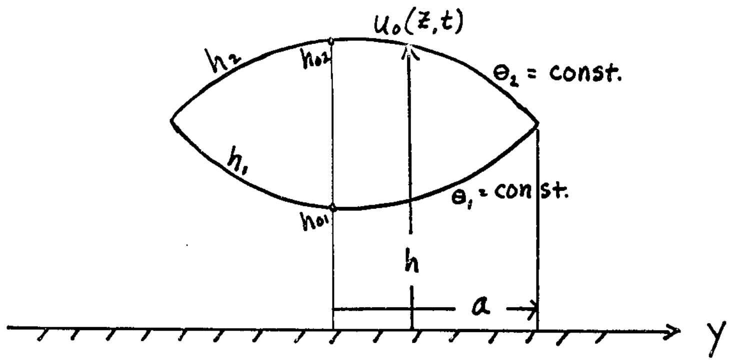

Equator

From continuity considerations, we have

$$\frac{1}{a}\frac{\partial \ln \theta}{\partial z} = \text{const.} = \frac{1}{a_0}\frac{\partial \ln \theta}{\partial z} = K$$

Assuming $u = u_0(z,t) + \frac{\beta y^2}{2}$ then $\frac{\partial u}{\partial z} = \frac{\partial u_0}{\partial z}$

From the thermal wind equation

$$g\frac{\partial \ln \theta}{\partial y} = \beta y \frac{\partial u}{\partial z}$$

we have

$$g\frac{\partial \ln \theta}{\partial z}\frac{\partial h}{\partial y} = \beta y \frac{\partial u_0}{\partial z}$$

$$gKa\frac{\partial h}{\partial y} = \beta y \frac{\partial u_0}{\partial z}$$

and integrating we obtain

$$(h - h_0) = \frac{\beta y^2}{2gKa}\frac{\partial u_0}{\partial z}$$

Assuming a wave of form as follows $u = U_0 \sin \frac{2\pi z}{L}$

we have $\left(\frac{\partial u}{\partial z}\right)_{MAX.} = \frac{2\pi U_0}{L}$.

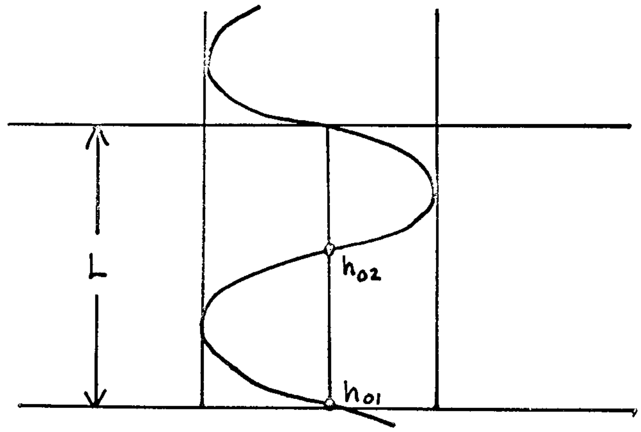

Since $h_{02} - h_{01} = \frac{L}{2}$ we have

$$h_1 - h_{01} = \frac{\beta y^2}{2gKa} \frac{2\pi U_0}{L}$$

$$h_2 - h_{02} = h_2 - (h_{01} + \frac{L}{2}) = - \frac{\beta y^2}{2gKa} \frac{2\pi U_0}{L}$$

$$(h_2 - h_1) - \frac{L}{2} = - \frac{\pi U_0 \beta y^2}{gKaL}$$

Now, θ_1 and θ_2 theoretically intersect in our model when $h_2 = h_1$; thus we can think of $h_2 - h_1 = 0$ as a "limiting" condition. With this assumption, we have

$$- \frac{L^2}{2} = - \frac{\pi U_0 \beta y^2}{gKa}$$

or

$$L^2 = \frac{2\pi U_0 \beta y^2}{gKa}$$

We would expect (or hope) that $\theta_1 \approx \theta_2$ at a distance greater than a; thus we set $y = Ma$ where $M > 1$.

Hence, $L^2 = \frac{2\pi U_0 \beta M^2 a}{gK}$

$$L = M\sqrt{2\beta\pi U_0 a/gK}$$

For $\beta = \dfrac{2\pi}{8.64 \times 3} \times 10^{-10}/m.\ sec.$

$g = 10\ m/sec^2$

and $a = 3^{\circ}$ latitude, we have $L \cong 2.5 M \times 10^{-3}\sqrt{U_0/K}$

For $\theta = \dfrac{3}{10^3}$ and $\dfrac{\Delta\theta}{\Delta z} = \dfrac{10}{10^3}$, $a = \dfrac{10^6}{3}$, we have $K \cong 10^{-10}$

and for

$$U_0 = 10\ m/sec.$$

$$L \cong 2.5 \times 10^{-3} M\sqrt{10^{11}}$$

$$\cong 0.8 \times 10^3 M$$

$$\sim M\ km.$$

Hence for $M = 10$ ($y = 30^{\circ}$ latitude), $L \sim 10\ km.$ which is a reasonable value for the wavelength.

Rudimentary Theory of Fluid Motion in the Ionosphere: ToStudy Slow Motion of "Air" at High Levels as Influenced by Ions Motion

We need an acceptable equation of motion that links the hydrodynamic and hydromagnetic motions.

We have good sets of equations for each.

We assume that the ions make up a fluid cable along the lines of magnetic force, and that the tension in the cable is given by $A(\dfrac{B^2}{4\pi\mu})$ where A is the area of the cable.

This results in the following set of equations where $u_i + v_i$ are both normal to the line of force for the ions.

$$\frac{\partial^2 u_i}{\partial t^2} - \frac{B^2}{4\rho_i \mu \pi}\frac{\partial^2 u_i}{\partial x^2} = -F\frac{\partial u_i}{\partial t}\sqrt{\left(\frac{\partial u_i}{\partial t}\right)^2 + \left(\frac{\partial v_i}{\partial t}\right)^2} + f v_i$$

$$\frac{\partial^2 v_i}{\partial t^2} - \frac{B^2}{4\rho_i \mu \pi}\frac{\partial^2 v_i}{\partial x^2} = -F\frac{\partial v_i}{\partial t}\sqrt{\left(\frac{\partial u_i}{\partial t}\right)^2 + \left(\frac{\partial v_i}{\partial t}\right)^2} - f u_i$$

$$-\frac{\partial \rho_i}{\partial t} = \bar{\nabla}\rho_i \mathbb{V}_i + K_i\frac{\partial T}{\partial t}.$$

The neutral particles have a similar set of equations and we assume the frictional drag of the ions carries them along or more important holds them stationary.

$$\frac{\partial u}{\partial t} + g\frac{\partial H}{\partial x} = f v + \frac{\rho_i}{\rho} F\frac{\partial u_i}{\partial t}\sqrt{\left(\frac{\partial u_i}{\partial t}\right)^2 + \left(\frac{\partial v_i}{\partial t}\right)^2}$$

$$\frac{\partial v}{\partial t} + g\frac{\partial H}{\partial x} = -f u + \frac{\rho_i}{\rho} F\frac{\partial v_i}{\partial t}\sqrt{\left(\frac{\partial u_i}{\partial t}\right)^2 + \left(\frac{\partial v_i}{\partial t}\right)^2}$$

$$-\frac{\partial \rho}{\partial t} = \bar{\nabla}\rho \mathbb{V} + K_m\frac{\partial T}{\partial t}.$$

There is at least a superficial similarity between the stability of vertical sheets of constant vorticity and material particles, and the stability of "vertical" magnetic lines of force coming into the pole carrying the ions. (See figure next page).

We can imagine a magneto meteorological coordinate system that follows constant vorticity up to 150 km and lines of force above, or we may think of an atmosphere-like ionosphere above an ocean-like atmosphere.

There can be radical and violent motions of the ionosphere and we hope to investigate their effect on the atmosphere.

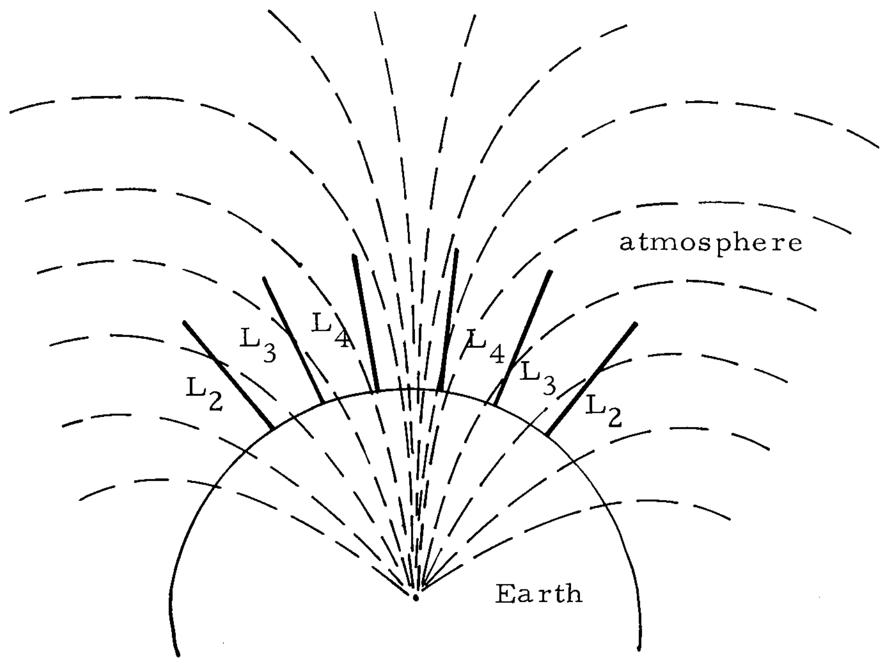

However, for the moment we will only discuss a polar vortex type motion in the mesosphere-stratosphere. The "displaced" magnetic pole can give us a polar vortex in the following way. The vertical lines of magnetic force carry the ionized particles with them and stir the neutral atmosphere. This serves as a "drag" to slow the winds in the ionosphere.

A solar event serves to increase the number of ions and to lower them and thus to increase the drag.

If the winds in the ionized layer are west winds,this results in an input of east winds.

If the winds in the ionized layer are east winds,this results in an input of west winds.

We assume that in the top of the meso-stratosphere where this action is most effective we usually have east winds. Thus, when a solar event lowers the ionosphere and increases the drag the result is an input of west winds.

These west winds work their way down as indicated by the formulas developed in Section III.

The drag gives us an excess of west wind (really of deficiency of east wind) or a Δu that is positive. This Δu results in values of $\frac{d^2 Y_i}{dt^2}$ and subsequent motion of the Y_i lines.

Note from the equation that there is a small "instantaneous" effect of a disturbance at all levels but it finally becomes more important at upper levels than in lower.

In Section III we have a discussion of several cases of increased solar activity being followed by increased easterlies in the auroral zone at 10 mb.

We feel that most of our work of showing solar influence on tropospheric weather patterns is done when we can show an effect at 10 mb. Also we feel that in the polar regions an effect that goes from 10 mb to 1000 mb could have gone from 0.1 mb to 10 mb and from 0.001 mb to 0.1 mb by almost exactly the same process. We have no difficulty showing significant disturbance at 0.001 mb so we feel there is little difficulty in postulating that disturbances propagate to 0.1 mb. We only have the gap from 60 km to 30 km or 0.1 mb to 10 mb as being made up of pure theoretical discussion.

Unsteady Motion in Atmospheric Cross Sections

We discussed the steady state flow in atmospheric cross sections in Appendix A, and we also discussed certain rudimentary time dependent problems (especially the time dependence at one level) previously in this section.

Now we would like to develop a fairly complete model giving the dynamics of an atmospheric cross section and from that show the path we are taking toward a solution of the problem in x, y, and z.

We assume a known three dimensional divergence (to keep from emphazing non-essentials, we make it zero), conservation of potential vorticity and of potential temperature, and that thermal wind equation holds. These assumptions are expressed as follows:

(1) $\frac{dA}{dt} = 0$

(2) $\frac{d}{dt}\left(\frac{\zeta + f}{D}\right) = 0$

(3) $\frac{d\theta}{dt} = 0$

(4) $\left[f_0 + \beta(y - y_0)\right]\frac{\partial u}{\partial z} = -\frac{g}{\theta}\frac{\partial \theta}{\partial y}$

where: $A = WD$

D is the vertical distance between two constant θ surfaces

W is the horizontal distance between two constant $\frac{\zeta+f}{D}$ surfaces.

Since we are dealing with cross sections with no derivatives with respect to "x", the divergence equation $\frac{\partial u}{\partial x} + \frac{\partial v}{\partial y} + \frac{\partial w}{\partial z} = 0$ becomes $\frac{\partial v}{\partial y} + \frac{\partial w}{\partial z} = 0$ which can be written $\frac{dA}{dt} = 0$, with A defined as above. With the use of $A = WD$, we can write the vorticity equation in a different form for cross sections as follows:

$$\frac{d}{dt}\left(\frac{\zeta+f}{D}\right) = \frac{d}{dt}\frac{W(\zeta+f)}{WD}$$

$$= \frac{1}{WD}\frac{d}{dt}W(\zeta+f) - \frac{W(\zeta+f)}{(WD)^2}\frac{d(WD)}{dt}$$

(5) $\quad \therefore \ \frac{d}{dt} W(\zeta + f) = 0$ for a non-divergent cross section.

Hence for a cross section, we have defined a new vorticity (5). We call this quantity L and we have

$$L = W(\zeta + f)$$

$$\frac{dL}{dt} = \frac{d}{dt} W(\zeta + f) = 0$$

If the relative vorticity is known we can draw lines of constant L on a cross section. Assuming this to be the case, we pick one of these lines and call it L_o. (We would hope that L_o is small, i.e., $L_o \sim \Delta L$ and that the lines of $L = L_i$ are vertical.)

We now define $Y = y - y_o$ and we make a finite difference approximation to ζ at $Y_i, u_i = u(Y_i)$ and $u_{i+1} = u(Y_{i+1})$ where Y_i and Y_{i+1} are the coordinates of L_i and L_{i+1} respectively. We note that $W_i = Y_{i+1} - Y_i$. Since $L = W(\zeta + f)$, we can write

(6) $$W_i\left[-\frac{(u_{i+1} - u_i)}{W_i} + f_o + \frac{\beta}{2}(Y_{i+1} + Y_i)\right] = L_i$$

or $$-(u_{i+1} - u_i) + f_o(Y_{i+1} - Y_i) + \frac{\beta}{2}(Y_{i+1}^2 - Y_i^2) = L_i$$

Rearranging, we have

$$\left[f_o Y_{i+1} + \frac{\beta Y_{i+1}^2}{2} - u_{i+1}\right] - \left[f_o Y_i + \frac{\beta Y_i^2}{2} - u_i\right] = L_i$$

$$\left[f_o Y_{i+1} + \frac{\beta Y_{i+1}^2}{2} - u_{i+1}\right] = \left[f_o Y_i + \frac{\beta Y_i^2}{2} - u_i\right] + L_i$$

By defining $M_i = \left[f_o Y_i + \frac{\beta Y_i^2}{2} - u_i\right], \quad i = 0, 1, 2, \ldots$

$$L_i = L_o + i\Delta L$$

we have $\quad M_{i+1} - M_i = L_i = L_o + i\Delta L$

and $$M_{i+1} = M_i + L_o + i\Delta L$$
$$= (i+1)L_o + \sum_{k=1}^{i} k\Delta L + M_o$$

(7) $$M_{i+1} = (i+1)L_o + \frac{i(i+1)}{2}\Delta L + M_o$$

which gives us relationships in the horizontal.

We note that any M_i can be expressed in terms of <u>any other</u> M_j. Thus we would expect that M_i = constant and $dM_i = 0$. This property will be very useful to us shortly.

From (7), we can write

$$u_i = f_o Y_i + \frac{\beta Y_i^2}{2} - (i+1)\left(\frac{2L_o + i\Delta L}{2}\right) - M_o \tag{8}$$

Equation (8) gives u_i in terms of Y_i.

Next, we will use the thermal wind equation to relate Y_i and h_i, where h_i is the height of the potential temperature surface θ_i.

From equation (4) and substituting $Y = y - y_o$, we have

$$\begin{aligned}(f_o + \beta Y_i)\frac{\partial u_i}{\partial z} &= -\frac{g}{\theta_i}\frac{\partial \theta_i}{\partial y} \\ &= -g\frac{\partial \ln \theta_i}{\partial y} \\ &= -g\frac{\partial \ln \theta_i}{\partial z}\frac{\partial h_i}{\partial y}, \text{ where } h_i = h(Y_i)\end{aligned}$$

Expressing in finite difference form, we have

$$(f_o + \beta Y_i)\frac{\partial u_i}{\partial z} \approx -g\frac{\ln\frac{\theta_{i+1}}{\theta_i}}{D_i}\frac{(h_{i+1} - h_i)}{W_i} \tag{9}$$

By differentiation we have from equation (8)

$$\frac{\partial u_i}{\partial z} = f_o\frac{\partial Y_i}{\partial z} + \beta Y_i\frac{\partial Y_i}{\partial z}, \tag{10}$$

since $\frac{\partial L_i}{\partial z} = 0$, $\frac{\partial M_o}{\partial z} = 0$ and $\frac{\partial \Delta L}{\partial z} = 0$

Substituting equation (10) into equation (9), we have

$$(f_o + \beta Y_i)\left(f_o\frac{\partial Y_i}{\partial z} + \beta Y_i\frac{\partial Y_i}{\partial z}\right) = -g\frac{\ln\frac{\theta_{i+1}}{\theta_i}}{D_i W_i}(h_{i+1} - h_i) \tag{11}$$

We now make use of the second equation of motion

$$\frac{dv}{dt} = -g\frac{\partial h}{\partial y} + (f_o + \beta Y)u$$

which we re-write using finite differences as follows

$$\frac{d^2 Y_i}{dt^2} = -g\frac{(h_{i+1} - h_i)}{W_i} + (f_o + \beta Y_i)u_i$$

(12) $$\frac{d^2Y_i}{dt^2} = -g\frac{(h_{i+1}-h_i)}{W_i} + (f_0+\beta Y_i)\left[f_0 Y_i + \frac{\beta Y_i}{2} - \left\{(i+1)\left(\frac{2L_0+i\Delta L}{2}\right)+M_0\right\}\right]$$

by using equation (8).

Since $\frac{d^2w}{dt^2} \approx 0$, we have $\frac{d^2Y_i}{dt^2} \approx \frac{\partial^2 Y_i}{\partial t^2}$. Using equation (11) we have

(13) $$\frac{\partial^2 Y_i}{\partial t^2} = \frac{D_i}{\ln\frac{\theta_{i+1}}{\theta_i}}(f_0+\beta Y_i)\left(f_0\frac{\partial Y_i}{\partial z} + \beta Y_i\frac{\partial Y_i}{\partial z}\right) + (f_0+\beta Y_i)\left[f_0 Y_i + \frac{\beta Y_i^2}{2} - \left\{(i+1)\left(\frac{2L_0+i\Delta L}{2}\right)+M_0\right\}\right]$$

Although equation (13) appears to be very complicated, we can illustrate it quite simply using graphical means.

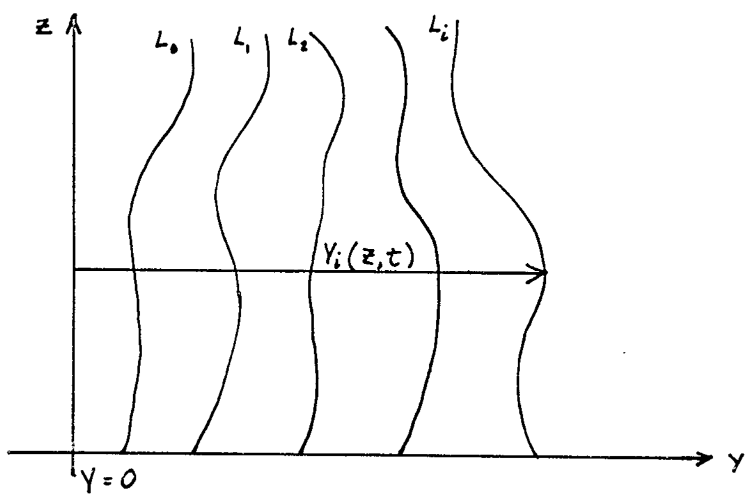

Recalling that we are dealing with cross sections, equation (14) is merely the equation for lines of constant vorticity q as they move in the y direction, giving values of $Y(z,t,q)$.

If we deal with cases where the Y_i are small (and $\beta Y_i << f_0$), then we can simplify equation (13) to a more useful form (still retaining its essential linear mathematical elements).

Thus we have

(14) $$\frac{\partial^2 Y_i}{\partial t^2} = \frac{D_i f_0^2}{\ln\frac{\theta_{i+1}}{\theta_i}}\frac{\partial Y_i}{\partial z} + \left[f_0^2 - \left\{\beta(i+1)\left(\frac{2L_0+i\Delta L}{2}\right)+M_0\right\}\right]Y_i$$

where for further simplification we have ignored the constant

$\left\{f_0(i+1)\left(\frac{2L_0+i\Delta L}{2}\right)+M_0\right\}$.

Let us now check to see whether a study by the method of characteristics would be fruitful. We write equation (14) as follows:

$$\frac{\partial U_i}{\partial t} - \frac{D_i f_0^2}{\ln\frac{\theta_{i+1}}{\theta_i}} \frac{\partial Y_i}{\partial z} = \left[f_0^2 - \left\{\beta(i+1)\left(\frac{2L_0+i\Delta L}{2}\right)+M_0\right\}\right] Y_i$$

$$\frac{\partial Y_i}{\partial t} = U_i$$

$\frac{\partial U_i}{\partial t}$	$\frac{\partial U_i}{\partial z}$	$\frac{\partial Y_i}{\partial t}$	$\frac{\partial Y_i}{\partial z}$
1			$\frac{D_i f_0^2}{\ln\frac{\theta_{i+1}}{\theta_i}}$
		1	
dt	dz		
		dt	dz

Hence, we see that $(dz)^2 = 0$. This equation has only the characteristic $\frac{dz}{dt} = 0$. Consequently, we cannot gain in the study of equation (14) by the method of characteristics.

In a previous study, reference [3], we discussed equation (14) in some detail when $\frac{\partial Y_i}{\partial z}$ is small enough to be neglected. We will now discuss it when $\frac{\partial Y_i}{\partial z}$ is the most prominent term.

We make a preliminary study of the equation

(15) $$\frac{\partial^2 Y}{\partial t^2} = \frac{1}{k^2}\frac{\partial Y}{\partial z} \qquad \text{with } k^2 > 0$$

This is the parabolic equation $\frac{\partial Y}{\partial z} = k^2 \frac{\partial^2 Y}{\partial t^2}$.

We will find solutions of it later but the general form is well known and is show below.

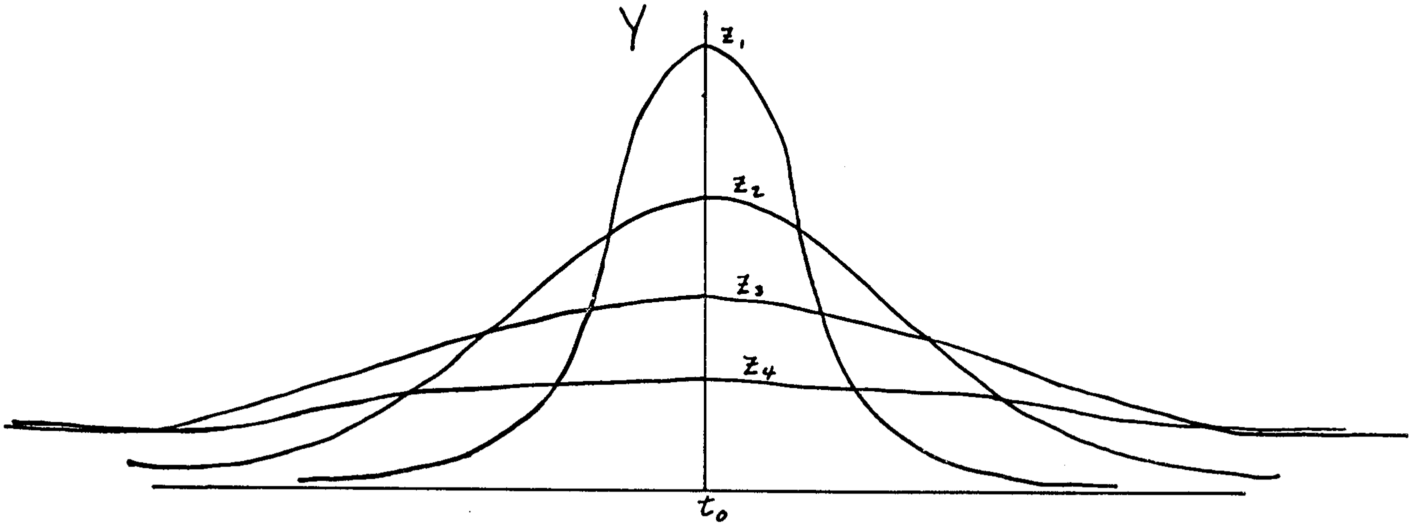

This shows that a long term weak disturbance at high altitude can build up to a short term strong disturbance at low altitude.

A plot of Y(z) for various times appears as follows.

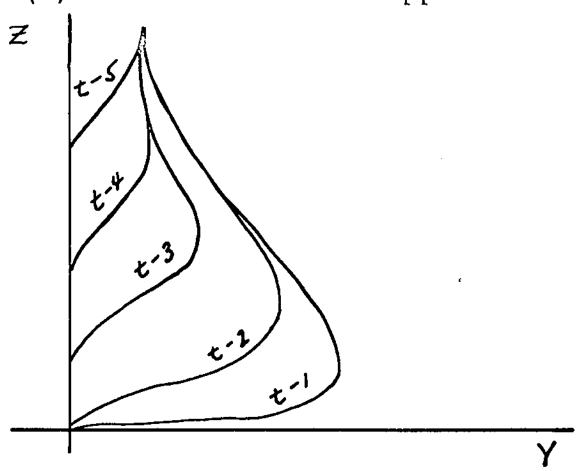

Notice that the maximum value of the disturbance grows and moves down.

We re-write equation 14) as follows

$$\frac{\partial Y_i}{\partial z} = \frac{\ln \frac{\theta_{i+1}}{\theta_i}}{f_0^2 D_i} \frac{\partial^2 Y_i}{\partial t^2} - \frac{\ln \frac{\theta_{i+1}}{\theta_i}}{f_0^2 D_i} \left[f_0^2 - \left\{ \beta(i+1)\left(\frac{2L_0 + i\Delta L}{2}\right) + M_0 \right\} \right] Y_i$$

This is a differential equation of the form

(16) $$\frac{\partial Y_i}{\partial z} = k_1^2 \frac{\partial^2 Y_i}{\partial t^2} - k_2^2 Y_i$$

We note that a solution $Y(\eta)$ of $b^2Y'' - Y' = 0$ is also a solution of equation (16) where

$$\eta\left(k_2^2 z + b\frac{k_2}{k_1}t\right)$$

Hence two solutions of equation (16) are

$$(17) \qquad \begin{aligned} Y_i &= Y_{i_{o\pm}}\, e^{\left(\frac{1\pm\sqrt{1+4b^2}}{2b^2}\right)\left(k_2^2 z + b\frac{k_2}{k_1}t\right)} \\ &= Y_{i_{o\pm}}\, e^{\left(\frac{1\pm\sqrt{1+4b^2}}{2b^2}\right)\left(k_2^2 z + \frac{b}{k_1k_2}t\right)} \end{aligned}$$

where

$$k_1^2 = \frac{\ln\frac{\theta_{i+1}}{\theta_i}}{f_o^2 D_i}$$

$$k_2^2 = k_1^2\left[f_o^2 - \left\{\beta(i+1)\left(\frac{2L_o + i\Delta L}{2}\right) + M_o\right\}\right]$$

The downward propagation speed c is equal to $\frac{b}{k_1k_2}$ where b is arbitrary. Hence,

$$(18) \qquad \begin{aligned} c &= \frac{b}{k_1k_2} \\ &= \frac{bf_o^2D_i}{\ln\frac{\theta_{i+1}}{\theta_i}\sqrt{f_o^2 - J_i}} \end{aligned}$$

where

$$J_i = \left\{\beta(i+1)\left(\frac{2L_o + i\Delta L}{2}\right) + M_o\right\}$$

It is worthwhile to examine one or two simple cases.

We note that when $J_i << f_o^2$, equation (18) reduces to

$$(19) \qquad c = \frac{bf_oD_i}{\ln\frac{\theta_{i+1}}{\theta_i}}$$

and for $b \geq 1$, the propagation speed is meteorologically instantaneous. In this case the speed c can be "adjusted" by choosing $b < 1$.

Also when $J_i \approx f_o^2$ (which is more likely), the speed c can be readily "adjusted" by choosing $b << 1$.

Equation (17) will be more fully investigated, by using varying values of b and for various Y_i, in a forthcoming paper.

We would probably like to discuss the effects of this model on a spherical earth. In this case we can write the continuity equation in the form

$$\frac{d}{dt} WD \sin\left(\frac{Y_i + Y_{i+1}}{2}\right) = 0$$

where Y_i and Y_{i+1} are expressed in degrees of latitude.

The pole needs special treatment. We would call the southern boundary of the polar cap Y_n.

The vorticity equation would be

$$\frac{\partial}{\partial t}\left(\frac{\Omega + \frac{U_m}{(90° - Y_m)}}{D}\right) = 0$$

and the continuity equation would be

$$\frac{\partial}{\partial t}\left(Y_m^2 D\right) = 0$$

The thermal wind equation would be

$$f \frac{\partial \omega r}{\partial z} = -\frac{g}{\theta}\frac{\partial \theta}{\partial r} \qquad \text{or}$$

this would be

$$r f \frac{\partial \omega}{\partial z} = -\frac{g}{\theta}\frac{\partial \theta}{\partial r} - \frac{\partial}{\partial z}\frac{\partial v}{\partial t} \qquad v = \frac{\partial a}{\partial t} r$$

$$\frac{\partial \log \theta}{\partial r} = -\frac{f}{g}\frac{\partial \omega}{\partial z} r - \frac{\partial^2 v}{\partial t\, \partial z} \qquad \frac{\partial Y_m}{\partial t} = \frac{\partial a}{\partial t} Y_m$$

which is the thermal wind equation for a polar cap.

$$\log \frac{\theta}{\theta_p} = -\frac{f}{2g}\frac{\partial \omega}{\partial z}\left(r^2 - r_p^2\right) - \frac{\partial^2 a}{\partial t\, \partial z}\left(r^2 - r_p\right)$$

$$\theta_m = \theta_p\, e^{-\frac{f}{2g}\frac{\partial \omega}{\partial z}\left(Y_m^2 - (90)^2\right)}$$

These modifications may be needed to discuss these flows.

REFERENCES

1. Ebdon, R. A., and R. G. Veryard, 1961: Fluctuations in equatorial stratospheric winds. Nature, 189, 791-793.

2. Reed, R. J., W. J. Campbell, L. A. Rasmussen and D. G. Rogers, 1961: Evidence of a downward propagating, annual wind r4versal in the equatorial stratosphere. J. Geophys. Res., 66, 813-818.

3. Freeman, Jr., J. C., L. Baer, and G. H. Jung, 1957: The bathystropic storm tide. J. Marine Res., 16, 12-22.

APPENDIX C

EXAMPLES OF THE RESPONSE OF THE TROPOSPHERE TO SOLAR EFFECTS

by

John C. Freeman, Jr.
W. H. Portig
Leon F. Graves

Response of Low Level Circulation

MacDonald (1960) and Shapiro and Ward (1962a) have shown that there is a response in the lower atmosphere to the solar storms. Shapiro and Ward found statistical significance for two events.

(1) An increase in the westerlies about 5 days after the K_p maximum.

(2) A decrease in the westerlies about 14 days after the K_p maximum.

Their event (1) is consistent with the increased cyclonic circulation found by MacDonald.

Thus we could say that the solar wind or the solar storm heats the upper mesosphere and causes divergence and anticyclonic circulation there. This divergence causes low level convergence and increased cyclonic circulation which reaches its peak in about 5 days. In about 14 days the anticyclonic circulation has worked its way to the troposphere.

The attempt by Freeman, Graves and Portig (1963) to show the effect of the solar wind on the earth weather is summarized in the following pages.

The model calls for increase in cyclonic activity in the polar troposphere as a first effect resulting from upper air divergence and low level convergence. The final effect is the ultimate arrival at the ground of the high level anticyclonic circulation.

The effects studied here were first found in detail by Shapiro and Ward and were emphasized by our work.

With this hypothesis in mind we have prepared graphs of solar, ionosphere, high atmosphere and tropospheric data for the period August and September, 1961.

We will describe the scales and outlines of those figures along with credit for their source.

Because we are concerned with solar-earth weather effects, each Figure 1-4 has the plot of the K_p magnetic index which we take to be a measure of the solar wind area and a plot of $Z1_p$ the west wind at 700 mb. (Since this is still summer we use the polar zonal index which we will see later contains most of the westerlies.)

Figure 1

SSN, the sun spot numbers as reported by Lincoln (1961, 1962). The vertical lines on the graphs denote weeks. The vertical scale for SSN is the observed relative sun spot number.

C_p, the planetary magnetic character index from Bartels (1962). The vertical scale is the accepted value of the index. It is a measure of magnetic disturbance.

A_p, the planetary magnetic A index from Bartels (1962). This is essentially an expanded K index but has its accepted scale and method of measurement from a magnetogram.

$Z1_p$, the polar zonal index of westerly wind speeds as used and reported by the Extended Forecast Section of the U.S. Weather Bureau. The dotted line is the five day running mean of this quantity plotted three times a week on the day the period ends.

K_p is the planetary magnetic K index from Bartels (1962) summed for the day indicated. This quantity has an accepted scale and we use it as a measure of the solar wind for the day. The dotted line is the 5 day running mean of K_p quantity plotted daily on the last day of the period.

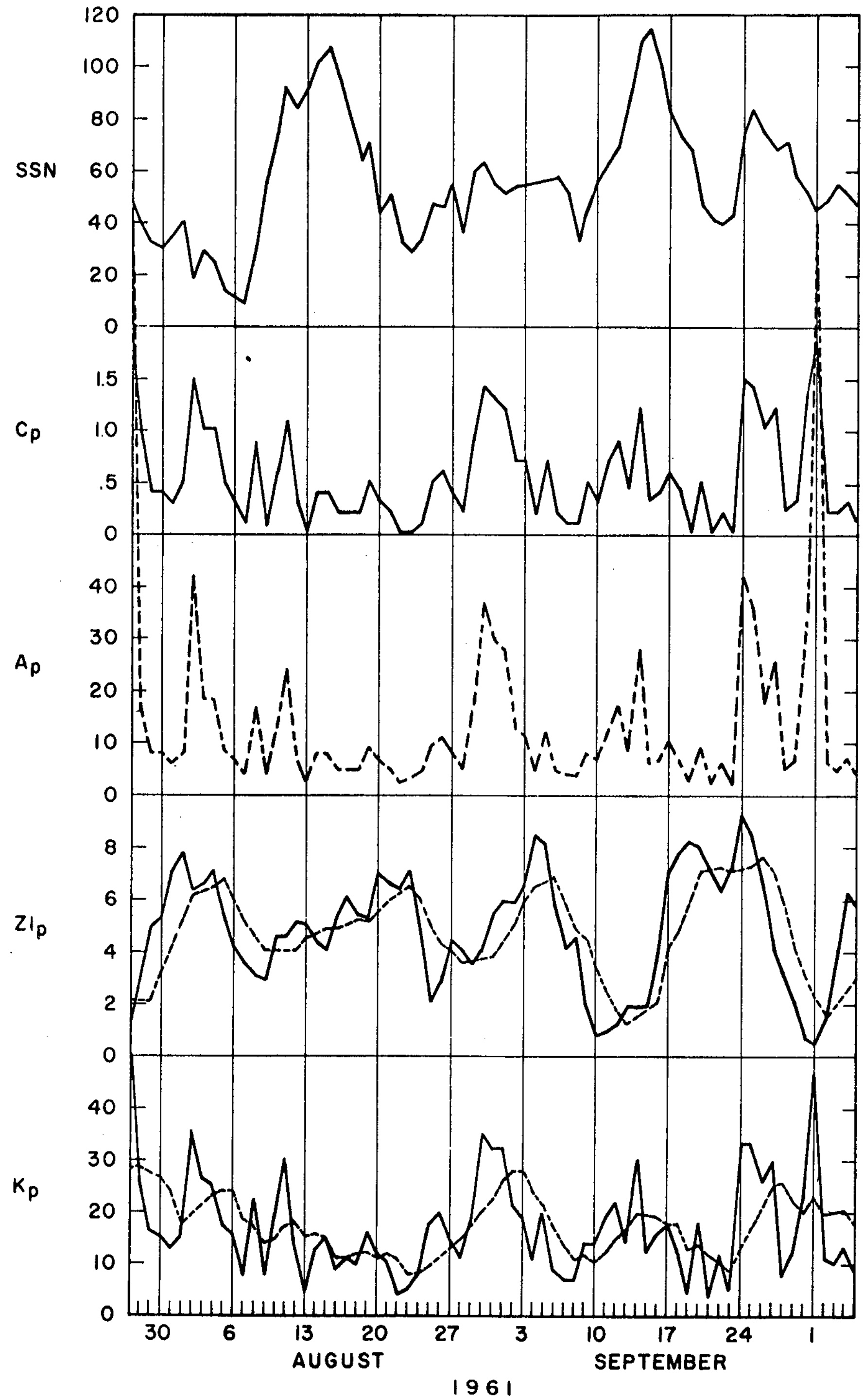

FIGURE 1
SOLAR AND MAGNETIC DATA

Figure 2

F_{10}, the flux of 10.7 cm wave length radio waves as reported by Jacchia (1963). He relates these waves to satellite drag and high atmosphere temperature as did King-Hele (1963). The vertical scale is in units of $10^{-22} W/m^2$ c/s band width.

F_{20}, the flux of 20 cm wave length radio waves.

D_{ST}. This is the $D_{ST}(H)$ from San Juan and Honolulu computed by J. W. Freeman (1963) after Akasofu. This is a special magnetic index used as a measure of the intensity of individual magnetic storms. Note that the maximum deviation of -100γ occurred in the magnetic storm of September 29 and 30.

R_M, J. W. Freeman's (1963) measure of the distance (on the sun side of the earth) at which there is a sharp cutoff in the count rate of the S_pL* charged particle detector. He assumes this is the boundary of the magnetosphere (and since it is practically the discovery observation, he is probably right). The figure for our period is plotted here. The units are km x 10^3.

R_M is taken as a measure of the solar wind. (This measure would be influenced by the preceding shock wave in the solar wind.

Figure 3

$P_R - P$, The corrected drag on the satellite 1961 δ_1 during the period indicated. Jacchia (1963) takes this as the best summary of satellite drag measurement made on six satellites during this period.

---

* S_pL. An electron energy spectrometer channel with pass band 90 kev to 50 kev.

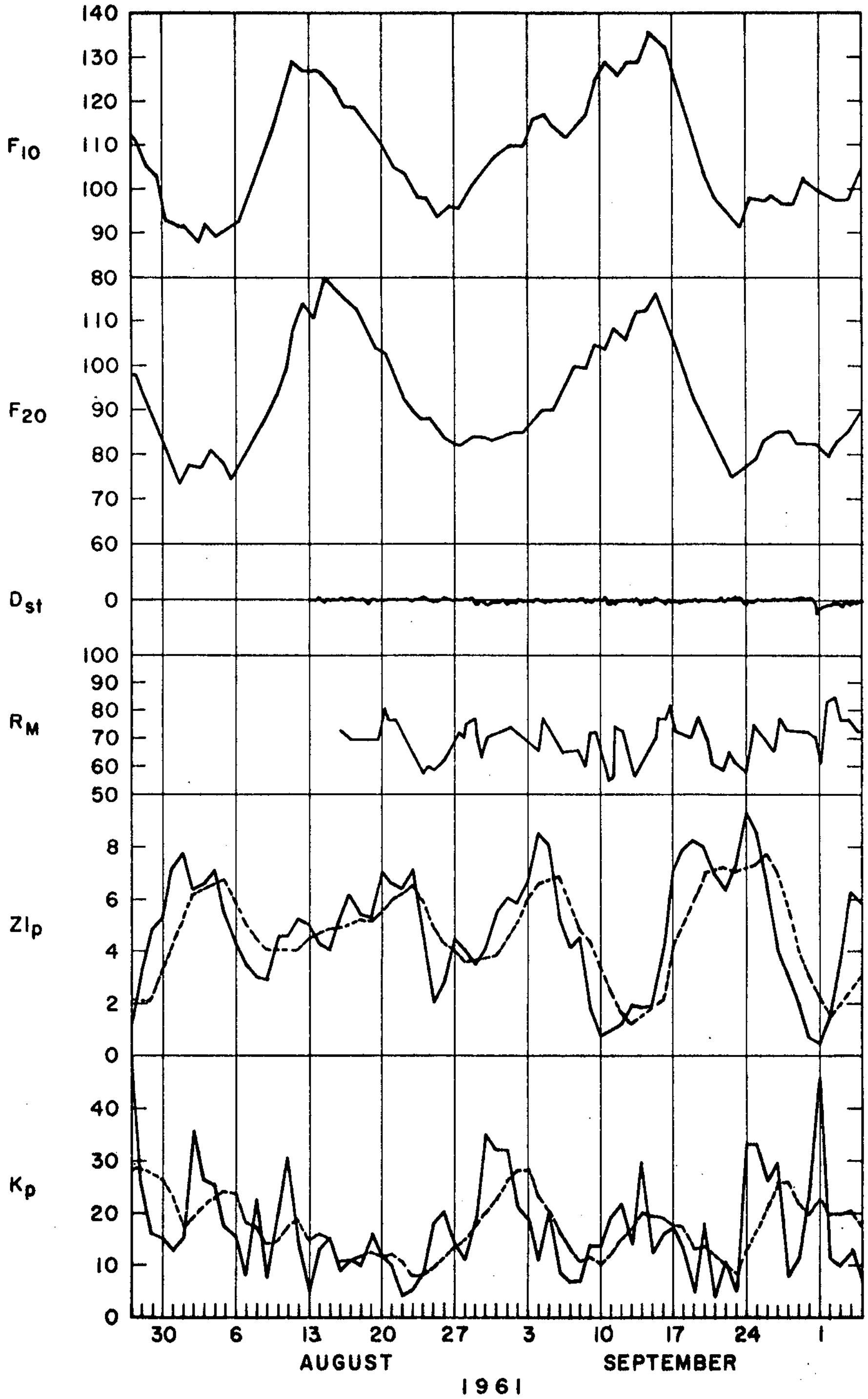

FIGURE 2

SOLAR AND MAGNETOSPHERE DATA

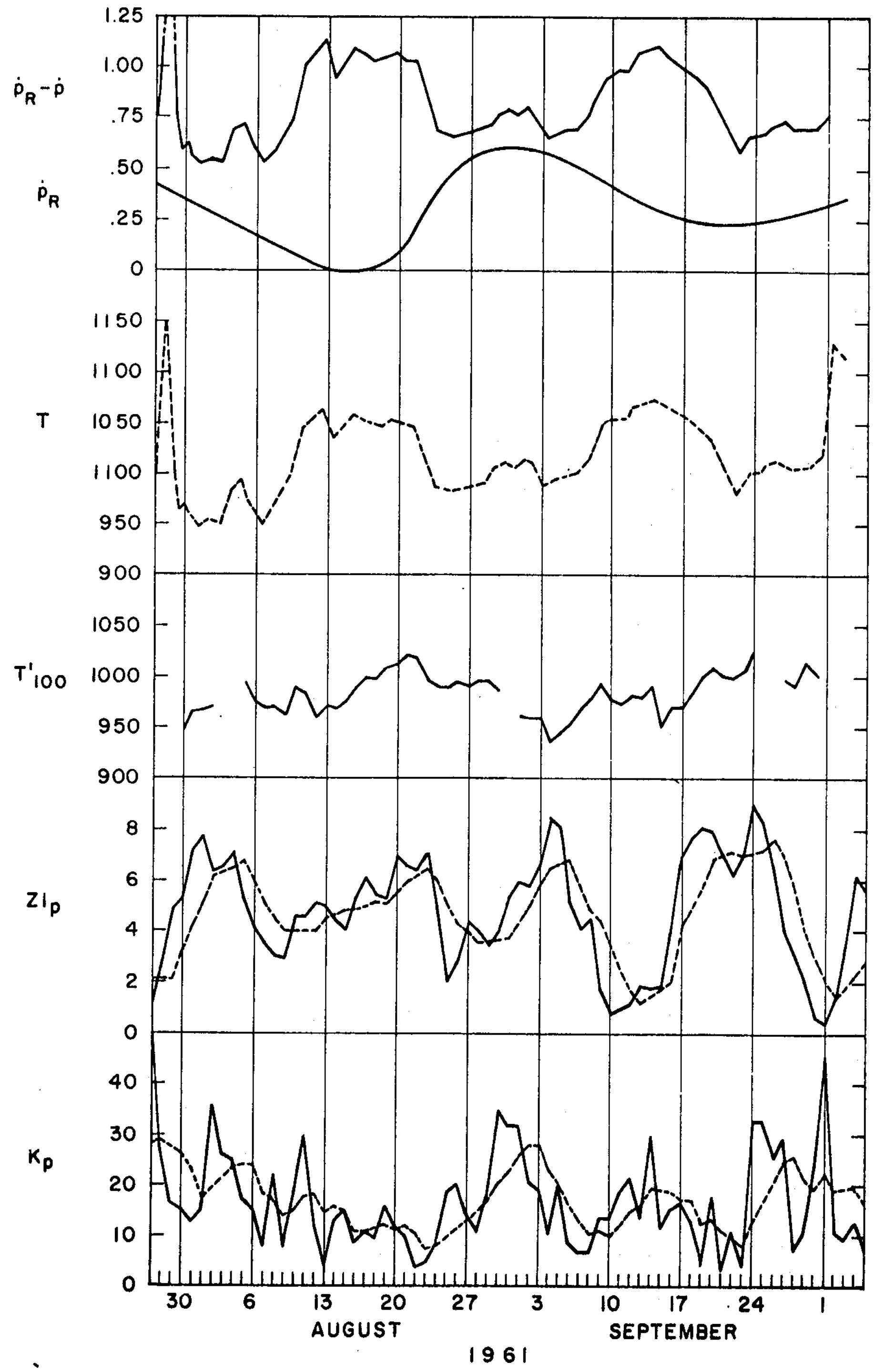

FIGURE 3
IONOSPHERE DATA

The radiation pressure is subtracted and the drag inverted in order to correlate with temperature. High temperature results in high drag. The satellites were at 350 to 650 km.

P_R, Radiation pressure drag. The scale is torrs/sec.

T , Jacchia's estimate of the temperature at satellite altitude. This would be the temperature in the high ionosphere in ^oK.

T'_{100}, Jacchia's (1963) standardized temperature. The temperature is "corrected" to $A_p = 0$ and 10.7 cm flux = 100. This is a measure of the accuracy of the fit of his method of temperature estimate.

Figure 4

L , An indication of the dates on which certain events are expected according to Shapiro (1959). As you go up three days you find a period of increased persistence begins. In five days a period of increased westerlies begins and in 13 days a period of decreased persistence and westerlies begins.

Δ_{lat} is the difference between the mean latitude of the 18, 200 feet height contour at 500 mb and the 19, 200 feet height contour at 500 mb (when they define the north and south boundaries of the westerlies). This is expected to vary inversely with the speed of the westerlies.

W-E. The maximum easterlies (usually near 80^o) are subtracted from the maximum westerlies to get the dotted curve. The solid curve is the mean zonal wind in the ring between 850 and 500 mb and

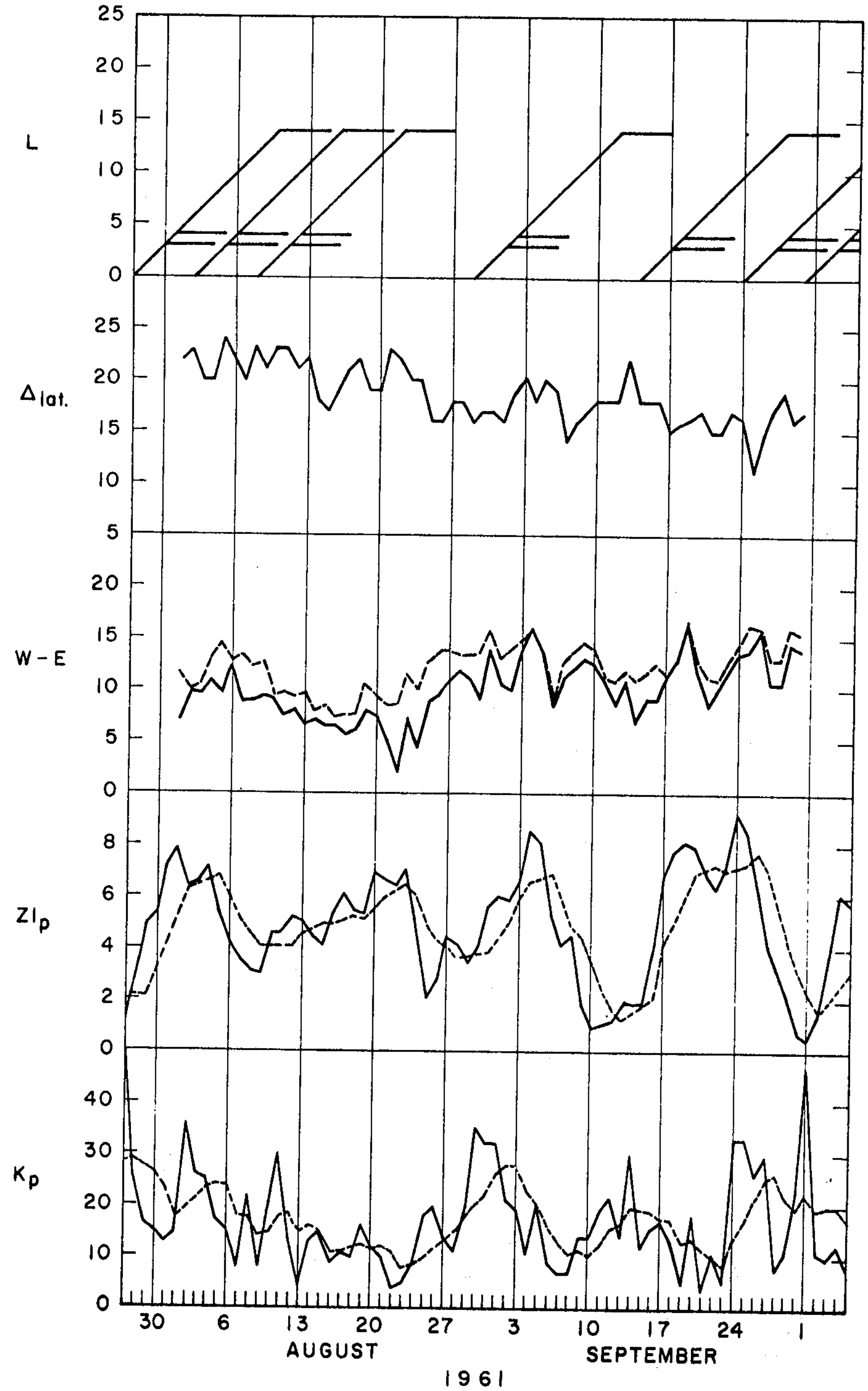

FIGURE 4
WIND AND MAGNETIC DATA

between $50^{\circ}N$ and $55^{\circ}N$ minus the mean zonal wind in the ring between 850 and 500 mb and between $80^{\circ}N$ and $85^{\circ}N$. The figure is based on computation furnished by A. Kreuger of the National Weather Satellite Center of the U. S. Weather Bureau.

In addition to these graphs, we made several subjective studies of the weather patterns at various levels over the whole world. We decided that the pattern of September 10 and 11 was vastly different from that of August 29 and 30. The southern and northern hemisphere flows at 500 mb were mostly strong westerlies on August 29 and 30. The 10 mb chart of Scherhag (1962) showed zonal flow with a ring of high pressure. On September 10 and 11 there were several blocks and cut-off highs and lows. Hurricanes and typhoons were a prominent feature of the map. The 10 mb flow showed a definite two cell (high and low) pattern on September 10 and 11. (The two cell pattern at 10 mb was firmly established by September 4 and at that time a surface high cell was over the magnetic pole. It progressed from east to west between September 4 and 11.)

These differences and the occurrence of a peak in the K_p index near August 29 led to the choice of August 30, September 3 and September 11 as days to emphasize in the study.

We made some quantitative studies of the differences between these days. The surface pressure distribution in the Northern Hemisphere north of 15° shows that the total weight of air on August 27 and September 10 was the same but that 50% of it was north of 34.2° on August 27 and 50% of it was north of 36.2° on September 10. Thus there was a pressure increase at the poles during this period and a pressure decrease in lower latitudes.

Even though the choice of September 10 and 11, 1961 by a laboratory in Houston as a day of significance in the weather is understandable (the landfall of Hurricane Carla occurred at this time), it also turned out to be a very fortunate choice. We were led back to August 29 as the day of arrival of an impulse at the magnetosphere, and the highest value of K_p for the period occurred during this magnetic storm. In addition, the other effects on ionospheric temperature postulated by Jacchia (1963) are all small (see Figure 2).

The period August 29 to September 12 is one of the few periods in these two months when neither the beginning nor the end of the expected solar wind effect is influenced by another solar wind storm or other solar effect.

The maximum 5-day running mean of K_p for August and September occurs in association with a disturbance that reached its peak August 30, 1961 (See Figure 1.) There were no other very large values of K_p between August 11 and September 14; hence, this K_p increase event was comparatively isolated in time. The sun spot numbers show a flat disturbed minimum during this period (Figure 1) and the 10 cm solar flux stays below 110 from August 20 to September 3. The radius of the magnetosphere is a minimum on the day the K_p index reaches a peak. Both of these are accepted indications of a strong solar wind. We assume that there was a marked increase in the solar wind on

August 30.

At a time when the 10 cm solar flux value (see Figure 3) indicates that a minimum should be expected in temperature (as measured by satellite drag), there is a small maximum which reaches its peak with the K_p index and R_M (see Figure 2). Since solar corpuscular effects are generally accepted as the heating mechanism for this kind of temperature change, we shall assume that it caused this heating. Since the satellite was not in the auroral zone we can surmise that this heating was more pronounced at the poles. Since the effects we study depend on gradients of temperature we are not too unhappy to see a small temperature change.

Accepting that the polar atmosphere at about 100 km and above was heated on August 29 or 30, what do we expect to happen to the lower layers? Following Ward and Shapiro we would expect persistence of patterns to be great starting the third day after the event and continuing for six days. This would be the period September 1-6. According to "Die Grosswetterlagen Mitteleuropas" of Amtsblatt des Deutschen Wetterdienstes, the same basic pattern lasted from August 26 to September 7. The analysis of Shapiro (1959) predicts (as the "lag flag" of Figure 4 indicates) that the period from September 12 to September 17 should be a period of change. The description from Germany says there were moderate westerly winds from September 8 to 13. They broke down on September 14 and became a marked meridional pattern. This independent observation of Shapiro's persistences probably adds to the significance of his study. However, since we are concerned with only one case we are not in a position to perform any statistical analysis.

Shapiro (1959) also estimates the effect on the zonal wind. His data was for all times of the year and to consider the westerlies at this time we must use the polar westerly index. Shapiro's study for the Western Hemisphere indicates that the maximum speed of the westerlies ($Z1_p$) should be September 3 and it occurred September 4 (see Figure 4). He indicates that the minimum should be September 11 and it occurred September 10.

We have several other wind indices:

Δ_{lat} in Figure 4 which includes lower latitudes over about 1/2 the hemisphere (it is not wind but a rough measure of it) shows strong westerlies September 6 and the weakest westerlies for a long period around September 13.

W-E covers a whole ring around the earth and it indicates a maximum difference between westerlies and easterlies near the pole on September 4 and a sustained minimum centered on September 13. This minimum corresponds to the longer time lag for weakening the westerlies that Shapiro* noted for Europe.

---

* Shapiro attempted to link the high persistence and weak westerlies with the statement that high persistence and strong westerlies go with large pressure systems and that low persistence and weak westerlies go with small pressure systems. We found this statement confusing until we recalled that he filters ordinary troughs and ridges; and by large systems, he means a polar low cell with two or three subtropical highs and by small systems, he means blocks and cut-off lows and highs.

With this noteworthy confirmation of a result that was found statistically significant on previous data, we are encouraged to study the rest of the two month period.

Study of the lag flags in Figure 4 indicates the following predictions and confirmations:

Predicted Westerlies		Observed Westerlies
August 1-9	High values	High values began July 29 and lasted until August 5.
August 10-18	Confused	Many peaks and valleys slowly rising.
August 19-25	Low values	Low values August 22 to 27.
August 26-31	No prediction	Rise begins on August 29.
September 1-6	High values	Peak on September 4.
September 7-11	No prediction	Low values.
September 12-17	Low values	Low values; rise begins on September 15.
September 18-22	High values	High values.
September 23-30	Confused	High values until September 27; then rapid decrease.

There are five unequivocal predictions possible during the two month period and all of them are correct.

Calculation of linear correlation coefficients between indices provided additional information to assist in evaluating the August-September 1961 weather. The entire series of daily data was used in calculating 5-day mean values. The 5-day means were identified by the ending date of the period for which the mean was being calculated.

The latitude difference between the 18,200 feet and 19,200 feet contour on the 500 mb chart showed a correlation coefficient of -0.6 with the 700 mb temperate zonal index for the westerlies. Since larger latitude differences are associated with slower westerlies, the results are in the expected direction.

The 5-day mean K_p (daily sum) index had a +0.1 linear correlation with the 700 mb zonal westerlies for the western quadrisphere. An attempt was also made to check the lag relationships between K_p and the zonal index for the 700 mb temperate westerlies with these results:

Lag:	0 day	2 day	4 day	5 day	6 day	13 day	14 day
	+0.1	-0.2	-0.4	-0.5	-0.6	-0.2	-0.3

Note that in common with most of the studies of geomagnetism and winds or pressure data, more happens between days 4 and 6 than at other times. When you recognize that during this period the polar westerlies and the temperate westerlies at 500 mb had a very high negative correlation, then this report becomes a fair confirmation of Shapiro's and Ward's findings and even indicates there is some possible profit in day to day correlation of K_p and the maximum westerlies.

The weather maps for August 30, September 3 and September 11 which we have chosen to be of particular interest are in Figure 7 (contained in the pocket in back of this report).

Surface maps show a striking difference between August 30 and September 11, especially in the low latitudes where hurricanes predominate on September 11. The map for September 3 perhaps has the seeds of the hurricane but they have not formed. The increased polar westerlies between August 30 and September 3 are noteworthy in Europe and the Pacific Ocean. The 500 mb chart shows an increase in blocking and meridional flow between August 30 and September 11, and the westerlies have significant jet streams far to the south on September 11. The 500 mb chart for September 3 shows the westerlies contracted into the pole but otherwise is much like the chart for August 30.

The 100 mb charts are all pretty much the same for all three days.

The 30 mb chart shows a very significant difference between August 30 and September 11 in that there is a polar low and a ring of high pressure on August 30 and a two cell non-polar pattern on September 11. It is also significant that the 30 mb chart for September 3 looks very much like the two cell 10 mb chart for September 11 except that a migration of the high cell from the magnetic pole to the west during the period has occurred.

REFERENCES

Akasofu, S.-I., and S. Chapman, 1960: The sudden commencement of geomagnetic storms. Vrania, 250, 1-35.

Bartels, Julius, 1962: Collection of geomagnetic planetary indices K_p and derived daily indices, A_p and C_p for the years 1932 to 1961. IAGA Bulletin No. 18, Amsterdam, North-Holland Publishing Co., 188 pp.

Blum, Ronald, 1963: The interaction between the geomagnetic field and the solar corpuscular radiation. Icarus, 1, 459-488.

Dessler, A. J., 1959: Ionospheric heating by hydromagnetic waves. J. Geophys. Res., 64, 397-401.

Dessler, A. J., 1962: Further comments on stability of interface between solar wind and geomagnetic field. J. Geophys. Res., 67, 4892-4894.

Dessler, A. J., and E. N. Parker, 1959: Hydromagnetic theory of geomagnetic storms. J. Geophys. Res., 64, 2239-2252.

Freeman, Jr., J. C., 1963a: On the thickness of a shock wave in the solar wind (See Appendix I).

Freeman, Jr., J. C., 1963b: A possible oscillation of the wind in the equatorial stratosphere with a period of 24 to 27 months (see Appendix II).

Freeman, Jr., J. C., 1963c: A possible inertial oscillation of the equatorial stratosphere (see Appendix III).

Freeman, J. W., 1963: The morphology of the electron distribution in the outer radiation zone and near the magnetospheric boundary as observed by Explorer XII. Doctorate dissertation, State University of Iowa, Iowa City, Iowa.

Harris, I. and W. Priester, 1962: Time-dependent structure of the upper atmosphere. J. Atmos. Sci., 19, 286-301.

Jacchia, L. G., 1963: Electromagnetic and corpuscular heating of the upper atmosphere. Space Res. III, Amsterdam, North-Holland Publishing Co., 3-18.

Johnson, F. S., 1961: Structure of the upper atmosphere. Satellite Environment Handbook, Stanford, California, Stanford University Press, 9-24.

King-Hele, D. G., 1963: Upper-atmosphere scale height and its variation with solar activity. Space Res. III, Amsterdam, North-Holland Publishing Co., p. 27.

Lincoln, J. Virginia, 1961: Geomagnetic and solar data. J. Geophys. Res., 66, 3949 and 4302.

Lincoln, J. Virginia, 1962: Geomagnetic and solar data. J. Geophys. Res., 67, 387 and 887.

Macdonald, N. J., and W. O. Roberts, 1960: Further evidence of a solar corpuscular influence on large-scale circulation at 300 mb J. Geophys. Res., 65, 529-534.

Macdonald, N. J. and W. O. Roberts, 1961: The effect of solar corpuscular emission on the development of large troughs in the troposphere. J. Meteor., 18, 116-118.

Miers, B. T., 1963: Zonal wind reversal between 30 and 80 km over the southwestern United States. J. Atmos. Sci., 20, 87-93.

Shapiro, Ralph, 1958: Some observations of the persistence of the surface pressure distribution. J. Meteor., 15, 435-439.

Shapiro, Ralph, 1959: A comparison of the response of the North American and European surface pressure distributions to large geomagnetic disturbances. J. Meteor., 16, 569-572.

Shapiro, Ralph and Fred Ward, 1962a: The harmonic persistence correlation and geomagnetic disturbance. J. Atmos. Sci., 19, 60-65.

Shapiro, Ralph and Fred Ward, 1962b: A neglected cycle in sunspot numbers, J. Atmos. Sci., 19, 506-508.

Snyder, C. W., Marcia Neugebauer and U. R. Rao, 1963: Preliminary results on interplanetary plasma from Mariner II (to be published).

Warwick, James W., 1959: Some remarks on the interaction of solar plasma and the geomagnetic field. J. Geophys. Res., 64, 389-396.

Willett, H. C., 1961: Research directed toward study of stmospheric reactions to changing conditions of solar activity. Final Report, Contract No. AF19(604)-3056.

Woodbridge, D. D., N. J. Macdonald and T. W. Pohrte, 1958: A possible relationship of geomagnetic disturbances to 300 mb trough development. J. Meteor., 15, 247-248.

SOURCES OF WEATHER ANALYSES

U. S. Weather Bureau copies of NWAC Northern Hemisphere working maps.

Die Grosswetterlagen Mitteleuropas, Amtsblatt des Deutschen Wetterdienstes.

Institut für Meteorologie und Geophysik der Freien Universität Berlin, "Preliminary Daily Northern Hemisphere 10-Millibar Synoptic Weather Maps of the Year 1961," Meteorologische Abhandlungen, Band XX.

Institut für Meteorologie und Geophysik der Freien Universität Berlin, "Preliminary Daily Northern Hemisphere 30-Millibar Synoptic Weather Maps of the Year 1961," Meteorologische Abhandlungen, Band XIX.

U. S. S. R. TSentral'nyi institut prognozov. Ezhednevnyi biulletin' pogody.

APPENDIX D

PLANETARY EFFECTS ON THE SUNSPOT CYCLE

by

W. H. Portig

ABSTRACT

It is shown that a considerable amount of the variations of the sunspot numbers are due to three periodicities. While one of them remains unexplained the other two coincide with periodicities in the movements of Jupiter and Saturn. These effects are so strong and their levels of statistical significance so high that new ways of thinking in planetary science seem imperative.

In order to apply statistical methods the original sunspot numbers have to be replaced by their square roots. The physical significance of this transformation is briefly discussed.

The periodicities which have been found are used to forecast the annual sunspot numbers for the years up to 2000 A.D.

I. Introduction

For a long time the variations of the number of sunspots have intrigued scientists. Many attempts have been made to analyze them but with relatively small success. In the last century, when such investigations began, the number of available data was not sufficient. Recently the power spectrum analysis has been applied which is too crude a method to be successful in this delicate time series.

The appearance of the time series of annual sunspot numbers should make it clear to a careful observer that there must be several periodicities of almost equal length involved. There are, with exception of the years around 1800, no obvious breaks in the phase angle which would justify the assumption that a periodicity begins at a certain time and fades away gradually. This is the case with daily sunspot numbers which, after the first appearance of a new group of sunspots, show a periodicity which reflects the rotation of the sun. New series of this type are out of phase with previous and future ones. No such phenomenon can be observed in annual sunspot numbers.

On the other hand, not much emphasis has been placed on the changes in the length of the sunspot cycle. The author is not aware that the shortening of the sunspot cycle, which took place in the beginning of this century, has aroused much attention in scientific circles. The years with sunspot maxima in this century were 1905, 1917, 1928, 1937, 1947, and 1957 which corresponds to a mean length of the cycle of 10.4 years, or, counting from World War I, of 10.0 years, and not of 11 years as is still generally assumed.

These types of irregularities in the annual sunspot numbers led the author to the belief that there must be several causes for the sunspots having almost equal wave lengths. The first attempts at analysis were made with the sunspot numbers as they are published. The results were encouraging and identical with those obtained with transformed sunspot numbers.

II. The Statistical Treatment

1. Transformed Sunspot Numbers

The original sunspot numbers have a property that makes it impossible to apply most of the statistical tests. This property is their extreme skew frequency distribution. In order to submit the sunspot numbers to statistical treatments it is advisable to transform them such that the frequency distribution of the transformed data does not differ too much from a normal distribution. It is not possible to find a transformation that produces a strict Gaussian distribution for two reasons: (1) A periodic function which resembles a sine curve always has a tendency toward a bimodal distribution. A periodic function with constant amplitude even has an extreme bimodal distribution which drops abruptly to zero beyond the two maxima (Portig, 1944). Since we intend to study the periodicities of the sunspots we do not want to destroy the bimodality by means of a transform.*

*Remark: All statistical significance tests known to the author overlook the fact that a periodic function cannot have a normal distribution, and that the better the periodicity the greater are the deviations from normality.

(2) The original data have a substantial number of zeros which cannot be eliminated by a transform. The normal distribution requires the frequencies to converge to zero when approaching the smallest value.

A transform which improves the statistical properties of the original sunspot numbers, S, - within the limitations just mentioned - is the square root of them. For convenience they are multiplied by 10 so that we use the variable $S' = 10\sqrt{S}$.

Figure 1 shows the frequency distributions of S and S'.

For the data from 1749 through 1961 the arithmetic mean of all 213 values of S' is 65.9, their standard deviation σ' being 29.79.

2. Analysis

It is extremely difficult to separate periodicities of almost equal length, and there is only one way to eliminate the intermingling of them. One must find a period for which all suspected periodicities are subharmonics. This period, totally covered with equally spaced data, has to be submitted to harmonic analysis for the selected subharmonics. Assuming that the periodicities are independent of each other such that their effects add up arithmetically, such harmonic analysis will separate them completely. When the periodicities have very closely the same length, or the ratio between their lengths is unfavorable, a very long series of data is required. This requirement excludes the majority of meteorological data from rigorous treatment in the search for periodicities. In the case of the sunspot numbers things are more favorable.

It is a trend of the present development in planetary science to

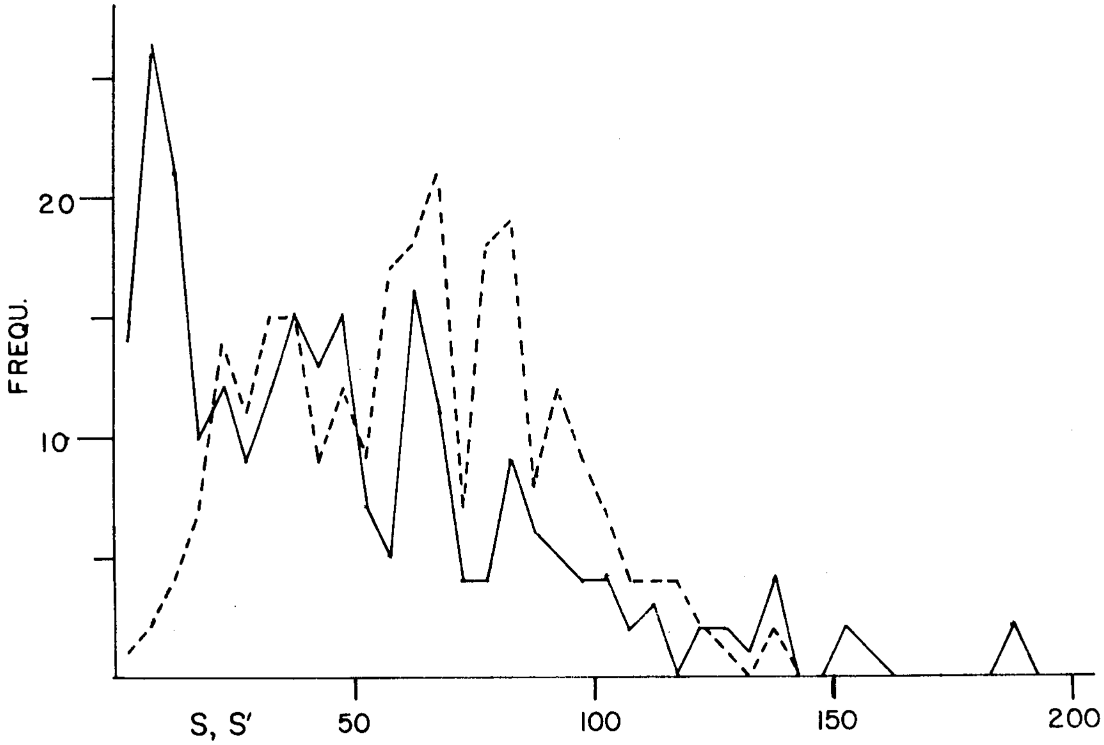

Figure 1. Frequency Distributions of S (——) and $S' = 10\sqrt{S}$ (- - - -)

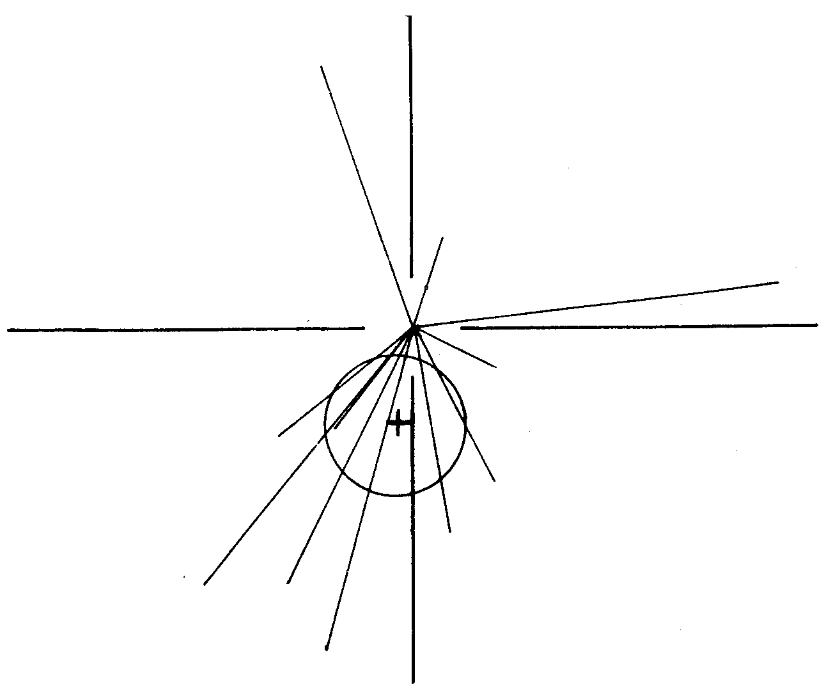

Figure 3. Harmonic Dial of Monthly Sunspot Numbers S' Analyzed for the Position of the Earth

study the tides that may be induced by the planets on the sun. It is tempting to relate the 11.86 years that Jupiter requires for one orbit with the approximate 11 year intervals in which the sunspot maxima are spaced. The sunspot data were arranged according to the positions of the planets in their orbits.

There was an unexpected difficulty in finding these positions. All books dealing with the motion of the planets, even the Encyclopaedia Brittanica, carefully list the seven elements which must be known to compute the position of a planet at any time; they fail, however, to give numerical values of these elements. It turned out that for our purpose it is sufficient to know the celestial longitudes of the planets at one certain moment and their times of a siderial orbit to the fourth digit. After some searching the celestial longitudes for 1850, January 1, were found (Clemence) and all other longitudes could be computed easily from these.

A relatively crude review showed that three planetary periodicities are strongly reflected in the sunspot numbers, viz.

(1) the siderial orbit time of Jupiter, 11.86 years;

(2) the "synodic" orbit time of Jupiter with respect to Saturn, i.e. the repetition time after which Jupiter and Saturn are in conjunction or opposition, 9.93 years;

(3) the siderial orbit of Uranus, 84.0 years.

Because of its length the latter factor is not yet amenable to rigorous statistical treatment.

The two remaining periodicities are very close to the 15th and 18th harmonics of a 178 year period. The differences are

$$11.86 - \frac{178}{15} = 11.86 - 11.87 = 0.01 \text{ year}$$

$$9.93 - \frac{178}{18} = 9.93 - 9.90 = 0.03 \text{ year}$$

After extracting these two periodicities, it was found that another harmonic remained, 178/16 = 11.125 years. This harmonic is well known from previous analyses (e.g., see Kuiper, 1953) and is still unexplained. The new aspect in this analysis is that it has been separated from planetary periodicities of similar lengths. This procedure is rigorous and has no ambiguities under the two assumptions that (a) the effects of the several periodicities are additive arithmetically, and (b) the effects can best be described by sine curves. Both assumptions are common in this type of work, but it seems advisable to state them formally and to remember them in the interpretation of the results.

3. Results

Schuster (quoted from Baur, 1939) developed a theory about the emergence of ficticious periodicities in any population of data. He relates the probability, W, that the analyzed amplitude, A, will exceed certain values to the number of data, N, and their standard deviation, σ, by introducing the ratio

$$k = \frac{\text{Amplitude A}}{\text{Expectancy E}}$$

where $E = \sigma\sqrt{\pi/N}$ and $W(k) = e^{-\frac{\pi}{4}k^2}$. In the example we have the standard deviation of the transformed sunspot number, $\sigma' = 27.3$, based on the first 178 observations. This leads to an expectancy $E = 3.62$ S'- units.

The harmonic analysis of the S' data gives for the

15th harmonic (11.87 years), A = 12.9, A/E = 3.6

18th harmonic (9.90 years), A = 11.05, A/E = 3.0

and for the residual

16th harmonic (11.125 years), A = 21.70, A/E = 6.0

Computing W we find that there is only 0.05, 0.085, and less than 10^{-5} of a percent probability, respectively, that the analyzed amplitudes are the products of mere chance.

Figure 2 shows in the upper three curves the three periodicities discussed here as they were obtained by harmonic analysis from the annual S' values of the 178 years, 1749 through 1926. The fourth curve is the arithmetic sum of the three. It is extrapolated to the year 2000; that is, its left hand part is repeated such that 1749 corresponds to 1927, etc.

The lowest part of the figure presents the original S' numbers. One sees that in spite of the very high probabilities for the reality of the analyzed curves there are considerable unexplained residues. One gets two subjective impressions, that (a) the amplitude of the S' numbers is subject to a multiplying (or some other functional) effect in addition to the additive ones; and (b) there is a long term wave which has not been covered by our analyses. The first of these conclusions cannot be investigated at the present time. The second is discussed briefly in the following paragraphs.

4. Other Periodicities

It is probable that the position of Uranus also has an influence on the number of sunspots. The literature on the effects of sunspots on climate mentions again and again a cycle of 80 to 90 years length (e.g. Willett, 1961). Uranus orbits the sun in 84 years. As mentioned above, this is too long an interval to be determined by rigorous mathematical methods from 213 years of data. Less rigorous methods are very encouraging and indicate a large amplitude of 13-14 S'-units. [If we could apply Schuster's criterion, this would mean that there is only 0.007% probability that this analyzed periodicity is the product of mere chance.]

Also, the position of the earth may have an effect on the sunspot numbers. In this case we have to use monthly data rather than annual. The effect is much smaller than that of the big planets, its amplitude being only 0.33 S'-units. Applying Schuster's test we would find that there is a probability of 98.5% that this result is nothing but a result of mere chance. There is another test which can be applied here. Harmonic constituents can be represented by vectors. If there are several of them there will be a mean vector, and circles can be drawn around its end representing probabilities in the same way as intervals counted from a scalar mean. Analyzing the monthly S' with respect to calendar months for 10 year periods, we arrive at the vectors shown in Figure 3. The cross denotes the end of the average vector. The circle around it represents its standard error. From the theory of harmonic dials we see that there is 86% probability that this distribution of vectors is not a result of

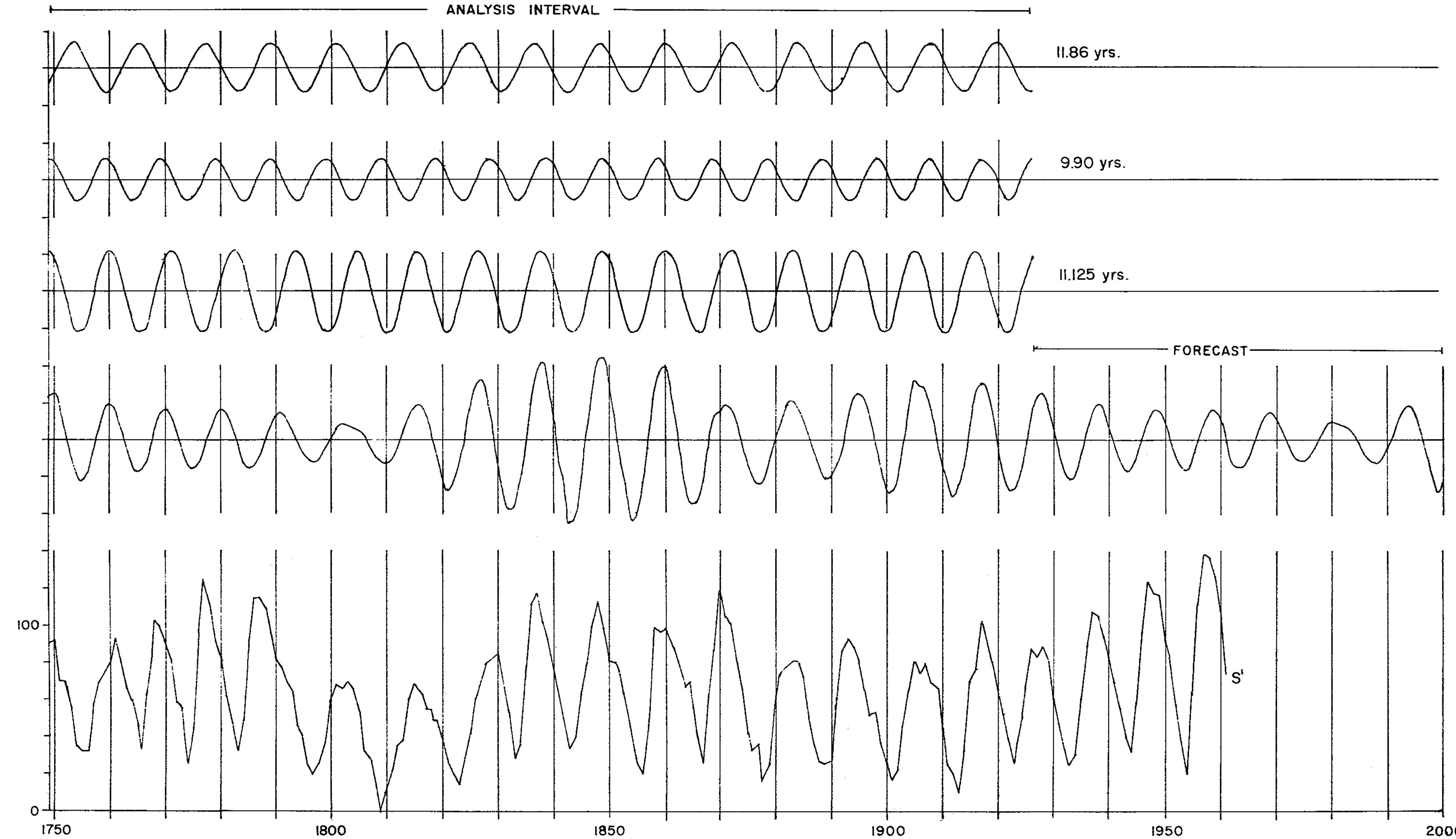

Figure 2. First three curves: Periodicities derived from sunspot numbers through harmonic analysis

Fourth curve: Arithmetic sum of the functions above

Fifth curve: Actual S' numbers

mere chance.

It is interesting to note that only the data obtained after 1849 have a harmonic dial of the characteristics presented in Figure 3. When we use earlier data the centroid of the dots is very close to the center of the dial. This seems to be a consequence of the fact that sunspot numbers before 1849 were estimated at a later time on the basis of old records. This feature, together with the change in the appearance of the harmonic dials for the data before and after 1849, adds to the confidence one may have in the resultant vector of Figure 3. This is, however, only a subjective feeling whereas the objective methods do not suggest a statistical significance of the result.

III. Astronomical Interpretation of the Results

The statistical evidence proves for Jupiter and Saturn, and suggests for Uranus and Earth, that there are positions which favor or impede the formation of sunspots. Figure 4 shows the positions of the planets which seem to be effective. The sun is in the center of the figure. The celestial longitude begins at the left and runs counterclockwise. The inner circle contains the "critical" positions of earth.* The next and the outer circles contain these positions for Jupiter and Uranus, respectively. The third circle indicates the positions of the radius vector on which Saturn, Jupiter, and the sun are lined up at "critical" times.

*Notice that the earth is positioned at the time of the autumnal equinox (September) in the direction, as seen from the sun, of the vernal equinox which is conventionally assigned the longitude 0°.

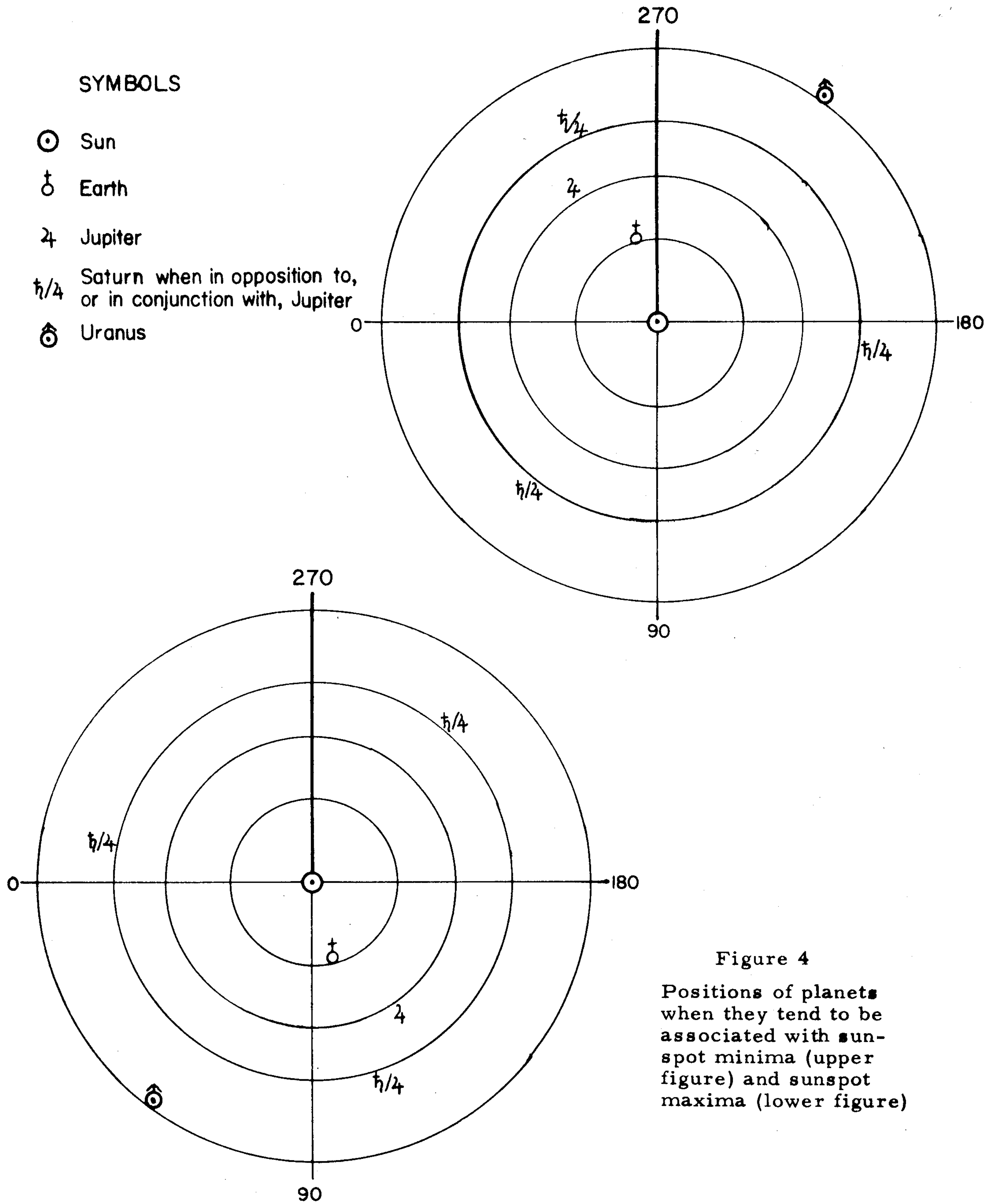

Figure 4

Positions of planets when they tend to be associated with sunspot minima (upper figure) and sunspot maxima (lower figure)

The same conditions are shown in another way in Figure 4A. For each of the orbits presented in Figure 4 the actual relationship between S' numbers and the celestial longitudes are plotted in polar coordinates. The center corresponds to $S' = 0$, and the circle to the arithmetic mean of all S', 66. The curves are the arithmetic means of all S' that were observed at the particular longitudes. Shadings emphasize longitudes of super- or subnormal solar activity as related to (or also produced by?) the planets.

Comparing the upper and lower diagrams in Figure 4, it is seen that there is a clustering of planetary positions near 270° longitude when the sunspots tend to have their minimum. Since the entire system moves in the direction of 270° it appears that planets preceding the sun tend to have a quieting effect on solar activity. This effect begins when the planet is still at longitudes smaller than 270° and reaches its maximum shortly thereafter. The solar system does not move parallel to the ecliptic. Figure 5 shows the vector of motion in its relation to the ecliptic, the plane in which we count celestial longitudes.

Only one of the three Saturn-Jupiter constellations fits into this scheme, and the author can suggest no explanation. It should be mentioned that the three places where Saturn and Jupiter meet shift slowly around the ecliptic. While Saturn reaches the same longitude every 29.46 years, the meeting repeats itself every [9.93, 19.86, and] 29.79 years, or 4° farther east. This is confirmed, though below statistical significance levels, by a computed increase of phase angle of 6 degrees per orbit.

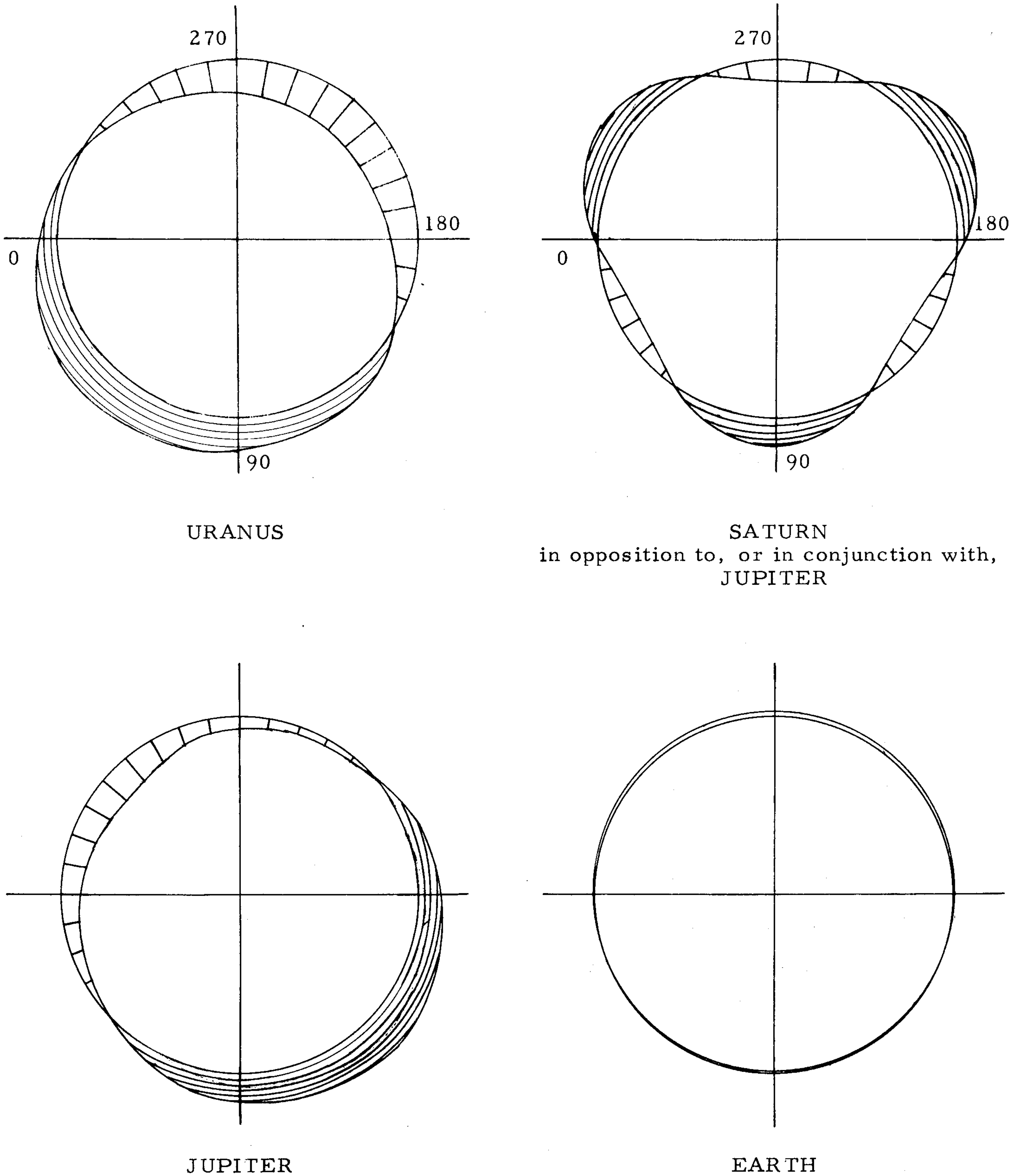

Figure 4A. Mean S' (transformed sunspot numbers) as a Function of the Positions of Planets.

0 is the celestial vernal equinox. 270 is the direction in which the entire solar system moves.

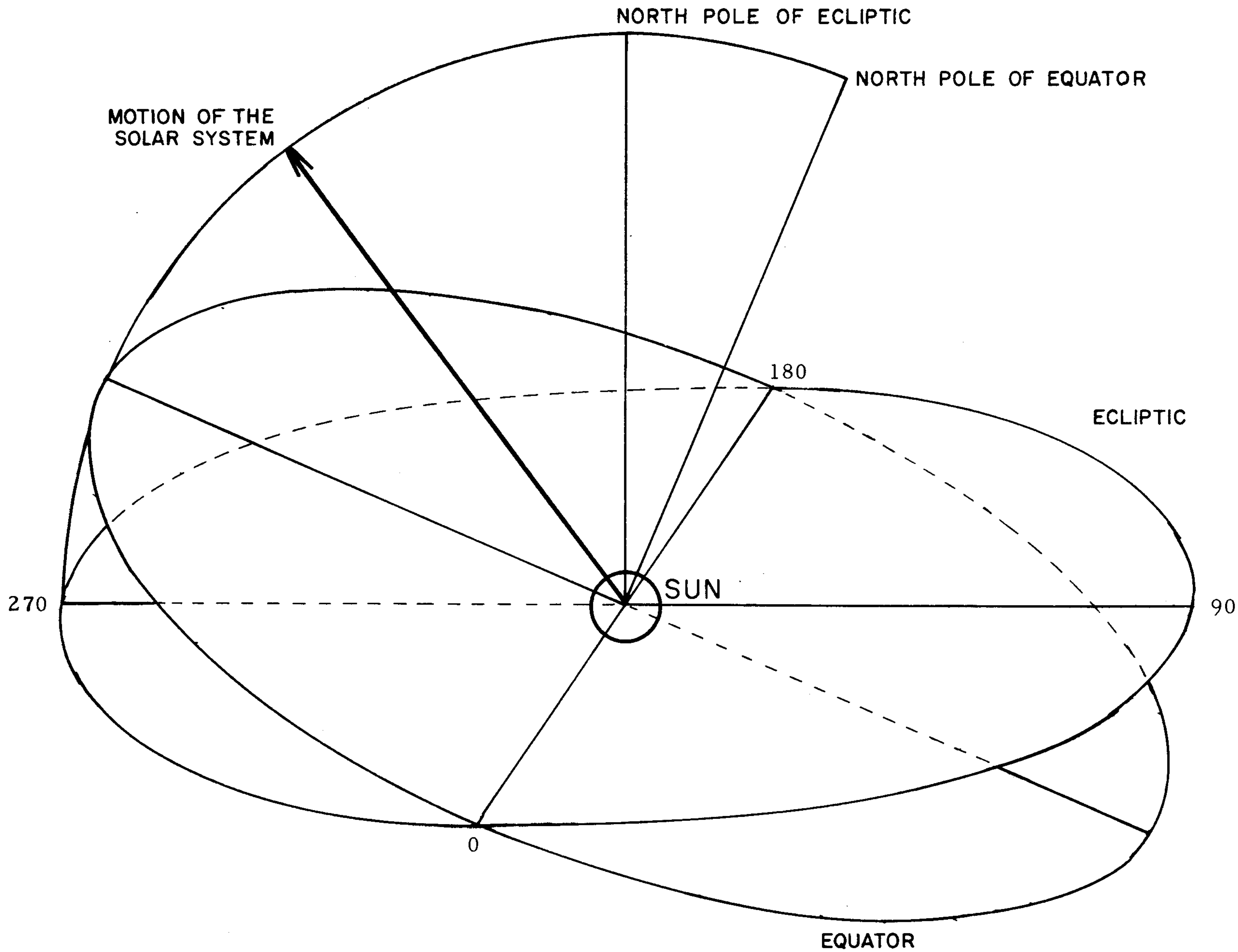

Figure 5. Motion of the Entire Solar System with Respect to the Ecliptic. The longitudes correspond to those of Figure 4. The planets move with increasing longitudes.

IV. Physical Justification for the Use of S'

Taking the root of the sunspot number means mathematically changing from a parameter that represents an area to one representing a line. In other words, S' represents the sunspot density along a line crossing the region with sunspots. This can be related more easily to the positions of the planets when we interpret their effects as tidal forces. Tidal forces on the sun are strongest just opposite the planet. This is especially true for the component perpendicular to the solar surface. This means that the tidal force in the radial direction is concentrated in one point from where it decreases in all directions. As a consequence of the sun's rotation and the movement of the planets, there is a tidal wave running over the sun's surface and its crest stretches in the meridional direction.

We can also try another interpretation. When we assume that the tidal forces exerted by the planets do not provide the energy for the intensity of the sunspots but that they only trigger their release, the diameter, d , of the area affected by the tidal triggering forces is more important than its area, $\frac{\pi d^2}{4}$. This would justify our relating the root of the sunspot number rather than the number itself to tidal forces.

The concepts in this section are only a weak attempt to bolster the modification required by the theory of statistics. The solar physicist has to decide what is actually the physical meaning of S' . As an excuse for our heuristic approach, it may be mentioned that the physical meaning of the original sunspot number is also not yet fully established.

V. Outlook

A physical hypothesis to explain the correlations between positions of the planets does not exist yet and should be developed. Further studies should be made which include the smaller planets and which scan all constellations, and not only those which are commensurate with full orbits (as above).

REFERENCES

Baur, F., 1939: Periodogrammanalyse. Meteorologisches Taschenbuch, ed. F. Linke, Vol. IV, p. 59.

Clemence, G. M., 1949: First-order Theory of Mars. Astronomical Papers, Vol. 11, Part 2, U. S. Government Printing Office, 1950 #8243.

Kuiper, G. P., editor, 1953: The Solar System, Part I, The Sun. The University of Chicago Press, Chicago, Ill., p. 336.

Portig, W. H., 1944: Haufigkeitsverteilung eifacher periodischer Funtionen (Frequency Distributions of Simple Periodic Functions). Annalen der Hydrographie und Maritimen Meteorologie, January, 35-37.

Willett, H. C., 1961: The pattern of solar climatic relationships. Annals of the New York Academy of Sciences, Vol. 95, Art. 1, 89-106 (especially p. 95).

REFERENCES

Brunt, D., 1939: Physical and Dynamical Meteorology. Second Edition, Cambridge.

Charney, J. G., 1951: Dynamic forecasting by numerical process. Compendium of Meteorology, Thomas F. Malone, editor, American Meteorological Society, Boston, 470-482.

Charney, J. G. and P. G. Drazin, 1961: Propagation of planetary-scale disturbances from the lower into the upper atmosphere. J. Geophys. Research, 66, 83-109.

Ebdon, R. A., and R. G. Veryard, 1961: Fluctuations in equatorial stratospheric winds. Nature, 189, 791-793.

Freeman, Jr., John C., Leon F. Graves, W. H. Portig, 1963: Investigation of Relations between Solar Variations and Weather on Earth as Shown by Satellite Data. Final Report, Contract No. NASw-724, National Aeronautics and Space Administration, Washington, D. C.

Freeman, Jr., John C., Leon F. Graves, P. Hanna, W. H. Portig, L. Armijo, and J. Burgmeier, 1964: The Effects of Internal Waves in the Easterlies on Mesoscale Weather Developments. Interim Report No. 1, Contract No. DA 28-043 AMC-00173(E), U. S. Army Electronics Command, Fort Monmouth, N. J.

Haurwitz, B., 1941: Dynamic Meteorology. New York, McGraw-Hill.

Hess, S. L., 1959: Introduction to Theoretical Meteorology. New York, Holt.

Jacchia, L. G., and J. Slowey, 1964: Atmospheric heating in the auroral zones: a preliminary analysis of the atmospheric drag of the Injun 3 Satellite. J. Geophys. Research, 69, 905-910.

Johnson, Francis S., 1965: Structure of the upper atmosphere. Satellite Environment Handbook, Second Edition, Stanford University Press, Stanford, California, 3-20.

King-Hele, D. G., 1964: The rotational speed of the upper atmosphere determined from changes in satellite orbits. Planetary and Space Science, Vol. 12, No. 9, 835-853.

Labitzke, K., 1965: On the mutual relation between stratosphere and troposphere during periods of stratospheric warmings in winter. J. of Appl. Meteor., Vol. 4, 91-99.

MacDonald, N. J., and W. O. Roberts, 1960: Further evidence of a solar corpuscular influence on large-scale circulation at 300 mb. J. Geophys. Research, 65, 529-534.

Ooyama, K., 1958: On the vertical propagation of a disturbance through the mesosphere. (Unpublished paper), Department of Meteorology and Oceanography, New York University.

Paetzold, H. K., 1963: Solar activity effects in the upper atmosphere deduced from satellite observations. In W. Priester, ed., Space Research III, North-Holland Publishing Co., Amsterdam, 28-52.

Reed, R. J., W. J. Campbell, L. A. Rasmussen, and D. G. Rogers, 1961: Evidence of a downward propagating, annual wind reversal in the equatorial stratosphere. J. Geophys. Research, 66, 813-818.

Scherhag, R., and Labitzke-Behr, K., 1963: Preliminary Daily Northern Hemisphere 10 mb Synoptic Weather Maps of the Year 1962. Inst. Met. u. Geoph. Freie Universität Berlin, Meteorologische Abhandlungen, Vol. 26.

Shapiro, Ralph and Fred Ward, 1962a: The harmonic persistence correlation and geomagnetic disturbance. J. Atmos. Science, 19, 60-65.

Snyder, C. W., and Neugebauer, M., 1963: Interplanetary Solar Wind Measurements by Mariner II. Paper presented at the Fourth International Space Science Symposium (Cospar), Warsaw.

Snyder, C. W., Neugebauer, M., and Rao, U. R., 1963: The solar wind velocity and its correlation with cosmic-ray variations and with solar and geomagnetic activity. J. Geophys. Research, 68, 6361-6370.

Takahashi, K., 1958: The effect of the change of solar activity on meteorological phenomena. Journal of the Meteorological Society of Japan, Series II, Vol. 36, 21-31.

Thompson, Philip D., 1961: Numerical Weather Analyses and Prediction. The Macmillan Co., New York.

Wurlitzer, G., 1958: Das Verhalten des Luftdrucks am Boden bei Schwankungen der erdmagnetischen Aktivität. Inst. Met. u. Geoph. Freie Univ. Berlin, Meteorologische Abhandlungen, Vol. 7, Part 2.

CORRECTIONS FOR FINAL REPORT SN-140A

PAGE	ERRATA			
before i	Add Explanatory Note (attached)			
iv	Add For Sections I, II, and III and page number R-1			
I-2	Change	absorbtion	to	absorption
I-9	"	Ooyoma	"	Ooyama
I-14	"	being	"	bring
I-15	"	viscous like	"	viscous-like
I-21	"	utlimately	"	ultimately
II-1	"	(Takahashi, 1958)	"	Takahashi (1958)
II-3	"	500 km/sec^{-1}	"	500 km sec^{-1}
	"	days	"	ways
II-5	"	which solar wind	"	which no solar wind
II-7	In title of Table 1 repair letter t in Arrangements			
	In last line, insert described			
II-10	Change	seasonally-adjusted	to	seasonally adjusted
	"	found day	"	found from day
II-15	"	Sea over Japan	"	Sea, over Japan
II-20	"	reason	"	season
II-31	"	index.)	"	index.
	"	insignificantly.	"	insignificantly).
	"	solstices:	"	solstices,
	"	So	"	so
II-32	"	Table 2	"	Table 5
II-33	"	ortoo	"	or too
II-37	"	Table 2	"	Table 5
II-38	Underline as indicated			
II-39	Change	Finds	to	Findings

PAGE	ERRATA			
II-39	Change	a	to	the
	"	emphasis vertical	"	emphasis on vertical
III-5	"	rate	"	rates
"	(twice)	for very small time*	"	plus very small terms*
III-8	Repair the letter e in especially			
III-9	Change	$\frac{\partial}{\partial t}$	to	$\frac{1}{2}\frac{\partial}{\partial t}$
III-13	"	1963)).	"	1963).
III-14	"	level of	"	level i of
	"	$k_1{}^2$	"	$k_{i1}{}^2$
	"	$k_2{}^2$	"	$k_{i2}{}^2$
III-15	"	k^2z	"	$k_{i1}{}^2z$
	"	For	"	for
III-16	"	R_m	"	R_{ni}
	"	theoretical	"	thermal
III-18	"	level. So	"	level so
	"	$\frac{\partial}{\partial z}\left[\frac{f}{2g}\Omega\frac{D_1}{D_0}\right.$	"	$\frac{\partial}{\partial z}\left[\frac{f}{2g}\Omega\frac{D_1}{D_0}\right]$
"	(twice)	$\left(\frac{1}{D}\frac{\partial D}{\partial t}\right),$	"	$\left(\frac{1}{D}\frac{\partial D}{\partial t}\right)_0$
A-1	Repair atmosphere, where and developed			
A-23	Change	(1953)	to	(1955)
A-30	"	$\frac{g(h_{m+1}\ h_m)\frac{\partial}{\partial z}}{\theta}$	"	$\frac{g(h_{m+1}-h_m)\frac{\partial\theta}{\partial z}}{\theta}$
A-33	"	x	"	z
A-34	"	$\partial z\,\partial Y$	"	$\partial z\,\partial y$
	"	$K_2/\frac{\partial^2\theta}{\partial z^2}$	"	$K_2\frac{\partial^2\theta}{\partial z^2}$
	"	$K_1K_2/\frac{\partial^2\theta}{\partial z^2}$	"	$K_1K_2\frac{\partial^2\theta}{\partial z^2}$
	"	$\frac{\partial^2\theta}{\partial\ ^2}$	"	$\frac{\partial^2\theta}{\partial y^2}$
	"	$\frac{\partial\theta}{\partial}$	"	$\frac{\partial\theta}{\partial z}$
	"	$\frac{\partial^2\theta}{\partial\ ^2}$	"	$\frac{\partial^2\theta}{\partial z^2}$
	"	$F''F'=\frac{K_sF}{F}$	"	$F''F'=\frac{K_sF'}{F}$

PAGE	ERRATA			
A-35	Change	$\sqrt{2K_6\bar{H}+K_6}$	to	$\sqrt{2K_5\bar{H}+K_6}$
	"	$H' C^{H}$	"	$\bar{H}' C^{\bar{H}}$
	"	$\bar{H}' = \frac{2ww' - K_6}{2K_6}$	"	$\bar{H}' = \frac{2ww'}{2K_5}$
	"	$\frac{2ww'}{2K_5} C \frac{w^2-K_6}{2K_5} = w$	"	$\frac{2ww'}{2K_5} C^{\frac{w^2-K_6}{2K_5}} = w$
	"	$\int_{w_0}^{w} C \frac{w^2-K_6}{2K_5} = K_5(y=y_0)$	"	$\int_{w_0}^{w} C^{\frac{w^2-K_6}{2K_5}} = K_5(w-w_0)$
A-37	Change title to: REFERENCES FOR APPENDIX A			
B-5	Omit as a bonus			
B-6	Change	or	to	, i.e.
	Remove spot from original and/or reproducible copy.			
B-9	Change	$-2\Omega\rho g$	to	$2\Omega\rho u - g\rho$
	"	V	"	v (lower case)
	Change	$\frac{\partial \rho}{\partial y}$	to	$\frac{\partial p}{\partial y}$
	" (twice)	β_{yu}	"	βyu
B-10	"	$g u$	"	g_u
	"	$+2\Omega u$	"	$-2\Omega u$
	"	$\gamma_u \frac{\partial D}{\partial y}$	"	$-\gamma_u \frac{\partial D}{\partial y}$
	"	$\frac{\partial u}{\partial t}$	"	$\frac{\partial a}{\partial t}$
	" (twice)	$-2\Omega u$	"	$+2\Omega u$
	Change	$-\frac{2\Omega\beta u^2}{g}$	"	$+\frac{2\Omega\beta u^2}{g}$
B-12	"	is sufficient	"	are sufficient
	"	respect z	"	respect to z
B-13	"	$\frac{1}{a}\frac{\partial u}{\partial t}$	"	$\frac{1}{a}\frac{\partial a}{\partial t}$
	"	$= const. = \frac{\frac{\partial u}{\partial z}/max.}{a_{max.}}$	"	$= const. = \frac{\left(\frac{\partial u}{\partial z}\right)_{max.}}{a_{max.}}$

PAGE		ERRATA			
B-13		Change	$\frac{\frac{\partial u}{\partial z\,min.}}{a_{max.}} a$	to	$\frac{\left(\frac{\partial u}{\partial z}\right)_{max.}}{a_{max.}} a$
		"	$u = u_o \cos\left(\frac{2\pi z}{2} - \frac{2\pi z}{T}\right)$	"	$u = u_o \cos\left(\frac{2\pi z}{L} - \frac{2\pi t}{T}\right)$
		"	$a = a_o \sin\left(\frac{2\pi z}{2} - \frac{2\pi t}{T}\right)$	"	$a = a_o \sin\left(\frac{2\pi z}{L} - \frac{2\pi t}{T}\right)$
B-14		"	$\beta_Y (u_A + \Delta u)$	"	$\beta y (u_A + \Delta u)$
B-15		Add to For $u_A = 0$ the following: and the values for Ω, β, g, and T given on page B-11, we get			
B-19		Change	magneto meteorological	to	magneto-meteorological
B-24		"	$+(f_o + \beta Y)u$	"	$+(f_o + \beta y)u$
B-27		Change	equation 14)	to	equation (14)
B-30		"	r4versal	"	reversal
		Change title to : REFERENCES FOR APPENDIX B			
C-1		Clean mark off original and/or reproducible copy			
C-2		Change	area	to	speed
	"	(twice)	sun spot	"	sunspot
		"	from a magnetogram	"	from magnetograms
C-4	"	(twice)	D_{ST}	"	D_{st}
		"	$P_R - P$,	"	$\dot{p}_R - \dot{p}$,
C-6		Clean spot off original and/or reproducible copy			
C-7		Change	P_R	to	$\dot{p}_R$
C-10		"	sun spot	"	sunspot
C-14		Omit last paragraph			
C-15		Omit the text on this page			
C-16		Change page number to C-15			
		Change title to : REFERENCES FOR APPENDIX C			
		(3 times) Omit (See and).			
		Add: ,Final Report, Contract NASw-724. where indicated			
C-17		Change page number to C-16			
C-18		" " " " C-17			

PAGE	ERRATA			
C-19	Change	TSentral 'nyi	to	TSentral'nyi
D-2	"	This	"	Such
	Underline daily			
	Underline annual			
D-7	Change	fiction fictitious		
D-8	"	page number to D-9 and change position of page.		
D-9	"	page number to D-10 and change position of page.		
D-10	"	page number to D-8 and change position of page.		
D-14	Fill in missing labels.			
D-18	Change	Haufigkeitsverteilung	to	Haüfigkeitsverteilung
	"	eifacher	"	einfacher
	"	period-	"	perio-
	"	ischer	"	discher
	"	Funtionen	"	Funktionen
	Omit January.			
	Change title to: REFERENCES FOR APPENDIX D			
R-1	Change title to: REFERENCES FOR SECTIONS I, II, AND III			
	"	capital letters to lower case where shown		
R-2	"	" " " " " " "		
	"	Analyses	to	analysis

EXPLANATORY NOTE

The sections of this report are not arranged in the order in which the work was carried out. Consequently, there are certain contradictions between Appendix C (written in 1963) and Section II (written in 1965).

Appendix A was begun in 1958 and final preparation was accomplished for this project. This work has been sponsored, during a period of several years, by the U. S. Air Force, the National Science Foundation and NASA. The concepts developed in Appendix A are necessary for understanding Sections I and III of the report.

The present (1966) addresses of the authors of this report are:

Dr. W. H. Portig
U. S. Army Tropic Test Center
Fort Clayton
Panama Canal Zone

Dr. Leon F. Graves
Physics Department
University of Houston
Houston, Texas

Mr. Peter Hanna
TRW Systems - Houston Operations
Space Park Drive
Nassau Bay, Texas

July 7, 1966

Dr. John C. Freeman, Jr.
Institute for Storm Research
3812 Montrose Boulevard
Houston, Texas 77006